Demonstration of an HTS SQUID system for nondestructive evaluation

Report for
US Air Force,
European Office of Aerospace Research and Development

Reference SPC-95-4018

by
Dr J.Kuznik,
Czech Academy of Sciences

on work with
Prof. G.B.Donaldson and Dr A.Cochran,
University of Strathclyde,
Department of Physics and Applied Physics,
Glasgow, Scotland. G4 0NG

31 July 1995

REPORT DOCUMENTATION PAGE

Form Approved OMB No. 0704-0188

1. AGENCY USE ONLY (Leave blank)	2. REPORT DATE	3. REPORT TYPE AND DATES COVERED
	31 July 1995	Final Report

4. TITLE AND SUBTITLE

Demonstration Of An HTS SQUID System For Nondestructive Evaluation

5. FUNDING NUMBERS

F6170895W0210

6. AUTHOR(S)

Dr. Jan Kuznik

7. PERFORMING ORGANIZATION NAME(S) AND ADDRESS(ES)

University of Strathclyde
Glasgow G4 0NG
United Kingdom

8. PERFORMING ORGANIZATION REPORT NUMBER

N/A

9. SPONSORING/MONITORING AGENCY NAME(S) AND ADDRESS(ES)

EOARD
PSC 802 BOX 14
FPO 09499-0200

10. SPONSORING/MONITORING AGENCY REPORT NUMBER

SPC 95-4018

11. SUPPLEMENTARY NOTES

Final report plus supporting documents on SQUIDS.

12a. DISTRIBUTION/AVAILABILITY STATEMENT

Approved for public release; distribution is unlimited.

12b. DISTRIBUTION CODE

A

13. ABSTRACT (Maximum 200 words)

This report results from a contract tasking University of Strathclyde as follows: This report describes the work done by Dr. Jan Kuznik at the University of Strathclyde from 1 May 1995 until 31 Jul 1995. In accordance with the proposal, the main objective was to illustrate the feasibility of an eddy current nondestructive evaluation (NDE) measurement system based on high-T_c SQUIDS in an ordinary laboratory environment without any magnetic shielding. A series of aluminum and steel samples with artificial and real cracks were investigated under these conditions.

14. SUBJECT TERMS

Nil

15. NUMBER OF PAGES

64

16. PRICE CODE

N/A

17. SECURITY CLASSIFICATION OF REPORT	18. SECURITY CLASSIFICATION OF THIS PAGE	19. SECURITY CLASSIFICATION OF ABSTRACT	20. LIMITATION OF ABSTRACT
UNCLASSIFIED	UNCLASSIFIED	UNCLASSIFIED	UL

1.0 Introduction

This report describes the work done by Dr Jan Kuznik at the University of Strathclyde from 1 May 1995 until 31 July 1995. In accordance with the proposal, the main objective was to illustrate the feasibility of an eddy current nondestructive evaluation (NDE) measurement system based on high-T_c SQUIDs in an ordinary laboratory environment without any magnetic shielding. A series of aluminium and steel samples with artificial and real cracks were investigated under these conditions.

The results suggest that a high-T_c SQUID system is a suitable tool for some NDE tasks. Some of these results have already been presented at the 2nd European Conference on Applied Superconductivity (see attached preprints [1,2]) and more papers will follow: two abstracts are attached [3,4].

2.0 The SQUID system

A custom made first order electronic gradiometer was used, one of the first of this type of system ever developed, and certainly the first optimised for NDE. We also made our own cryostat, again optimised for NDE. Both were used with existing, custom built, computer controlled NDE scanning apparatus and data processing software.

2.1 SQUIDs and electronics

The sensors are commercially available Conductus Mr SQUIDs. These are very small and are therefore poor sensors from the point of view of sensitivity. Specially designed electronics were needed to achieve 10 pT/$\sqrt{\text{Hz}}$ sensitivity for each SQUID. Even with this high value, the separate output of each SQUID was dominated by external noise in unshielded environments, but this was no longer the case with the electronic gradiometer. With a 25 mm baseline, its performance was excellent: power line interference was suppressed by more than 30 dB and most of the noise spikes such as switching glitches from day to day activity inside the building vanished as well (see [1] Figure 2, attached).

The SQUID electronics used a classical modulation scheme at 180 kHz, with detection of second harmonics at 360 kHz. The output bandwidth of the phase locked loop was about 50 kHz; this covers the range of useful frequencies for investigation of aluminium samples and provides the necessary higher than usual slew rate needed in electronic gradiometer instruments. Bias reversal was not needed because 1/f noise is dominated by environmental interference in unshielded environments and eddy current measurements do not need the sub-Hz sensitivity of some other SQUID measurements.

Our measurements used a slightly unusual geometry (see [1] Figure 1, attached) with the two SQUIDs placed perpendicular to the investigated surface, and separated by 25 mm in the horizontal direction. We thus detected the x derivative of the field component B_x. This design was mostly dictated by the shape of Conductus sensor, but it proved quite successful when appropriate excitation schemes were used: it has been used for the most advanced NDE measurements ever achieved with a high-T_c system.

2.2 Cryostat

During all our measurements the SQUID system was placed in a cotton-epoxy composite (Tufnol) LN_2 cryostat (see [1] Figure 1, attached). No magnetic or high frequency screening was used. This was only possible because the SQUID electronics itself was placed on top of the cryostat thus reducing the RF pickup. The layout also showed how a compact system for practical applications could be assembled.

3.0 Sample excitation

We used three excitation techniques (see [2] Figure 2, attached).

3.1 Direct current injection

Given the sensitivity of the SQUID system, only a few milliamperes needed to be fed into the sample. Direct current injection is the easiest laboratory method, and provides moderate sensitivity to flaws. Nevertheless, spatial resolution is not very good with our gradiometer geometry because of the physical separation of the SQUIDs and their total 11 mm stand-off from the base of the cryostat, and interference from currents flowing around the sides of a specimen is difficult to avoid.

3.2 Spiral loop eddy current excitation

For this technique, a spiral induction coil, made from a PCB track with four or more turns, was located below the cryostat in the middle of the SQUID gradiometer. The necessary ac excitation current was higher; typically 100 mA. This method gave the best spatial resolution, determined by the 4.5 mm diameter of the coil and its small stand-off from the specimen: the much larger gradiometer baseline and stand-off do not matter in this case. We achieved approximately 5 mm as a typical resolution. Unfortunately this method is useful only for surface flaw detection since the field of the coil is similar to that of a magnetic dipole and is therefore strongly attenuated inside the metal; subsurface crack detection with the small coil was hard even for our biggest artificial cracks.

3.3 Double-D excitation

For this, a wire loop formed into two D-shapes was wound around the tail of the cryostat with the maximum current flowing in the straight middle section. This method gives moderate spatial resolution but much higher sensitivity to subsurface flaws. It was used, amongst others, for the detection of a real crack in the pressure vessel outlined in the next section.

4.0 The samples

We used a variety of steel and aluminium samples. The most interesting are outlined in this section.

4.1 Aluminium plates

For most measurements, we used standard aircraft-grade (Al7075-T651) aluminium samples 300 x 300 x 13 mm with simulated flaws machined in the middle of one surface. The biggest flaw was a 40 x 6 x 6 mm slot and the smallest an arc section slit cut by a 45 mm diameter circular saw blade 0.15 mm thick to a maximum depth of 1.8 mm. Flaws were detected on both the upper (surface) and lower (subsurface) sides of the plate.

4.2 A steel plate

We made one measurement on a section of steel hull plate supplied by the UK DRA. This had approximately the same dimensions as the aluminium, but the flaw was an artificially induced fatigue crack. The main problems with steel are the large remanent fields and the distortion the ferromagnetic material causes in the Earth's field. These severely disturb the SQUID, since in the high-Tc case, the SQUID itself has to see the whole field rather than the effects of field gradient usually applied to a low-T_c SQUID by a gradiometric flux transformer. Since high-T_c flux transformers are not yet available, we made the experiment easier by demagnetizing the plate.

4.3 A pressure vessel section

A real sample from a failed pressure vessel was supplied by British Gas. Such a vessel is a laminate comprising an internal aluminium core and external fibreglass reinforcement a few millimetres thick. This is a good candidate for eddy current SQUID NDE since the presence of fibreglass makes conventional eddy current and ultrasonic flaw detection impossible from the exterior. The successful detection of an invisible crack in this sample was a significant achievement in our work.

5.0 Results

In this section, we briefly summarise the specimens we have inspected, the techniques used and their results.

- Specimen: V-shaped wire (see [1] Figure 3, attached)
  Material: Copper
  Flaw: Not applicable
  Technique: Directly injected current
  Results: Clear images of wires, showing characteristic signature of gradiometer and poor spatial resolution
  Conclusion: Stand-off and baseline dimensions limit the effectiveness of the system for mapping fields generated by excitation intrinsic in specimen

- Specimen: Plate (see [2] Figure 3, attached)
  Material: Aluminium
  Flaw: Surface slot 6 mm wide, 40 mm long and 6 mm deep
  Technique: Directly injected current
  Results: Successful detection of slot, superimposed on large artefacts caused by current flow around sides of plate
  Conclusion: SQUID system can map widespread current flows very effectively; these will often obscure flaw indications in practical applications

- Specimen: Plate
  Material: Aluminium 7075-T651 (see [1] Figure 4, attached)
  Flaw: Arc section slit 150 μm wide, 1.8 mm maximum depth in upper surface
  Technique: Eddy current - four turn, 4.5 mm diameter spiral coil
  Results: Successful detection with good signal to noise ratio (SNR) at stand-offs from 1.5 to 4.5 mm
  Conclusion: Small surface flaws are detectable even at stand-offs which allow interposed insulating surface layers; spatial resolution is good with small excitation coils at low stand-offs

- Specimen: 13 mm thick plate (publication will follow)
  Material: Aluminium 7075-T651
  Flaw: Two arc section slits 150 μm wide, maximum depths 6.5 and 3 mm in lower surface
  Technique: Eddy current - 63 mm diameter, single filament double-D excitation coil
  Results: Successful detection of deep slit with reasonable SNR; some indication of shallow slit.
  Conclusion: Some technical development of the system is needed to detect small flaws very deep beneath the surface of aluminium

- Specimen: Section of cylindrical pressure vessel with fibreglass reinforcement (publication will follow)
  Material: Aluminium
  Flaw: Fatigue crack induced in aluminium by pressure cycling
  Technique: Eddy current - double-D excitation coil
  Results: Successful detection of flaw with good SNR
  Conclusion: SQUID systems may be useful where surface layers prevent other techniques being used

- Specimen: UK DRA (UK Navy) hull plate (publication will follow)
  Material: Demagnetised mild steel
  Flaw: Artificially induced fatigue crack
  Technique: Eddy current - double-D excitation coil
  Results: Successful detection of flaw, but with poor SNR
  Conclusion: High-T_c SQUIDs can be used only with difficulty with steel specimens

In all cases, the excitation frequencies were in the 70 Hz to 3 kHz range and excitation currents, whether directly injected or in induction coils, were between 10 and 100 mA. Field amplitudes varied from a few hundred nanotesla for directly injected current mapping to a few hundred picotesla for some eddy current measurements.

6.0 Conclusions

We have demonstrated one of the first electronic gradiometers based on high-T_c SQUIDs in use for NDE. We have made measurements on real and artificial flaws in aluminium and steel and have shown that the apparatus can be used in a convenient and efficient manner in an unshielded environment. We consider that there should be several practical applications for such a system when the effectiveness of more common methods such as ultrasound and magnetic particle inspection is inadequate.

7.0 Acknowledgements

We acknowledge the assistance of Mr C.Carr, a UK EPSRC funded research student, in some of the measurements. We also acknowledge the support of the UK EPSRC which allowed us to develop the equipment we have shown to work successfully here.

8.0 References

[1] J.Kuznik, C.Carr, A.Cochran, L.N.C.Morgan and G.B.Donaldson, "First order electronic gradiometry with simple HTS SQUIDs and optimised electronics", presented at 2nd Eur. Conf. on Appl. Supercond., Edinburgh, 1995.

[2] A.Cochran, J.Kuznik, C.Carr, L.N.C.Morgan and G.B.Donaldson," Experimental results in non-destructive evaluation with HTS SQUIDs", presented at 2nd Eur. Conf. on Appl. Supercond., Edinburgh, 1995.

[3] A.Cochran, G.B.Donaldson, C.Carr, D.McA.McKirdy, M.E.Walker, U.Klein, A.McNab and J.Kuznik, "Recent progress in SQUIDs as sensors for electromagnetic NDE", to be presented at International Workshop on Electromagnetic NDE, London, 1995.

[4] A.Cochran, G.B.Donaldson, D.McA.McKirdy, M.E.Walker, U.Klein, C.Carr, J.Kuznik and A.McNab, "Advances in the theory and practice of SQUID ", to be presented at 22nd Annual Rev. of Progress in Quantitative NDE, Seattle, 1995.

Presented at 2nd European Conference on Applied Superconductivity (EUCAS'95), Edinburgh, July 1995.

First order electronic gradiometry with simple HTS SQUIDs and optimised electronics

J Kuznik*, C Carr , A Cochran , L N C Morgan+ and G B Donaldson

University of Strathclyde, Department of Physics and Applied Physics, John Anderson Building, 107 Rottenrow, Glasgow, G4 0NG, UK.

* Presently visiting from Institute of Physics, Czech Academy of Sciences, Prague, Czech Republic.

+ Now with BT Laboratories, Martlesham Heath, Ipswich, IP5 7RZ, UK.

Abstract. We have constructed a complete system for first order electronic gradiometry, including instrumentation and cryostat, based on two commercial high temperature superconductor Mr SQUID devices. The combined white noise level of the two SQUIDs is 10^{-11} T/√Hz. The system was designed for non-destructive evaluation in unshielded environments and therefore has a bandwidth of at least 30 kHz, needed to provide enough slew rate to stay in the flux locked loop under laboratory conditions. The SQUIDs are oriented vertically to measure a component of horizontal field depending on probe rotation. Their separation is 25 mm and they are positioned approximately 7 mm from the base of the cryostat, which is 4 mm thick in total. Here, we outline the electronic and cryogenic hardware and present results demonstrating fundamental performance. These are based on noise measurements in low noise and unshielded environments; on mapping a V-shaped current-carrying wire to illustrate spatial resolution; and on eddy current detection of a slit in an aluminium specimen.

1. Introduction

The problems to be overcome to use high temperature superconductor (HTS) SQUIDs (superconducting quantum interference devices) for nondestructive evaluation (NDE) are quite different from those for many other applications. For example, consider the simple biomagnetic magnetocardiographic measurement [1], in which SQUID noise levels are critical, particularly at low frequencies, necessitating relatively large pick-up areas and films and Josephson junctions of the highest quality for HTS implementations.

In contrast, HTS SQUIDs for NDE can be simple commercial devices such as the Conductus Mr SQUID [2]. Although low frequency measurements are of interest, this probably indicates a minimum of as much as 10 Hz or more, since lower frequencies may make inspection too slow to be practical. The maximum frequency is also higher; typically a few tens of kHz: above this the performance of other sensors makes it difficult to justify using SQUIDs. A further difference is that it is unlikely that practical NDE can involve magnetic shielding

In summary, a SQUID NDE system should have the following attributes: as much insensitivity as possible to external interference; an adequate white noise level (relatively high 1/f noise is possible); and a bandwidth from 10 Hz to a few tens of kHz. Other positive attributes include high spatial resolution and convenient, easy to handle cryogenics.

In the past, we have tried to satisfy these requirements [3] with systems based on single HTS SQUIDs (and with low temperature superconductor (LTS) devices [4]: the requirements are the same. No matter how familiar liquid helium seems to those working with LTS SQUIDs, the dominant LTS problem has always been cryogenic inconvenience.) However, although the intrinsic white noise level and field sensitivities of the HTS systems were adequate, upper bandwidth was poor and susceptibility to external interference without resorting to magnetic shielding made the signal to noise ratio (SNR) too low for many measurements.

2. Electronic gradiometer

In our new system, shown in Figure 1, the two Mr SQUIDs are mounted vertically 25 mm apart. They are standard commercial items, the only difference being truncation of the PCB immediately below the SQUID encapsulation to allow them to be positioned as close as possible to room temperature specimens outside the cryostat (i.e. with minimum lift-off). The probe itself is spring-loaded to press the PCBs on the bottom of the cryostat. This both minimises lift-off (about 11 mm including cryostat tail thickness) and provides the positive location for the SQUIDs which is essential for accurate computer modelling. There is no adjustment of relative SQUID position: the SQUIDs are bolted to a Tufnol mounting piece, oriented back to back.

Each SQUID is connected to a separate channel in the electronics via its own multicomponent matching circuit. The bandwidth of each channel extends from DC to 30 kHz, and the white noise level is $10^{-4}\Phi_0/\sqrt{\text{Hz}}$. Typical SQUID NDE field amplitudes in the range of nT or hundreds of pT provide signals from a few mV down to hundreds of μV. The electronics themselves are fabricated in a modular fashion in a multiboard headbox mounted directly on the SQUID probe. Only the ±15 V DC power supply is separate.

Individual outputs from each SQUID are available and the electronics also include a simple circuit to provide the difference (quasi-first order gradient) signal directly. The output range is ±10 V. To maintain the flux-locked loop in the presence of large fields, for example when inspecting steel specimens, multiple resets may occur, triggered by either SQUID separately or by an out of range difference. The short, 1 ms reset period is therefore valuable.

The SQUID probe and electronics are mounted in our own cryostat with the usual refine-

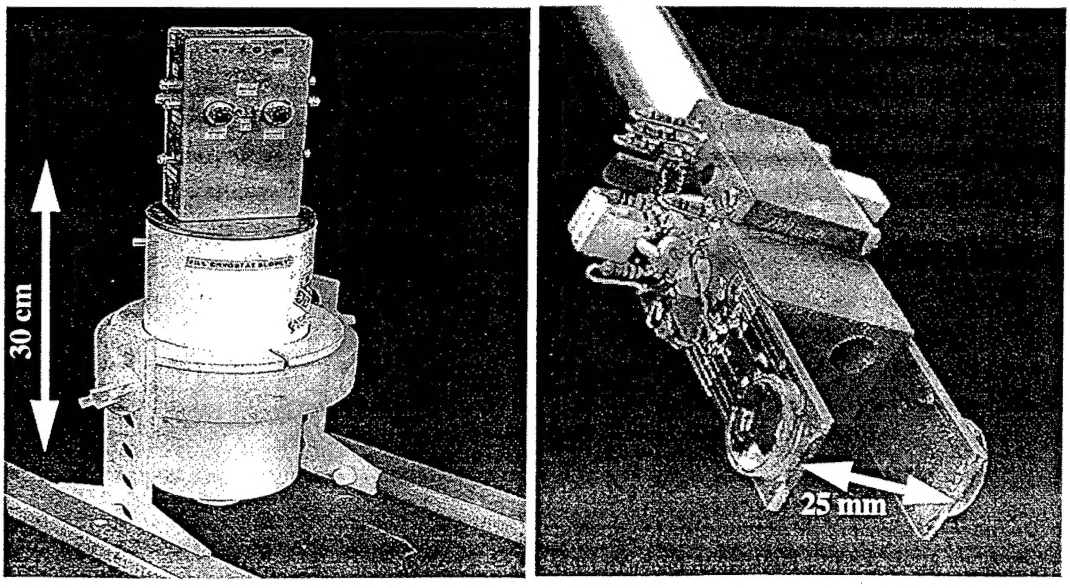

Figure 1. The complete electronic gradiometer, and the SQUID configuration.

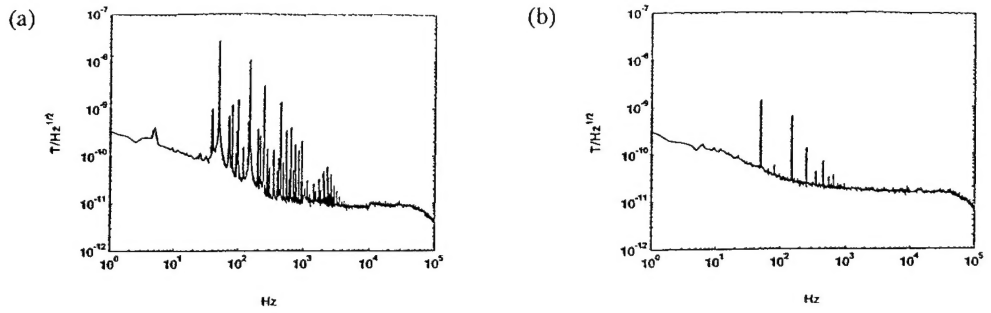

Figure 2. Noise measurements made in the open laboratory (a) single SQUID (b) electronic gradiometer.

ments of an insulating vacuum space, superinsulation and an activated charcoal getter. The cryostat's unusual characteristics are small size (diameter 150 mm, overall length 300 mm) chosen to provide a 24 hour hold time, all-Tufnol (cotton-epoxy composite) construction to obviate electromagnetic screening, and relatively small, 4 mm tail thickness.

3. Performance

We tested the system first in the Wellcome Biomagnetism Unit at the Southern General Hospital, Glasgow. This has an eddy current shielded aluminium room [5] to which an RF-shielding door has recently been added for low noise measurements. Our results showed that the white noise floor was less than 10^{-11} T/$\sqrt{\text{Hz}}$ for the two SQUIDs and slightly higher for the gradiometer. The 1/f corner frequency was 100Hz. According to a comparison with noise measurements made in mumetal shielding, most of the 1/f noise component is environmental but the white noise level is given by the SQUIDs themselves.

We repeated the measurements with the equipment in position unshielded in the NDE scanner in the Superconducting Devices Research Group laboratory at Strathclyde University, with the results shown in Figure 2. Clearly, the single SQUID is susceptible to a great deal of interference, while the gradiometer, despite its simplicity, gets rid of all but the largest peaks.

Figure 3 is an x-y scan above a >-shaped wire carrying a 14 mA, 270 Hz current. In the present apparatus, the SQUIDs are aligned vertically and measure horizontal field. We would have preferred horizontal alignment (to measure vertical fields) but reorientation would have meant either making the tail of the cryostat inconveniently large or truncating the other end of the SQUID-mounting PCBs, including cutting through tracks. Figure 3 therefore illustrates how the present 11 mm minimum lift-off gives relatively poor spatial resolution. However, it also demonstrates the stability and adequate SNR of both the single SQUID and the gradiometer in the open laboratory, even during computer-controlled, stepper-motor energised scanning.

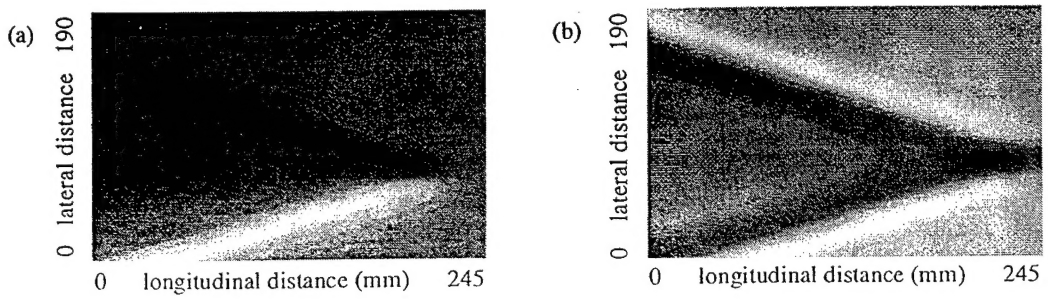

Figure 3. Maps of >-shaped current-carrying wire from (a) single SQUID (520 nT p-p) (b) electronic gradiometer (353 nT p-p). Dark areas are negative, light positive.

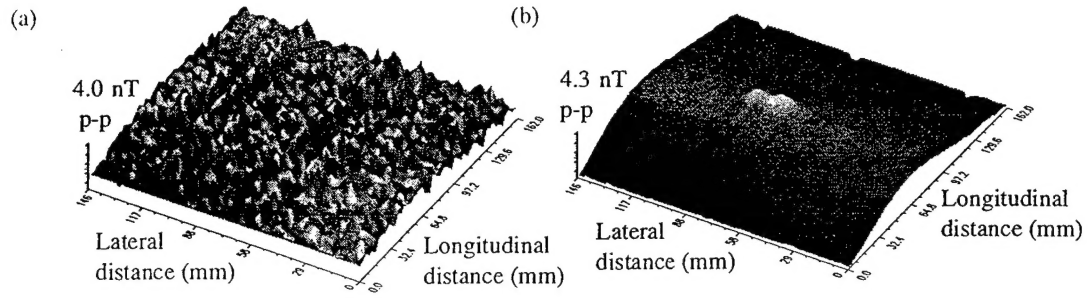

Figure 4. Eddy current maps of an aluminium plate with a single small surface slit.
(a) single SQUID and (b) electronic gradiometer.

Although the current-carrying wire illustrates the response of the system to a particular source, it gives no indication of real performance for NDE. This is dealt with in more detail elsewhere [6]. Here, we give the single example in Figure 4. This shows maps of an aluminium plate with a small slit in the surface. This slit has an arc section with a 45 mm diameter. Its maximum depth is 1.8 mm, surface length approximately 20 mm and width 150 μm. It was mapped by applying a 77 mA 2.7 kHz current to a 5 turn, 4.5 mm diameter spiral coil fabricated on epoxy glass PCB. The inner to outer connection was made by aluminium wire bonding. This coil was mounted beneath the cryostat centrally between the SQUIDs. The aluminium plate was positioned as close as possible to the coil.

Figure 4 clearly shows that spatial resolution is improved if a small, well defined source is positioned close to the specimen, no matter what the SQUID lift-off. Also apparent is that the fundamental SNR of this experiment is much lower than the one illustrated in Figure 3 and the difference in noise (i.e. interference) level between the single SQUID and gradiometer is much greater - in fact, the experiment would have failed if only a single SQUID had been used.

4. Conclusions

We have designed and built a complete two SQUID electronic gradiometer based on Conductus Mr SQUIDs and optimised for NDE. With it, we are able to exploit the fundamental performance of the SQUIDs properly for the first time in an open laboratory environment. We have demonstrated this here and elsewhere [6] with a selection of typical experimental results.

The authors acknowledge support from the US AFOSR, UK EPSRC, Oxford Instruments, The Royal Society of Edinburgh and the UK DRA.

References

[1] Wikswo J P Jnr 1995 *IEEE Trans. Appl. Superconductivity* 5 2

[2] Conductus Inc.1992 *Mr SQUID: A high T_c superconductor SQUID system for undergraduate laboratories*

[3] Cochran A, Macfarlane J C, Morgan L N C, Kuznik J, Weston R, Hao L, Bowman R M and Donaldson G B 1994 *IEEE Trans. Appl. Superconductivity* 4 3 123 - 234

[4] Cochran A, Morgan L N C, Bowman R M, Kirk K J and Donaldson G B1993 *IEEE Trans. Appl. Superconductivity* 3 1 1926-1929

[5] Bain R J P, Donaldson G B, Pegrum C M, Maas P. and Weir A I 1991 *Extended abstracts of the 8th International Conference on Biomagnetism*, Munster, Germany

[6] Cochran A, Kuznik J, Carr C, Morgan L N C and Donaldson G B *Presented at EUCAS '95.*

Presented at 2nd European Conference on Applied Superconductivity (EUCAS'95), Edinburgh, July 1995.

Experimental results in non-destructive evaluation with HTS SQUIDs

A Cochran, J Kuznik*, C Carr, L N C Morgan+ and G B Donaldson

University of Strathclyde, Department of Physics and Applied Physics, John Anderson Building, 107 Rottenrow, Glasgow, G4 0NG, UK.

* Presently visiting from Institute of Physics, Czech Academy of Sciences, Prague, Czech Republic.

+ Now with BT Laboratories, Martlesham Heath, Ipswich, Suffolk, IP5 7RZ.

Abstract. Until now, most experiments demonstrating the use of superconducting quantum interference devices (SQUIDs) for non-destructive evaluation have been based on liquid helium temperature equipment. However, experience of high temperature superconductor (HTS) SQUIDs is growing and we have recently begun to make almost routine measurements with them. Here we outline the developments in experimental apparatus which have allowed this and present some of our results, obtained in the open laboratory using a first order electronic gradiometer based on two simple bare HTS SQUIDs.

1. Introduction

We have been carrying out experiments in non-destructive evaluation (NDE) using superconducting quantum interference devices (SQUIDs) at Strathclyde University for more than ten years. Initially, we used low temperature superconductor (LTS) SQUIDs, gradiometers and cryostats similar to those in use at the time for biomagnetic measurements. However, we soon realised that the needs of NDE were quite different, and a long development process began.

Once it was known, soon after their discovery, that high temperature superconductors (HTSs) could be used for SQUIDs, efforts began to exploit them for NDE. Only simple experiments were possible with the first crude devices [1] but it was immediately clear that the convenience of liquid nitrogen cooling (LN_2) would be a vital factor in the adoption of SQUIDs by the wider NDE community.

The Conductus Mr SQUID [2] can now, arguably, be seen as a breakthrough in SQUID NDE. For the first time, an HTS SQUID was available which needed little special handling and which could be guaranteed to work through a series of experiments. However, few people considered that such a small sensor (with an effective pick-up area 70 μm square [3]) could have practical applications. Here, we demonstrate that this may not be true, at least in NDE.

2. Recent developments

For our first investigations of NDE with HTS SQUIDs, we used systems based on single SQUIDs. These showed that the sensors merited further investigation, though the results

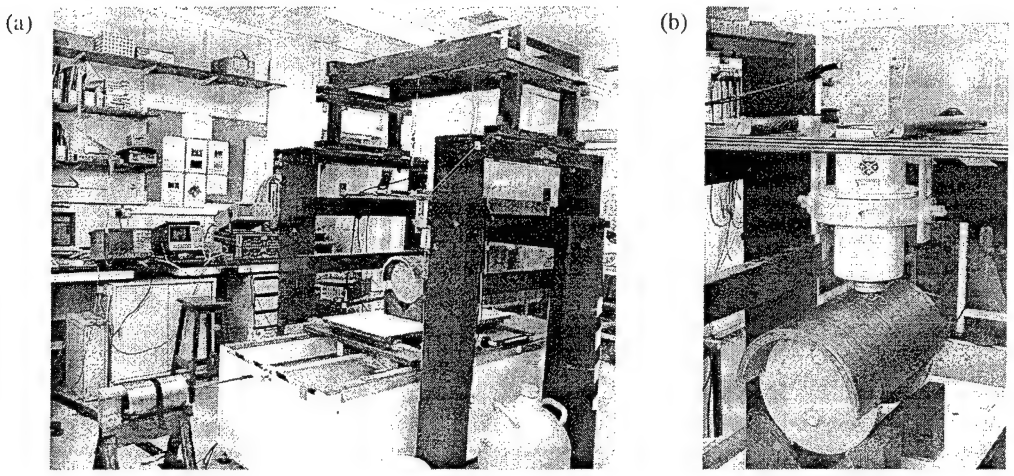

Figure 1. The NDE system in the open laboratory at Strathclyde University. (a) overall view and (b) detail showing HTS SQUID system, in this case above a section of pressure vessel

themselves, in NDE terms, were indicative only of possible future developments.

More recently, we have developed a system based on two Mr SQUIDs for simple electronic gradiometry. The other parameters of this system (described in more detail elsewhere [4]) were also optimised for NDE. They include a bandwidth of more than 30 kHz and a non-magnetic, non-conductive cryostat with a small (4 mm) LN_2 to room temperature separation.

After basic characterisation in low noise and open laboratory environments, the new gradiometer was incorporated into our existing SQUID NDE scanning, data acquisition and processing system. This has four major parts, some recently enhanced, as shown in Figure 1.

The *cryostat support gantry* is a timber frame (intended for large LTS cryostats) from which the small HTS system is suspended on two nylon arms. Precise lift-off adjustment is achieved by moving the specimen on an adjustable marble plinth.

Primary movement of the *x-y scanning bed* is longitudinal, effected by a lead screw from a shielded stepper motor and controlled via feedback from a non-magnetic shaft-encoder driven by the bed. Lateral motion is by a ratcheted rack and pinion mechanism to avoid the need for another stepper motor which, moving bodily, would act as a magnetic anomaly in its own right. Recent improvements include a choice of eight different scan patterns, one of them step and repeat which has proved crucial in the inspection of a mild steel specimen.

The stepper motor and the instrumentation for ac excitation signal generation (a two channel waveform synthesiser) and SQUID output demodulation (two EG&G 5210 dual channel lock-in amplifiers) are controlled by C++ software running on a *PC*. This also performs data acquisition, directly from the lock-ins via GPIB, or through an analogue input card.

After acquiring a complete magnetic map, it is transferred to our HP 9000/700 series *workstations* for examination and archival. Since a single scan produces at least four x-y sets of data at mm resolutions - for example quadrature ac components from one SQUID and the gradiometer - rapid processing and display is essential.

3. Experimental results

The results we present here were obtained using the three different excitation methods shown in Figure 2: direct injection of ac current, and eddy current induction using either a single turn

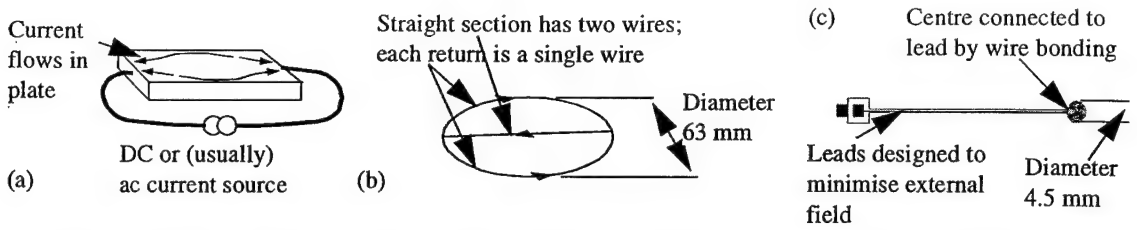

Figure 2. Excitation methods. (a) direct current injection, (b) double-D induction coil and (c) spiral coil

63 mm diameter coil with a double-D layout or a 4.5 mm diameter, 5 turn spiral coil made as a PCB with an aluminium wire bond from the centre out.

3.1. Direct injection of current

The specimen we used for this was an aluminium plate approximately 300 mm square and 13 mm thick, with a central slot 6.5 mm deep, 6 mm wide and 40 mm long. Although this is not a realistic NDE specimen, it serves to illustrate the performance of our system. Injecting a 140 mA ac signal at 530 Hz into it perpendicular to the slot gave the results shown in Figure 3.

The single SQUID result shows no indication of the slot because large signals from the current spreading out around the sides of the plate dominate and because the small signals from the slot are buried in environmental interference, itself too small to be seen on the same scale as the large signals. However, the gradiometer result clearly shows the expected peak at one end of the slot and trough at the other. There are two benefits of using a gradiometer here: the large *but distant* signals from spreading current are reduced, and interference is also reduced.

3.2. Eddy current induction with a double-D layout

For this experiment, we used the specimen described in Section 3.1, but turned over so that the slot was 6.5 mm beneath the scanned surface. In this case, although the slot is large, the 6.5 mm subsurface distance is also large in NDE terms. Note that superficially similar specimens made from separate layers [5] are electromagnetically quite different since in them current flows only around the sides of a slot whereas in our case current also flows over the slot, making the distortion more diffuse and difficult to detect.

The double-D coil of Figure 2(b) was used because field decay into the plate because of coil geometry is much slower than with a smaller coil. The ac signal in the coil was 140 mA at 270 Hz. The result from the gradiometer only is shown in Figure 4. In this case, we would expect the response to be given by two dimensional convolution of the gradiometer's spatial response, the shape of the coil (modified by lift-off), and the shape of the slot. This is indeed what appears.

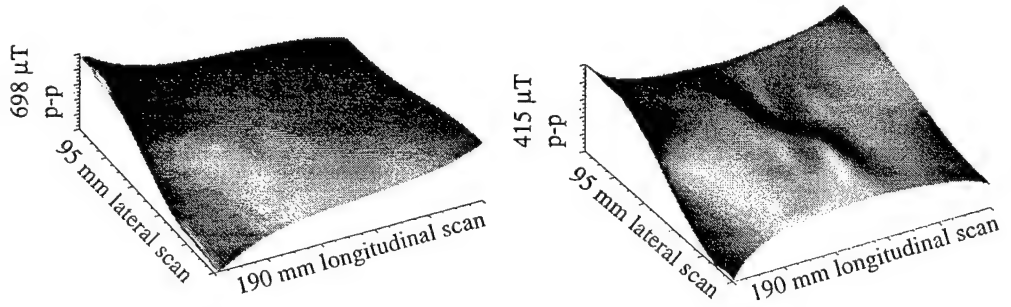

Figure 3. Directly injected current mapping. (a) single SQUID and (b) gradiometer

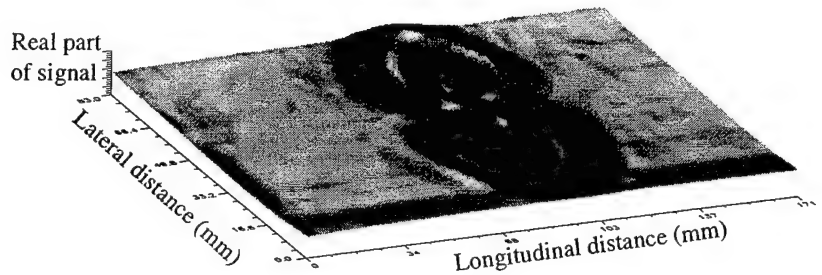

Figure 4. Eddy current mapping of a subsurface feature. The complicated response is mainly the result of the geometry of the double-D induction coil

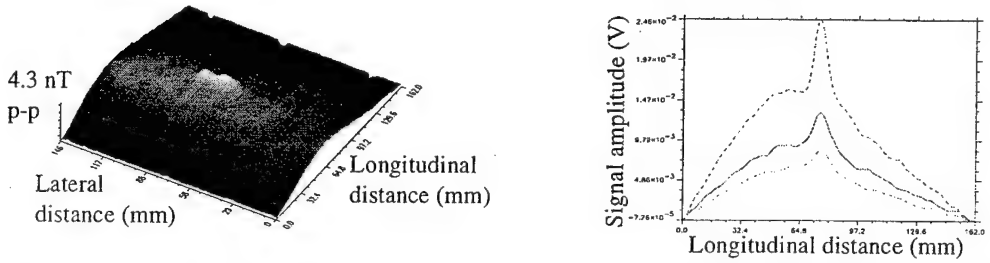

Figure 5. Eddy current mapping of a surface slit with a spiral coil. (a) Complete gradiometer result at 4.5 mm lift-off and (b) sections at lift-offs of 1.5 (upper), 3 (middle) and 4.5 mm (lower).

3.3. Eddy current induction with a small spiral coil

For our third experiment, we attached the spiral coil in Figure 2 to the cryostat and used a 47 mA 2.7 kHz ac signal. The specimen was another aluminium plate, 12.5 mm thick with a much smaller slit in its upper surface with a surface length around 20 mm, a width of 150 μm, with an arc profile 1.8 mm at its deepest and 45 mm in diameter. The results shown in Figure 5, and compared with Figure 4, clearly indicate how high spatial resolution can be achieved using a small source, even with relatively distant SQUIDs. Detection of such a small feature at lift-offs corresponding to thick layers of surface protection is noteworthy in itself for NDE.

4. Conclusions

We have demonstrated how the simplest possible HTS SQUID first order electronic gradiometer can be used as part of a well-specified SQUID NDE system working entirely without shielding to achieve results approaching the quality of those obtained with LTS systems.

The authors are supported by UK EPSRC, UK MoD/DRA, The Royal Society of Edinburgh and Oxford Instruments Ltd.

References

[1] Bowman R M, Macfarlane J C, Cochran A, Kirk K J, Pegrum C M and Donaldson G B 1993 *Supercond. Sci. Technol.* **6** 2 91 - 95

[2] Conductus Inc. 1992 *Mr SQUID: A high T_c superconductor SQUID system for undergraduate laboratories*

[3] Cochran A, Macfarlane J C, Morgan L N C, Kuznik J, Weston R, Hao L, Bowman R M and Donaldson G B 1994 *IEEE Trans. Appl. Superconductivity* **4** 3 123 - 234

[4] Kuznik J, Carr C, Cochran A, Morgan L N C and Donaldson G B *Presented at EUCAS'95*

[5] Alzayed N S, Fan C-x, Lu D F, Wong K W, Chester M and Knapp D C, 1994 *IEEE Trans. Appl. Superconductivity* **4** 2 81 - 86

To be presented at 22nd Annual Review of Progress in Quantitative NDE (QNDE'95), Seattle, August 1995. (Paper in preparation)

Advances in the Theory and Practice of SQUID NDE

A.Cochran, G.B.Donaldson, D.McA.McKirdy, M.E.Walker, U.Klein, C.Carr

Superconducting Devices Research Group, Department of Physics and Applied Physics, University of Strathclyde, Glasgow, Scotland, G4 0NG

J.Kuznik

Institute of Physics, Czech Academy of Sciences, Prague, Czech Republic.

A.McNab

Ultrasonics Research Group, University of Strathclyde, Department of Electronic and Electrical Engineering, Glasgow, Scotland, G1 1XW

Abstract We have been studying the use of the superconducting quantum interference device (SQUID) for electromagnetic nondestructive evaluation (EM NDE) for some years because it offers high sensitivity - permitting high stand-offs or very small excitation signals - and maintains this sensitivity from DC to high frequencies. However, the SQUID also has drawbacks, including the need for cryogenic temperatures and differential configurations to make measurements possible in environmental electromagnetic fields. In this paper, we describe three areas of progress. In integrated devices, the SQUID and pick-up coils are combined on a common substrate. We contrast this with wire wound pick-up coil configurations and combinations of discrete SQUIDs, both of which may suffice for NDE without a need for specialised microelectronic fabrication. Our second topic is modelling. SQUID performance is relatively easy to model macroscopically but still difficult to determine experimentally, so simulation using our own code and a commercial finite element package is particularly valuable. The final topic is practical systems design, which is allowing SQUIDs to be engineered into increasingly efficient cryogenic systems with optimised instrumentation. We present recent results to demonstrate current performance.

To be presented at International Workshop on Electromagnetic Nondestructive Evaluation (ENDE London), London, September 1995. (Paper in preparation)

Recent Progress in SQUIDs as Sensors for Electromagnetic NDE

A.Cochran, G.B.Donaldson, C.Carr, D. McA. McKirdy, M.E.Walker, U.Klein

Superconducting Devices Research Group, Department of Physics and Applied Physics, University of Strathclyde, Glasgow, Scotland, G4 0NG

A. McNab

Ultrasonics Research Group, University of Strathclyde, Department of Electronic and Electrical Engineering, Glasgow, Scotland, G1 1XW

J.Kuznik

Institute of Physics, Czech Academy of Sciences, Prague, Czech Republic.

Abstract. The properties of the superconducting quantum interference device (SQUID) makes it attractive for electromagnetic non-destructive evaluation: its potentially sub-picotesla sensitivity permits high lift-offs or very small excitation signals, and this sensitivity is maintained from megahertz frequencies down to DC, allowing thin skin and deep subsurface measurements. However, there are penalties, most importantly the need for cryogenic temperatures: although liquid helium is no longer necessary, there are still many difficulties in high temperature superconductor (HTS) SQUID fabrication which must be solved before reliable operation in liquid nitrogen is possible. In addition, the SQUID must be configured for differential detection since the small signals it detects can be swamped by environmental fields. Nevertheless, research is under way and progress is being made. Practical systems engineering is meeting cryogenic demands more efficiently and leading to refinements in instrumentation and other equipment. Essential simulation tools are being developed, based on the finite element and volume integral methods, made easier by the fact that though SQUIDs are still more difficult to work with than other sensors, they are relatively easy to simulate macroscopically. Finally, the integration of thin film SQUIDs with superconducting pick-up coils is being investigated as a way to increase signal to noise ratio, overcome packaging problems, and allow sensor arrays to be used.

Presented at International Workshop on Electromagnetic NDE (ENDE '95) London September 1995.

Recent Progress in SQUIDs as Sensors for Electromagnetic NDE

Sandy COCHRAN, Gordon B. DONALDSON, Chris CARR, David McA.McKIRDY, Morag E. WALKER and Udo KLEIN
Superconducting Devices Research Group, Department of Physics and Applied Physics, University of Strathclyde, Glasgow, Scotland. G4 0NG.

Alistair McNAB
Ultrasonics Research Group, Department of Electronic and Electrical Engineering, University of Strathclyde, Glasgow, Scotland. G1 1XW.

Jan KUZNIK
Institute of Physics, Czech Academy of Sciences, Prague, Czech Republic.

Abstract. The properties of the superconducting quantum interference device (SQUID) make it attractive for electromagnetic non-destructive evaluation: its sub-nanotesla sensitivity permits high lift-offs or very small excitation signals, and this sensitivity is maintained from megahertz frequencies down to DC, allowing thin skin and deep subsurface measurements. However, there are drawbacks, most importantly the need for cryogenic temperatures: although liquid helium is no longer necessary, there are still many difficulties to be solved in high temperature superconductor (HTS) SQUID fabrication before reliable operation in the more convenient liquid nitrogen is possible. In addition, the SQUID must be configured for differential operation otherwise the small signals it detects are swamped by environmental fields. Nevertheless, research is under way and progress is being made. Practical systems engineering is meeting cryogenic demands more efficiently and leading to refinements in instrumentation and other equipment. Essential simulation tools are being developed, based on the finite element and volume integral methods, and their results are being compared with experimental measurements. Finally, the integration of thin film SQUIDs with superconducting pick-up coils is being investigated as a way to reduce costs and increase signal to noise ratio.

1. Introduction

Since superconducting sensors are still a relatively new topic in NDE, we begin by summarising their history and properties.

1.1. Historical

Low temperature superconductor (LTS) materials superconduct at around 4.2 K (-269°C), the temperature of liquid helium (LHe), and high temperature superconductor (HTS) materials at around 77 K (-196°C), the temperature of liquid nitrogen (LN_2). Under these conditions, they have no electrical resistance and they exhibit the Meissner effect, that is, they

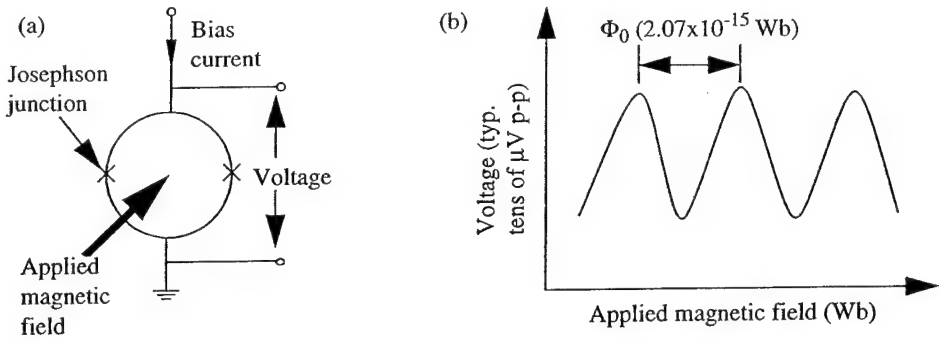

Figure 1. (a) Electrical symbol for the SQUID and (b) V-Φ characteristic.

expel all internal magnetic flux except in a thin skin called the London penetration depth. If a superconducting ring is formed, flux threading it is quantised into integer multiples of the flux quantum, $\Phi_0 = 2.07 \times 10^{-15}$ Wb, by screening currents in the ring. If this ring is interrupted by weak links, called Josephson junctions, which superconduct only up to some small critical current, a SQUID (superconducting quantum interference device) is formed [1], with the electrical symbol in Fig.1(a). This has a voltage response which is periodic in the flux quantum with a typical amplitude of a few tens of microvolts, as shown in Fig. 1(b). Connected to feedback electronics to linearise the response, it is the most sensitive detector of magnetic flux yet invented.

SQUIDs were first developed using LTS materials in the 1960s and became available commercially in the early 1970s as relatively crude niobium devices with single Josephson junctions formed by a mechanical point contact between a screw and bulk material. The reliability of this design was limited and in the early 1980s it was superseded by thin film devices fabricated with microelectronic film deposition and photolithographic patterning processes. Thin film LTS SQUIDs are now made routinely at many sites around the world.

The technology of superconducting devices was advanced in 1986 by the discovery of the HTS materials, principally $YBa_2Cu_3O_{7-\delta}$ which superconducts up to 92 K. Though this is still a low temperature in everyday terms, the ability to use LN_2-cooling led to the belief that many previously impractical applications, including NDE, would become practical. That this has not yet been justified is due more to the crystalline nature of HTS materials [2] than a mistaken estimate of the importance of the increased operating temperature.

Development of HTS SQUIDs began soon after the discovery of the materials and subsequently there has been an enormous international effort to develop a thin film device technology [3], without, as yet, conclusive results. Nevertheless, though many academic and industrial groups continue to study fabrication, simple HTS SQUIDs are readily available to researchers in fields such as NDE, from at least two commercial sources [4].

Interest in the use of SQUIDs for NDE began in the early 1980s as a result of the demands of two applications of static field magnetic sensing at very high lift-offs: detection of buried steel pipelines [5] and detection of gross flaws in subsea steel structures [6]. In neither case has any commercial potential been realised, mainly because the early LHe systems would have been too expensive to engineer to a practical level and HTS SQUIDs are not yet a satisfactory substitute for static field sensing. However, the interest in SQUID NDE at the time of the discovery of HTS materials allowed the higher profile of superconductivity as a whole to be turned into real support, the results of which are now becoming apparent.

In the remainder of this paper we discuss three topics which can be assigned approximately to the past, the present and the future. After several years of scientific development, systems design has reached the point at which engineering input is more important than exploration of fundamental configurations [7]. With the existence of several

established systems comes the need to verify simulation techniques [8] and to explore data processing, including inversion [9]. Finally, there are as yet untested SQUID sensor designs which may provide better performance: here we consider the case in which the SQUID is integrated with a thin film pick-up coil on a monolithic substrate [10].

1.2. Technical

Consider two devices which illustrate the important characteristics of the SQUID for NDE. Both are DC SQUIDs, with two Josephson junctions and a square washer loop outline. The first is an LTS device made at Strathclyde University [11]. Its sensitivity is approximately 20 fT/√Hz, and its bandwidth with standard electronics, is from DC to about 10 kHz. The second is a simple commercial HTS SQUID [12]. It is smaller, with a sensing area approximately 70 μm square and a sensitivity of approximately 20 pT/√Hz. With custom built electronics, its bandwidth is from DC to 33 kHz.

It is clear that in comparison with, for example, a typical laboratory mains field of 200 nT p-p at 50 Hz, SQUID sensitivities are so high that special techniques are needed to reduce the effects of environmental interference. (We have made NDE-type measurements without these [13]; the results were poor compared with those presented here.) The behaviour of other non-resonant sensors is worth mentioning here. In general, Hall-effect devices have much poorer sensitivity and slightly larger sensing areas though their bandwidth may be higher. Fluxgate magnetometers are more sensitive than Hall-effect devices but their bandwidths are smaller and sensing areas much larger.

There are four techniques which allow the sensitivity of the SQUID to be exploited. The most obvious is to make measurements in a magnetically shielded environment [14]. This can be impractical because of the cost (measured in tens of thousands of dollars) and limited size (a few cubic metres or less) of the shielding, though its adoption in an installation similar to those used for radiographic testing is not inconceivable.

The other three techniques, illustrated in Fig. 2, relate to the sensor configuration.

Fig. 2(a) shows the configuration of almost all LTS SQUIDs in the past, including many in NDE systems [14 - 16]. The SQUID is surrounded by a superconducting cylinder to shield it from all environmental fields. To couple the signal to it, a coil is placed inside the shield, connected by screw terminals to an external wire-wound pick-up coil, counterwound for example as in Fig. 2(a), so that it is sensitive to (the spatial gradients of) fields generated by nearby, signal sources and insensitive to (uniform) fields from distant, interference

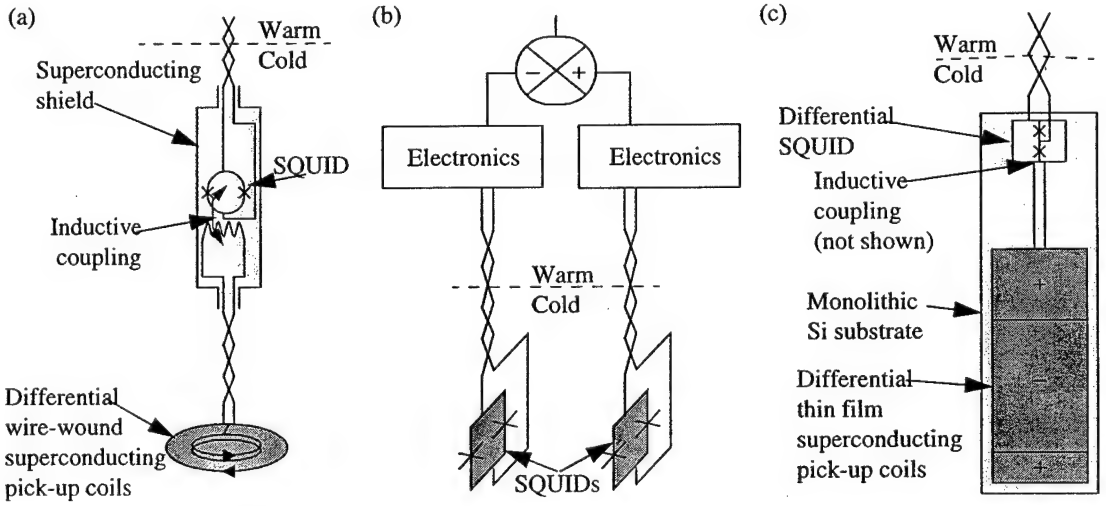

Figure 2. Three practical SQUID configurations. In each case, the sensing area is indicated by dark shading.

sources. This is called gradiometry. Pick-up coils for SQUID NDE are typically 1 to 5 mm in diameter. Since they, the screw terminals and the coupling coil in the shield all superconduct, static and ac fields are sensed. The critical component is the fine gauge superconducting wire for the pick-up coils. LTS wire is readily available, for example in niobium, but fine gauge HTS wire has not yet been developed and there is little prospect of this in the foreseeable future. This restricts the wire-wound configuration to LHe systems which find little acceptance outside superconductivity laboratories.

Fig. 2(b) shows the configuration under most active development, called electronic gradiometry. Two bare SQUIDs are exposed to magnetic fields comprising interference and signals, and the difference between their outputs is recorded. As before, this relies on distant interference sources generating the same field at the two SQUID positions while nearby signal sources generate different fields. The critical components here are the electronics which must track both broadband, large amplitude interference and typically narrowband, small amplitude signals in their entirety for each channel. At least three experimental electronic gradiometry systems have been developed and two are being applied to NDE [18, 19]. We describe ours in Section 2.1.

Fig. 2(c) shows a third configuration which may, in future, overcome both the lack of fine gauge HTS wire and the need for sophisticated electronics. In it, the gradiometric operation is hard-wired as in Fig. 2(a) but in thin film form realisable in either LTS or HTS materials. Since the SQUID is unshielded, it is itself configured as a small gradiometer to make it insensitive to environmental interference. The planar pick-up coils are multilayer superconductor-insulator-superconductor (SIS) structures tightly inductively coupled to the SQUID. The critical parts here are the SQUID and pick-up coil designs; we discuss these in Section 4.

2. An HTS Electronic Gradiometer

We have recently developed a simple HTS electronic gradiometer specifically for NDE, as shown in Fig. 3, and we have made several measurements with it.

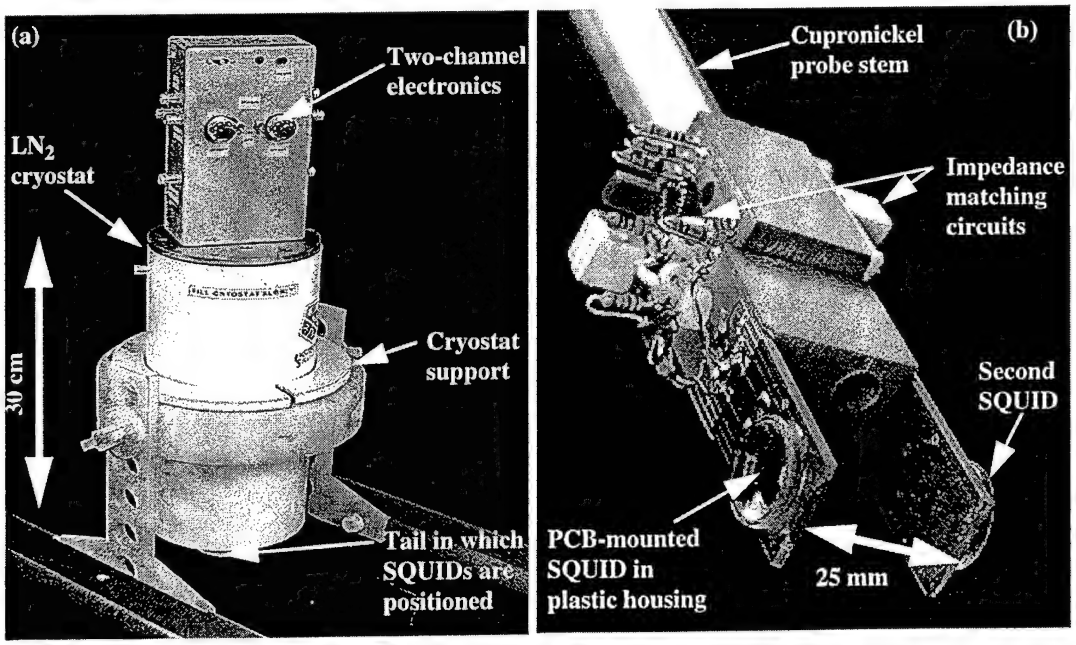

Figure 3. (a) The complete electronic gradiometer, and (b) the SQUID configuration.

2.1. Equipment

Since 1990, a great deal of optimisation of cryostats for SQUID NDE has taken place to avoid the use of copper and aluminium as structural and thermal shielding materials (these are acceptable for static but not ac measurements) and to overcome the fact that most cryostats are designed to remain cold for a given time rather than for easy handling. Several attempts have also been made to increase spatial resolution by minimising the distance from the cold SQUID sensor to the room temperature specimen. A distance of about 1 mm [16] is now possible; ingenious solutions may reduce this further, but 4 mm is a realistic figure for less extreme designs. In any case, it was recently realised that minimising this distance is useful only if the excitation source is in the specimen, for example for directly injected or corrosion current mapping [15,20], or must be far from the specimen, as in the case of a superconducting magnet for static field polarisation [21]. If, instead, a small external source such as an induction coil is placed between the cryostat and the specimen, the distance from the sensor to the specimen affects only signal amplitude; given the sensitivity of the SQUID, this is generally more than adequate anyway.

Taking these factors into account, we built the cryostat shown in Fig. 3(a) with bonded inner and outer cotton-epoxy composite skins separated by a vacuum space and aluminised mylar (superinsulation). The SQUIDs are positioned in the tail which is 4 mm thick in total, including a vacuum gap. The overall length of the cryostat is 333 mm, its diameter is 150 mm and it holds 1.5 l of LN_2 which lasts at least 24 hours. It must be used upright.

There are few precedents to aid the design of an electronic gradiometer for NDE but constructional constraints are common. In our case, the commercial SQUIDs [12] are PCB-mounted in plastic housings making horizontal positioning difficult. We therefore positioned them vertically, to measure horizontal fields B_x or B_y depending on cryostat orientation. The probe spring-loads the SQUIDs downwards to keep them 11 mm from the base of the cryostat to improve the accuracy of modelling and data processing. We chose a horizontal separation of 25 mm as shown in Fig. 3(b).

SQUID electronics usually comprise a probe head, housing a preamplifier, and a bench unit with front panel controls and a display, to provide a flexible laboratory instrument. Because our design was specifically for NDE, we were able to build complete two-channel electronics and a differencing stage into the probe-head box. This means that once the system is set up, connection to it is through one coaxial signal cable and one DC power cable. The specification is given in Table 1.

In use, the complete system is hung from a wooden frame above a heavy duty, computer controlled, magnetically quiet, x-y scanning system in an unshielded laboratory [13]. The scanner has a maximum load of 100 kg and sub-mm positioning accuracy. We usually limit scan speeds to 10 mm/sec because of its partly nylon construction, and all our measurements have been made with the specimen moving beneath the stationary cryostat.

Table 1. NDE Electronic Gradiometer Specification

SQUIDs	2 x Conductus HTS "Mr SQUID"
Sensing area (each SQUID)	70 x 70 μm
SQUID separation	25 mm
Bandwidth	DC to 33 kHz
Noise level	10 pT/√Hz at 1 kHz
Voltage response	3 V/μT
Signal outputs	Chan. 1, Chan. 2, Chan.1 - Chan.2

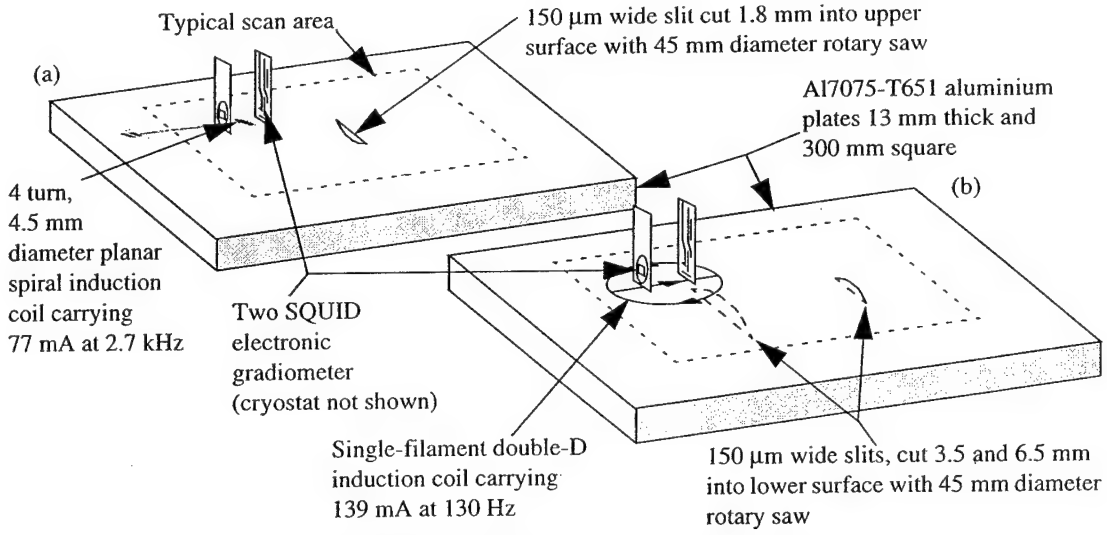

Figure 4. Specimens and techniques used to detect features in them: (a) surface slit and (b) subsurface slits.

2.2. *Results*

We have tested aluminium and steel specimens, detecting flaws ranging from milled slots several millimetres wide to real fatigue cracks. We have used both directly injected and eddy current excitation techniques. Here, we present eddy current results for narrow arc-section slits representing developing cracks, as shown in Fig. 4.

First consider Fig. 4(a), showing a specimen with a small surface slit and a 4.5 mm diameter 4 turn planar induction coil. Results from an x-y scan with a coil stand-off of 3 mm (giving a SQUID stand-off of 14 mm) are shown in Fig. 5. In this case, we recorded signals from both the gradiometer and one of the SQUIDs. Fig 5(b) shows that the gradiometer is much less susceptible to interference than the single SQUID: in fact, there is no indication of the slit in Fig. 5(a). Using the gradiometer, noise is reduced by typically 20 to 30 dB.

We repeated the measurement with two other coil stand-offs, 1.5 and 4.5 mm. Fig. 6 shows longitudinal sections through each result. Clearly the slit can still be detected even at 4.5 mm, indicating the possibility of inspection through non-conductive surface layers.

The specimen in Fig. 4(b) is considerably more difficult to inspect successfully. The depth of the slits beneath the surface prevents the use of the 4.5 mm diameter planar coil because its magnetic dipole-like field decay with distance, combined with the screening effects of the aluminium, make the signal too small. Instead, we used the single filament 63 mm diameter double-D coil shown in Fig. 4(b). The field from this suffers less free-space attenuation over a distance of a few millimetres and the geometry of the coil makes it possible to adjust its

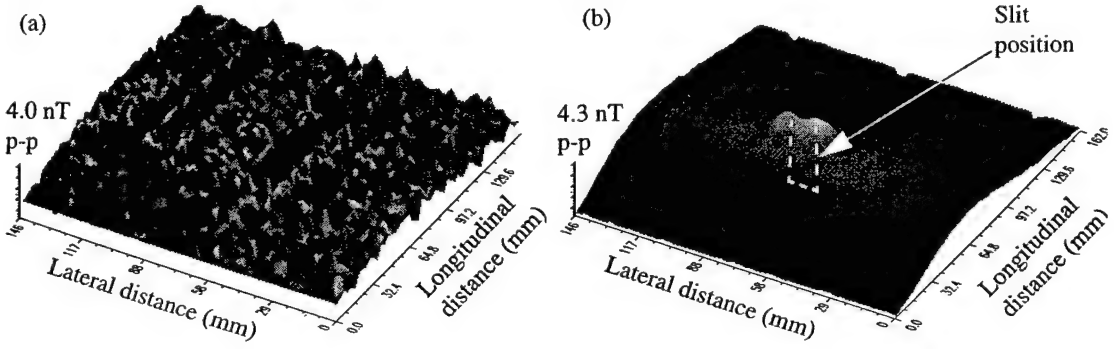

Figure 5. Eddy current images of a small surface slit: (a) single SQUID and (b) electronic gradiometer.

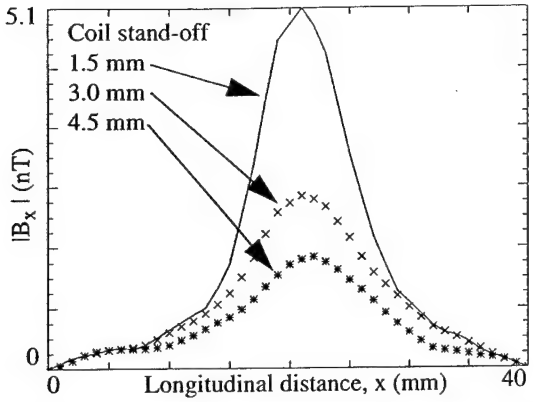

Figure 6. Surface slit responses at different stand-offs.

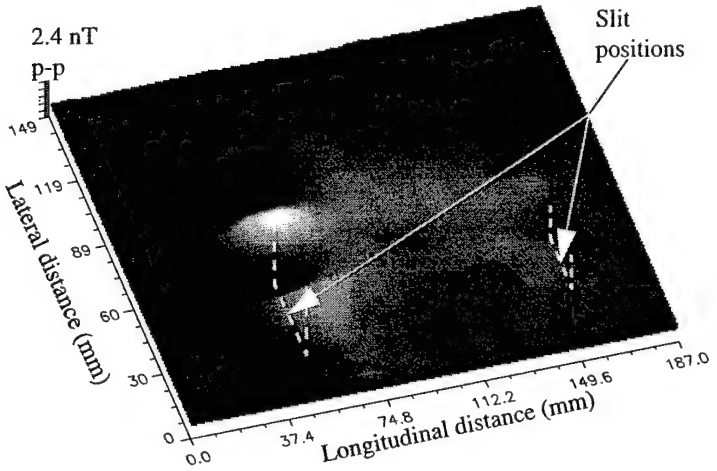

Figure 7. Eddy current image of two slits, 6.5 and 9.5 mm below the surface of an aluminium plate.

orientation so that the SQUIDs sense only a fraction of the unperturbed excitation field. The result is shown in Fig. 7. Signal to noise ratio (SNR) is poorer than for the surface slit, and the geometry of the double-D makes the response more complicated. However, it is predictable [8] and the deep slit has been detected successfully as a pair of peaks and troughs.

The other slit is almost invisible, clearly indicating a limit of our particular system. However, this is not a fundamental limitation of the SQUID as a sensor: other results [18] show that admittedly larger features can be detected through as much as 36 mm of aluminium. Our system could be improved by introducing a second mechanical adjustment as well as double-D coil orientation so that the two SQUIDs detect even less of the excitation field. This would allow the amplitude of the field to be increased, increasing SNR and therefore sensitivity to signals from smaller or deeper features.

3. Modelling and simulation

Our electronic gradiometer design was dictated more by practical constraints than theoretical optimisation. Nevertheless, models of SQUID NDE are important for three reasons. Firstly, experience of equipment construction is making it increasingly easy to transform theoretical designs into practical systems. Secondly, with care it is possible to define the parameters of experimental measurements very accurately to make them a useful source of data to verify modelling techniques. Thirdly, this accuracy of definition should permit automatic processing, for example to obtain crack dimensions from a map of magnetic field [9].

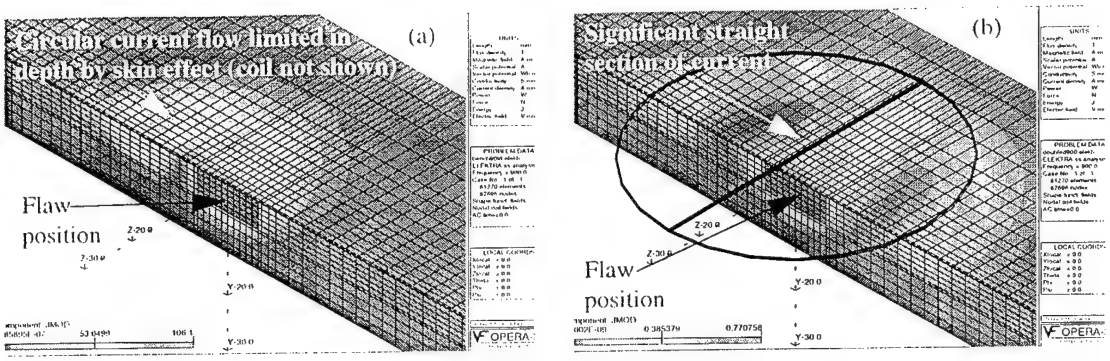

Figure 8. FEM simulation of a specimen containing a rectangular flaw 12.6 mm long, 5 mm deep and 0.28 mm wide: (a) the current flow induced in it by a circular coil and (b) by the double-D coil shown.

We use three modelling techniques: the finite element method (FEM), the volume integral method (VIM), and numerical calculation of responses to elementary sources. In each case, we assume that a small SQUID or filamentary pick-up coil has no effect on the field it is sensing. The SQUID acts as an almost ideal point sensor so there is no need for it to appear explicitly in the model and the pick-up coil can be included by simple spatial integration. This has been verified by comparison of several theoretical and experimental results.

3.1. The Finite Element Method

To explore the FEM, we identified Vector Fields OPERA and ELEKTRA [22] as the most appropriate package and we have used it to solve various problems, including benchmarks. Our experience has highlighted several practical issues.

For the scale of problem typical of SQUID NDE, meshes comprise around 80,000 nodes. We solve them on a Hewlett Packard 9000-715/100 workstation with 160 MB memory and 5 GB disk. For a single flaw and source position, the calculation time is several hours and several hundred megabytes of disk space are needed. Given these onerous overheads, we have so far limited our studies to the effects of different coil geometries, observed via current flow amplitudes in the specimen, as illustrated in Fig. 8. We have also investigated different operating frequencies, run as sub-cases to speed up the process, obtaining results corresponding well with experimental measurements [23]. However, at present the overheads of three dimensional FEM make simulation of even unidimensional scanning impractical, and we must instead turn to a faster but less general technique for this.

3.2. The Volume Integral Method

A basic expression of the VIM for eddy current testing is [24]:

$$\boldsymbol{E}(\boldsymbol{r}) - (\sigma_f - \sigma_s)\int_{V'} (\boldsymbol{G}(\boldsymbol{r},\boldsymbol{r}') \cdot \boldsymbol{E}(\boldsymbol{r}'))dV' = \boldsymbol{E}^0(\boldsymbol{r}) \qquad (1)$$

where $\boldsymbol{E}(\boldsymbol{r})$ is the total electric field; σ_f and σ_s are the flaw and specimen conductivities respectively; $\boldsymbol{G}(\boldsymbol{r},\boldsymbol{r}')$ is the Green's tensor appropriate to an unflawed specimen; V' is the volume occupied by the flaw; and $\boldsymbol{E}^0(\boldsymbol{r})$ is the electric field induced in an unflawed specimen by the induction coil. $\boldsymbol{r} = (x,y,z)$ and $\boldsymbol{r}' = (x',y',z')$ are the observer and source coordinate vectors. The electric field, $\boldsymbol{E}(\boldsymbol{r})$, is then transformed into magnetic field, using [9]

$$B_x(\boldsymbol{r}) = \left(\frac{\sigma_s - \sigma_f}{i\omega m_x^0}\right)\int_V (\boldsymbol{E}(\boldsymbol{r}) \cdot \boldsymbol{E}^0(\boldsymbol{r}))dV \qquad (2)$$

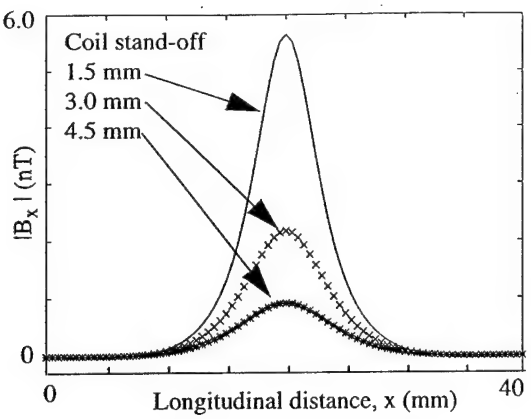

Figure 9. Theoretical surface slit responses at different stand-offs (cf. Fig. 6).

where $\omega = 2\pi f$, f is the excitation frequency; m_x^0 is the magnetic moment of an x-oriented sense coil (since reciprocity is used); and $\boldsymbol{E}^0(\boldsymbol{r})$ is again the electric field induced in the unflawed specimen, but now by the sense coil.

A crucial advantage of the VIM is that the problem is solved only in the volume of the flaw, rather than in the entire specimen. This makes it faster than the FEM, by as much as three orders of magnitude in our work. The disadvantage is that the information provided by it is more limited, as are possible specimen geometries and material parameters.

Fig. 9 is an illustration of the VIM, used to simulate the results in Fig. 6. The reasonable agreement in terms of amplitude is important because it allows estimation of minimum detectable flaw dimensions from simulation and knowledge of SQUID sensitivity and interference levels. However, the VIM results underestimate the width of the responses by about 25%. We intend to make further experimental measurements to identify the reasons for this.

3.3. Elementary Source Modelling

Our third simulation technique is numerical calculation of responses to elementary sources such as the magnetic dipole, the infinite current-carrying wire and the current dipole. The current dipole is, of course, the most general of these but the other two are also useful because special numerical solutions are available and corresponding experimental sources are easy to set up. In the next section we illustrate elementary source modelling in the development of integrated sensors.

4. Integrated sensors

In Section 2.1 we described integration of a SQUID and pick-up coils into a single sensor. Here we outline a practical implementation and its advantages and disadvantages for NDE.

4.1. Implementation

Integrated devices are fabricated in a similar way to conventional integrated circuits, using clean room conditions to deposit high quality thin films on a silicon wafer. In our work, these are principally superconducting niobium and insulating silicon dioxide. They are patterned photolithographically to define the SQUID and its Josephson junctions, a planar coil coupling it to the pick-up coils, and the pick-up coils themselves. Layer thicknesses are typically a few hundred nanometres or less and feature sizes vary from about 5 μm to 1 mm.

Fig. 10 is a composite view of a photolithography mask set for devices we are

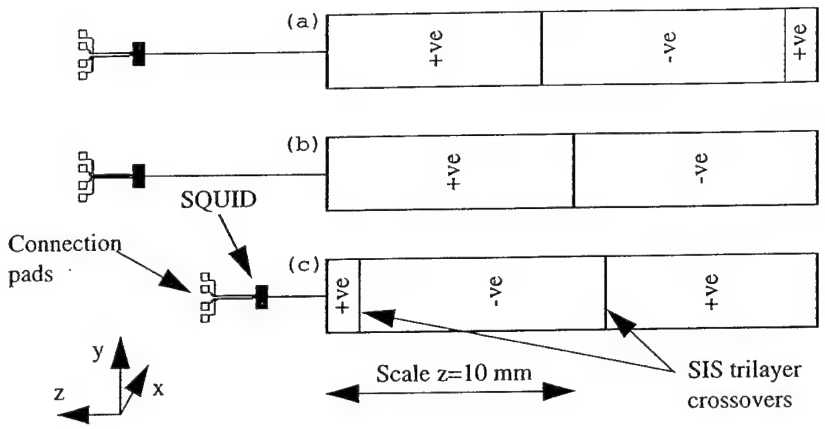

Figure 10. Mask design for planar first order gradiometers (a) and (c) asymmetric and (b) symmetric.

developing [10]. The connection pads are gold plated to bond to a printed circuit board using ultrasonic wire bonding. The SQUID is a double washer design [11] which acts as a very small gradiometer (its outer dimensions are 420 x 960 μm), so that it is unperturbed by most environmental fields. It is connected to the pick-up coils by 15 μm wide tracks in an SIS trilayer arrangement to reduce external coupling to them. The pick-up coils have 20 x 3 mm rectangular single layer outlines connected side to side by SIS trilayer crossovers.

There are three layouts in Fig. 10. Fig. 10(b) is a conventional first-order symmetric gradiometer - that is, the layout is symmetrical about its midpoint, it rejects uniform fields and senses first-order field gradients, dB_x/dz, and higher. Its spatial response is also symmetrical about its midpoint, with an intrinsic 1/z far-field characteristic. Figs. 10(a) and (c) are first-order singly asymmetric designs [19]. It is possible to add any number of crossovers to a gradiometer, at chosen positions within a given range, to make it asymmetric. The original field rejection order is maintained by calculating the position of the other crossovers accordingly [25]. In Figs. 10(a) and (c), uniform fields are rejected as before, but in each case the single additional crossover changes the spatial response to higher order field gradients very significantly, so that beyond the end nearest the additional crossover it exhibits a zero-crossing and local amplitude maximum.

The theoretical responses of the symmetric and asymmetric gradiometers to an on-axis magnetic dipole, M_x, are shown in Fig. 11. The symmetric design is more sensitive at practical stand-offs in the 1 to 20 mm range, but the response of the asymmetric design can also be exploited in two ways. If the gradiometer is oriented as in Fig. 10(a), the response to a magnetic dipole representing a specimen approximately 6 mm beneath it will be enhanced relative to the response to sources at other distances. If, on the other hand, the gradiometer is

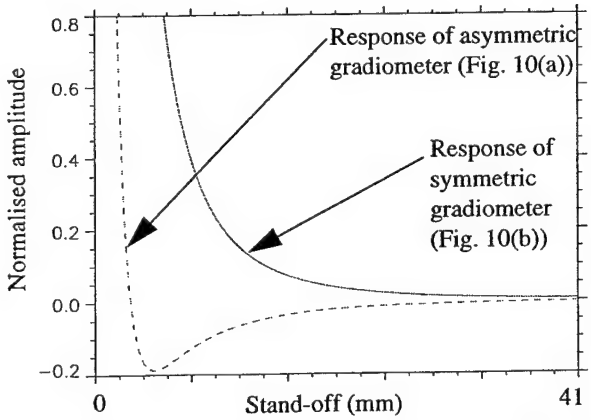

Figure 11. Simulated responses of symmetric and asymmetric gradiometers to an on-axis magnetic dipole

inverted as in Fig. 10(c), the specimen response will be similar to that of the symmetric design, but the magnetic dipole-like anomaly formed by the SQUID can be placed at the zero crossing so that it does not distort the gradiometer response and imbalance is avoided.

4.2. Advantages and Disadvantages

The principal advantages of the integrated device come from its manufacturing process. To make measurements in hostile environments, electronic gradiometers will always need better instrumentation than hard-wired designs, particularly in terms of bandwidth, and both they [18] and wire-wound pick-up coils [21] usually need precise low temperature mechanisms to reduce gradiometer imbalance. These arrangements can be expensive. In contrast, integrated devices are intrinsically well balanced and neither the superconducting shield used with wire-wound pick-up coils nor the multiple devices for electronic gradiometry are needed. Furthermore, once a fabrication process is established it is straightforward to design mask sets and still easier to fabricate many devices with them. Since these are solid state, they are robust and reliable, and their small size and light weight make them ideal for NDE, in which thermal cooling capacity is strongly related to inconvenience and cost.

Integrated devices also have disadvantages. The planar configuration limits the field components which can be measured; measuring fields normal to the surface of a specimen is more difficult than measuring parallel fields. More importantly, it is expensive to maintain a fabrication process even in well established LTS technology and multilayer HTS processes are still far from reliable [2]. The integrated approach therefore presupposes either a large and as yet non-existent market for the sensors [26] or a few critical applications in NDE or other fields such as biomedical imaging to bear the development and maintenance costs.

5. Conclusions

Progress is being made in several areas of SQUID NDE research. In the past, our work was based principally on LTS systems with wire-wound pick-up coils and magnetically shielded SQUIDs [15, 21]. More recently, we have developed an electronic gradiometer using HTS SQUIDs [7] which we have demonstrated on a number of specimens, presenting results here and elsewhere [17]. It is important to realise that the performance of this system is hardly superior to that of previous LTS ones, but that it is a much more practical tool.

The success of HTS measurements has led to an increased need for and interest in modelling. We are using the FEM [22], the VIM [24] and our own code for this and comparison of experimental and simulated results has begun. In the longer term, we anticipate combining the benefits of HTS and hard-wired gradiometers in the integrated devices we are presently designing and prototyping using LTS technology [11].

Acknowledgements

The authors are supported by the UK EPSRC and MoD, BP/The Royal Society of Edinburgh, Oxford Instruments Ltd., Quantum Magnetics, and the US AFOSR.

References

1. J.Clarke, SQUIDs: Theory and Practice. In: H.Weinstock and R.Ralston (Eds.), The New Superconducting Electronics, Kluwer Academic Publishers, Dordrecht (1993) 123 - 180.

2. A.Braginski, Thin Film Structure. In: H.Weinstock and R.Ralston (Eds.), The New Superconducting Electronics, Kluwer Academic Publishers, Dordrecht (1993) 89 - 122.
3. For example, at the last Applied Superconductivity Conference (ASC'94, Boston, October 1994), there were 140 papers from 110 research groups on subjects directly related to HTS SQUIDs and enabling technologies.
4. Conductus Inc., 969 West Maude Ave., Sunnyvale, CA 94086, USA; FIT, Postfach 1147, D-31158 Bad Salzdetfurth, Germany.
5. H.Weinstock and M.Nisenoff, Nondestructive Evaluation of Metallic Structures Using a SQUID Gradiometer. In H.D.Hahlbohm and H.Lubbig (Eds.), SQUID'85, de Gruyter, Berlin (1985) 853 - 858.
6. R.J.P.Bain, G.B.Donaldson, S.Evanson and G.Hayward, SQUID Gradiometric Detection of Flaws in Ferromagnetic Structures. In: H.D.Hahlbohm and H.Lubbig (Eds.), SQUID'85, de Gruyter, Berlin (1985) 841 - 846
7. For example, J.Kuznik, C.Carr, A.Cochran, L.N.C.Morgan and G.B.Donaldson, First Order Electronic Gradiometry with Simple HTS SQUIDs and Optimised Electronics, to be published in *Proc. 2nd Eur. Conf. on Appl. Supercond.*, IoP Conf. Proc. Series (1995).
8. D.McA.McKirdy, A.Cochran, A.McNab and G.B.Donaldson, Using SQUIDs to Solve Some Current Problems in Eddy Current Testing, to be published in *Proc. 2nd Eur. Conf. on Appl. Supercond.*, IoP Conf. Proc. Series (1995).
9. D.McA.McKirdy, A.Cochran, A.McNab and G.B.Donaldson, Theoretical Consideration of Fatigue Crack Detection and Characterisation Using SQUID Sensors, *these Proceedings*.
10. U.Klein, M.E.Walker, A.Cochran, D.Hutson, R.G.Weston and C.M.Pegrum, Simulation and Experimental Characterisation of Planar Asymmetric SQUID Gradiometers, *Proc. 5th Int. Superconductive Electronics Conf.*, Nagoya (1995).
11. G.Lang et al., Performance of a Second Order Integrated Planar Gradiometer in the Earth's Field, to be published in *Proc. 2nd Eur. Conf. on Appl. Supercond.*, IoP Conf. Proc. Series, (1995).
12. Conductus Inc., Mr SQUID: a High T_c Superconductor SQUID System for Undergraduate Laboratories, User Manual (1992).
13. A.Cochran, J.C.Macfarlane, L.N.C.Morgan, J.Kuznik, R.Weston, L.Hao, R.M.Bowman and G.B.Donaldson, Using a 77 K SQUID to Measure Magnetic Fields for NDE, *IEEE Trans. Appl. Supercond.*, **4** (1994) 128 - 135.
14. J.P.Wikswo Jr., J.M.van Egeraat, Y.P.Ma, N.G.Sepulveda, D.J.Staton, S.Tan and R.S.Wijesinghe, Instrumentation and Techniques for High Resolution Magnetic Imaging. In: A.F.Gmitro, P.S.Idell and I.J.LaHaie (Eds.), Digital Image Synethesis and Inverse Optics, SPIE Proc. **1351** (1990) 438 - 471.
15. A. Cochran,G. B. Donaldson, L. N. C. Morgan, R. M. Bowman and K. J. Kirk, SQUIDs for NDT: the Technology and its Capabilities, *Brit. J. NDT* **35** (1993) 173 - 182.
16. A.D.Hibbs, R.E.Sager, D.W.Cox, T.H.Aukerman, T.A.Sage and R.S.Landis, A High Resolution Magnetic Imaging System based on a SQUID Magnetometer, *Rev. Sci. Inst.* **63** (1992) 3652 - 3658.
17. A.Cochran, J.Kuznik, C.Carr, L.N.C.Morgan and G.B.Donaldson, Experimental Results in Non-destructive Evaluation with HTS SQUIDs, to be published in *Proc. 2nd Eur. Conf. on Appl. Supercond.*, IoP Conf. Proc. Series (1995).
18. Y.Tavrin, H.-J. Krause, W.Wolf, V.Glyantsev, J.Schubert, W.Zander and H.Bousack, Eddy Current Technique with High Temperature SQUID for Nondestructive Evaluation of Nonmagnetic Metallic Structures, accepted for publication in *Cryogenics* (1995).
19. G.B.Donaldson, C.M.Pegrum and R.J.P.Bain, Integrated Thin Film SQUID Instruments. In: H.D.Hahlbohm and H.Lubbig (Eds.), SQUID'85, de Gruyter, Berlin (1985) 729 - 759.
20. A.D.Hibbs, R.Chung and J.S.Pence, Corrosion Current Measurements with a High Resolution Scanning Magnetometer. In: D.O.Thompson and D.E.Chimenti (Eds.) Review of Progress in Quantitative NDE, vol. 13A, Plenum Press, New York (1993) 1955 - 1962.
21. A.Cochran, G.B.Donaldson, S.Evanson and R.J.P.Bain, First Generation SQUID-based Non-destructive Testing System, *IEE Proc. A* **140** (1993) 113 - 120.
22. Vector Fields Ltd., OPERA and ELEKTRA FEM Software, Kidlington, Oxford, OX5 1JE, UK.
23. L.N.C.Morgan, C.Carr, A.Cochran, D.McA.McKirdy and G.B.Donaldson, Electromagnetic Nondestructive Evaluation with Simple HTS SQUIDs: Measurements and Modelling, *IEEE Trans. Appl. Supercond.* **5** (1995) 3127 - 3130.
24. D. McA. McKirdy, Recent Improvements to the Application of the Volume Integral Method of Eddy Current Modelling, *J. Nondestr. Eval.* **8** 1 (1986) 45 - 52.
25. A.E.Jones and R.J.P.Bain, A Generalisation of Planar Magnetic Gradiometer Design via Orthogonal Polynomials, *J. Computational Phys.* **118** (1995) 191 - 197.
26. M.G.Silk, T.E.Dixon and D.J.MacKeith, Review of Opportunities for Advanced Sensors in Non-destructive Testing, *Insight* **36** (1994) 256 - 263.

Presented at Review of Progress in Quantitative NDE (QNDE'95) Seattle, August 1995.

ADVANCES IN THE THEORY AND PRACTICE OF SQUID NDE

A.Cochran, G.B.Donaldson, C.Carr, D.McA.McKirdy, M.E.Walker, U.Klein
Superconducting Devices Research Group
Department of Physics and Applied Physics
University of Strathclyde
Glasgow, Scotland, G4 0NG

J.Kuznik
Institute of Physics
Czech Academy of Sciences
Prague, Czech Republic

A. McNab
Ultrasonics Research Group
Department of Electronic and Electrical Engineering
University of Strathclyde
Glasgow, Scotland, G1 1XW

INTRODUCTION

The superconducting quantum interference device (SQUID) holds great promise for electromagnetic nondestructive evaluation (NDE) because it offers high sensitivity - permitting high lift-offs or very small excitation signals - and maintains this sensitivity from DC to high frequencies [1]. In eddy current NDE, this allows an induction coil to comprise only a few turns, or even a single filament, without a high permeability core, and makes forward modelling and inverse processing easier, since the induction source is well defined and the SQUID itself closely approximates an ideal sensor. However, the SQUID also has practical drawbacks, including the need for cryogenic temperatures and for differential configurations for measurements in environmental fields. Until very recently, almost all SQUID NDE systems were based on low temperature superconductors (LTSs), but the first measurements with high temperature superconductor (HTS) SQUIDs are now being reported [2 - 4].

In this paper, we describe our recent progress in three areas. We compare and contrast devices in which the SQUID and pick-up coils are integrated on a monolithic substrate [5] with the use of wire wound pick-up coils and magnetically shielded SQUIDs [6] and with arrangements of discrete SQUIDs combined electronically [7]. Our second topic is modelling. Although experimental systems are becoming more user-friendly, some aspects of SQUID NDE are still easier to study by macroscopic modelling. For this we use the finite element method, the volume integral method and our own code based on numerical calculation of

responses to elementary sources [8]. Finally, we deal with the ways SQUIDs are being engineered into increasingly efficient cryogenic systems with optimised instrumentation. We describe our most recent system and present results to demonstrate its performance [9].

PRACTICAL SQUID CONFIGURATIONS

Apart from the very expensive provision of a magnetically shielded environment, three techniques, outlined in Figure 1, are used to allow the SQUID's sub-nanotesla sensitivity to be exploited in environments where electromagnetic interference can be many hundreds of nanotesla or more.

Figure 1(a) illustrates how almost all LTS SQUIDs were configured in the past, including in NDE. A superconducting cylinder surrounds the SQUID, shielding it from all environmental fields. To allow the SQUID to sense the signal field, a coil is placed inside the shield, coupled inductively to the SQUID and galvanometrically to an external counterwound pick-up coil such as the example in Figure 1(a). This coil is sensitive to the spatial gradients of fields generated by nearby signal sources and at the same time insensitive to uniform fields from distant interference sources. For NDE, each winding would typically comprise a few turns with 1 to 5 mm diameters. Because the complete input circuit is superconducting, the configuration senses static and ac fields. Unfortunately, although fine gauge superconducting wire for the pick-up coils is readily available in LTS materials, suitable HTS wire has not yet been developed. The configuration is therefore limited to liquid helium temperature systems which have found little acceptance outside superconductivity laboratories.

Electronic gradiometry is the configuration under most active development at present. In the example illustrated in Figure 1(b), two bare SQUIDs are exposed to the full range of environmental magnetic fields, including interference and signals, and their outputs are differenced. For interference to be rejected successfully, its sources must be distant compared with the SQUID separation so that they produce the same SQUID outputs, while nearby signal sources produce different outputs. The performance of the electronics before

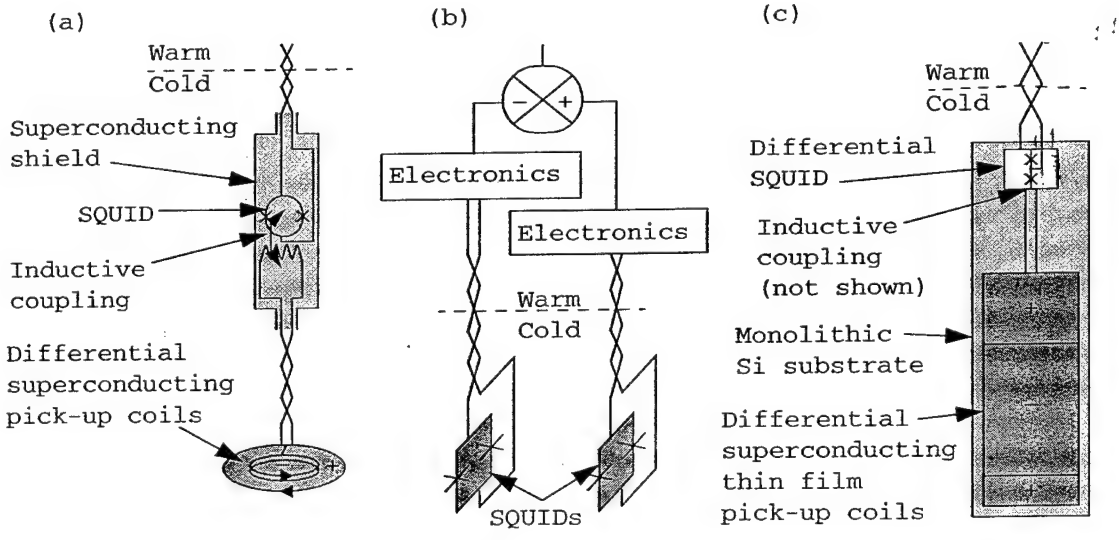

Figure 1. Practical configurations for SQUID measurements: (a) wire-wound pick-up coils and shielded SQUID, (b) electronic gradiometry and (c) integrated SQUID-gradiometer. Sense areas are indicated by dark shading.

differencing is crucial here, since they have to track both broadband, large amplitude interference and typically narrowband, small amplitude signals. At least three electronic gradiometers have been developed for research and two are being used to investigate NDE problems [4, 7]. We present results from our own in a later section.

Figure 2(c) shows a third configuration which may, in future, overcome both the lack of fine gauge HTS wire and the need for sophisticated electronics. Here, the gradiometry is hard-wired as in Figure 2(a) but in thin film form realisable in both LTS and HTS. Since the SQUID is unshielded, its sensitivity to environmental interference is minimised by using a double washer design. The planar pick-up coils are superconductor/insulator multilayer structures inductively coupled to the SQUID by planar spiral coils deposited on top of the SQUID washer. As well as the many established design rules for LTS devices, the geometries of the SQUID and the pick-up coil are critical in this configuration. We report on theoretical and experimental studies elsewhere [5].

MODELLING

The development of mathematical models of SQUID NDE is important for three reasons. Firstly, experience of equipment construction is making it increasingly easy to transform theoretical, computer aided designs into practical systems. Secondly, verification of new modelling techniques is aided by the simple nature of the experimental parameters; for example, in electronic gradiometry the SQUIDs behave as ideal point sensors with a uniform spectral response over several frequency decades. Thirdly, the same simple definitions make SQUID NDE a good candidate for automatic processing, for example using inverse techniques which require accurate forward problem definitions. We therefore use three modelling techniques: the finite element method (FEM), the volume integral method (VIM), and numerical calculation of responses to elementary sources.

OPERA and ELEKTRA [10] are our FEM packages. For a typical SQUID NDE problem, the mesh comprises around 80,000 nodes. We solve it on a Hewlett Packard 9000/715/100 workstation with 160 MB memory and 5 GB disk. For a single flaw such as a narrow rectangular slit and a source such as the 63 mm diameter double-D induction coil described later, the solution takes several hours. Given this onerous overhead, we have limited our FEM studies to the effects of different coil geometries, observed via current flow amplitudes in the specimen, and of different induction frequencies, in the latter case obtaining results which corresponded well with experimental measurements [11].

Although the flexibility of FEM in terms of specimen and flaw geometries and specimen materials is excellent, it is not yet fast enough for complete simulation of two-dimensional (2D) scans, and we have instead turned to the faster but less flexible VIM for this. Our implementation is dealt with in more detail elsewhere [8] but its practical advantage is that the numerical solution takes place only in the volume of the flaw. We have found this makes a difference of as much as three orders of magnitude in calculation time and both unidimensional (1D) and 2D scans have been simulated successfully [12].

The third technique is numerical calculation of responses to elementary sources such as the current-carrying wire, the current dipole and the magnetic dipole. The current dipole is, of course, the most general of these but the other two are useful because mathematical solutions are readily available and equivalent experimental sources are easy to set up. An example is shown in Figure 2(a). A return loop of wire carrying 13.9 mA rms at 270 Hz was arranged in a large V-shape and a 2D scan was made, with two SQUIDs oriented as shown. The experimental result was compared with simple theory for sections through the scan, for

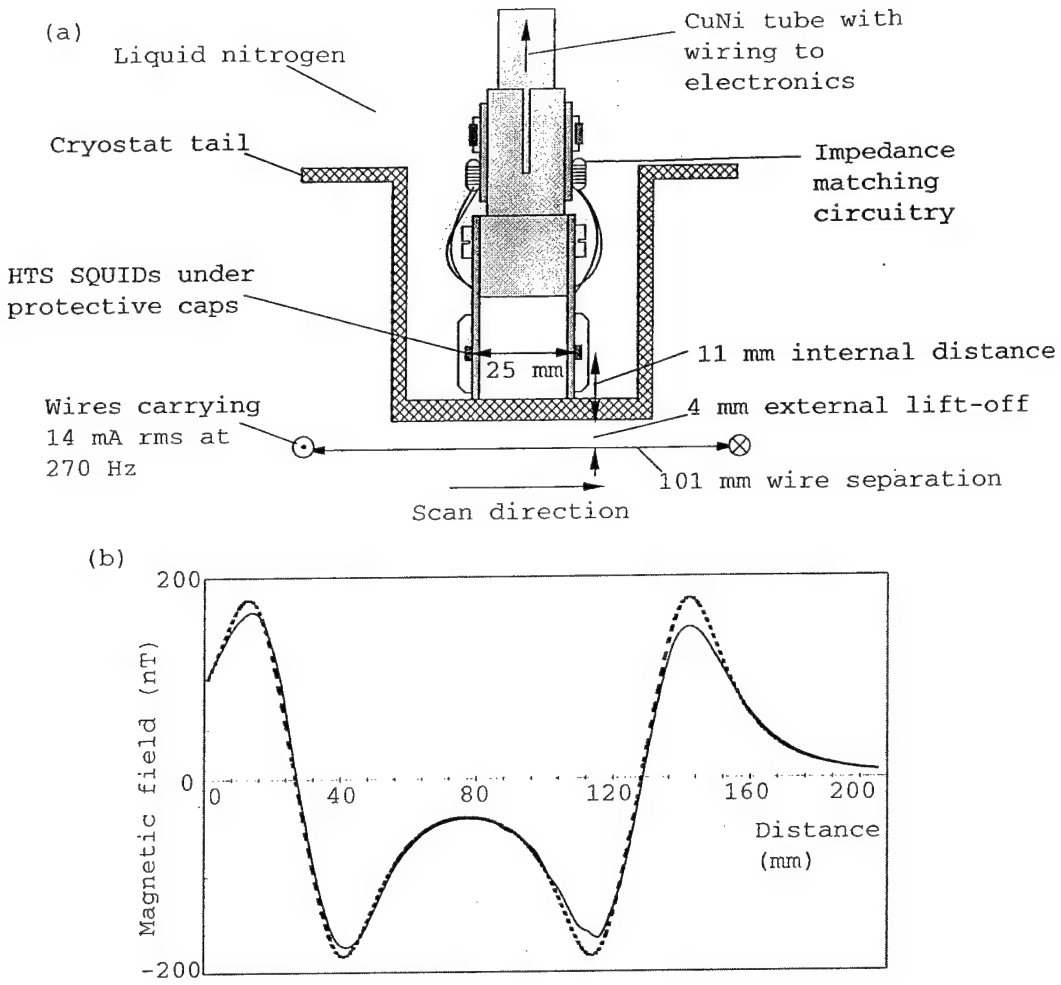

Figure 2. (a) Arrangement of two SQUIDs as an electronic gradiometer above a return loop of current carrying wire and (b) magnetic field measured during scanning (solid line) and its theoretical equivalent (broken line).

example with a wire separation of 101 mm as shown in Figure 2(b). The correspondence is clear, indicating that absolute amplitude calibration is reasonably accurate and that ac signals with amplitudes similar to or less than the environmental noise level (200 nT is a typical electrical mains field in our laboratory) can be measured with high signal to noise ratios (SNRs).

SYSTEMS DESIGN

Our recent practical work on NDE has mainly concerned the development and demonstration of the HTS SQUID electronic gradiometer shown in outline in Figure 1(a) and in more detail in Figure 2(a). Here, we concentrate on it, although in the past we have used wire-wound pick-up coils in an LTS system, and we have an existing programme to develop integrated devices, initially prototyped in LTS. It is important to realise that electronic gradiometry using HTS SQUIDs is indeed a new technique, but the real benefits are only in terms of convenience: the performance is no better than could have been achieved several years ago, with sufficient effort, in LTS. The system we have developed is shown fully in Figure 3. It is based on commercial SQUIDs, with our own cryostat, electronics, magnetically- quiet scanning system and software.

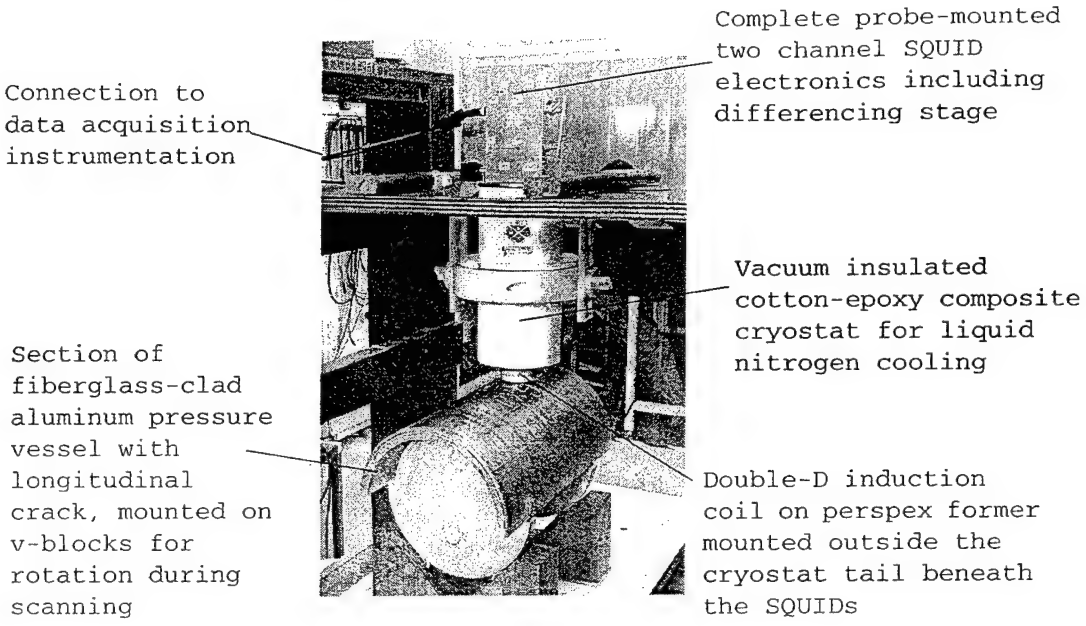

Figure 3. HTS SQUID electronic gradiometer for NDE in magnetically-quiet scanning equipment.

The insulation in the liquid nitrogen cryostat is based on a conventional combination of vacuum space, charcoal getter and aluminized mylar superinsulation. However, to minimise electromagnetic screening the cryostat is constructed entirely of bonded cotton-epoxy composite material, except for a vacuum valve and some aluminium components at the upper, probe-mounting end, well away from the sensors so that eddy-current distortion of ac fields is unlikely. It is 150 mm in diameter and 333 mm long with a tail 50 mm in external diameter and 4 mm thick at the base. The hold time is at least 24 hours. Although the overall dimensions and weight are acceptable for some practical applications, it must be used upright: ways to overcome this exist but have not yet been investigated in HTS systems.

The two SQUIDs are spring-loaded downwards so that their position can be determined accurately, 11 mm from the base of the cryostat tail. Unlike other systems [4], there is no fine position adjustment mechanism to null the gradiometer output. The vertical SQUID orientation was dictated by the dimensions of the mounting boards and the cryostat tail; in practice, this was found to be an effective orientation for several types of inspection. The SQUIDs themselves have sensing areas approximately 70 μm square and the intrinsic field noise level is approximately 10 pT/√Hz.

The electronics have two separate channels, each with a 33 kHz bandwidth, and a differencing stage. The output signal is 3 V/μT over a ±10 V range, extended as necessary by automatic resetting. Usually the difference between the channels is recorded, but outputs are also available to record each channel separately. The difference output provides a typical SNR enhancement of 20 to 30 dB.

The induction coil we used for the results here has the 63 mm diameter double-D configuration shown in Figure 4(a). It was driven, via fine twisted-pair wiring, by a current source connected to a Hewlett Packard waveform synthesizer, and the single channel and difference outputs from the SQUID electronics were synchronously demodulated using two EG&G dual channel (quadrature) lock-in amplifiers. Their readings were recorded via GPIB connections to the PC which also controlled the waveform synthesizer and the scanner.

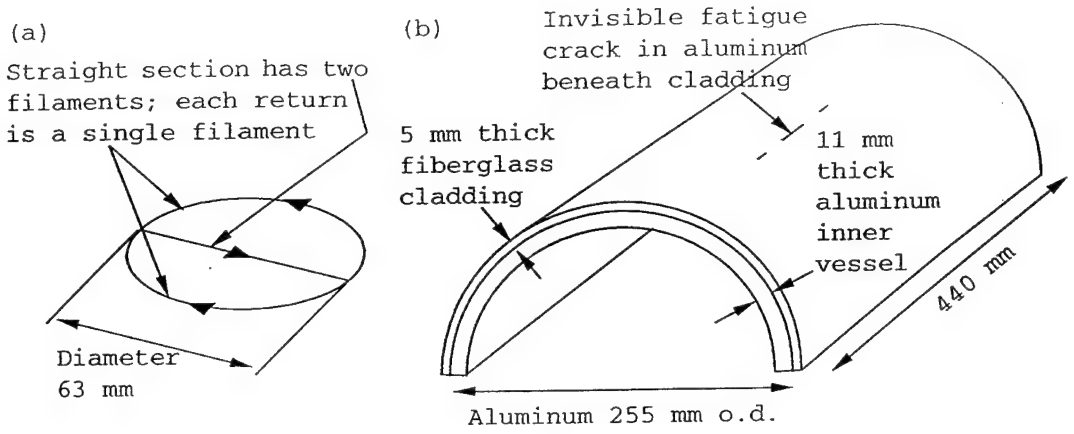

Figure 4. (a) Induction coil configuration (perspex former not shown) and (b) specimen cut from a fiberglass-clad aluminum pressure vessel (not to scale).

The scanner, built from wood and a variety of plastics, has a 2D scanning bed with longitudinal motion effected by a lead screw from a magnetically-shielded stepper motor and controlled via feedback from a non-magnetic shaft-encoder driven by the bed. For the measurements described here, lateral scanning was unnecessary; instead, the specimen was rotated manually, running on glass bearings in wooden v-blocks.

DEMONSTRATION

The specimen we consider here is shown in Figure 4. It was supplied by British Gas, as a section from a fiberglass-clad aluminum pressure vessel which had been cycled 40,000 times until it failed because of the growth of a crack through the aluminum. This is a quite intractable problem for NDE because poor acoustic propagation through the fiberglass into the aluminum makes ultrasonic inspection difficult and conventional eddy current testing has limited effectiveness at the relatively high minimum lift-off imposed by the cladding.

We raster scanned the specimen longitudinally, rotating it by 3° (6.67 mm on the surface of the aluminum) after each scan. The straight section of the double-D induction coil, carrying a 270 Hz, 77 mA current, was oriented perpendicular to the length of the specimen (shown approximately in Figure 4) at a 2 mm radial lift-off from the fiberglass. The SQUIDs were oriented perpendicular to the straight section of the double-D to minimize direct detection of the induction field and maximize sensitivity to circumferential fields around the specimen.

We first recorded complete 2D maps of the in-phase and quadrature components of the gradiometer output then, in a separate test at a smaller lift-off, we repeated the scan directly above the crack, this time recording single SQUID and gradiometer outputs.

First consider the 2D maps transformed into the magnitude and phase components shown in Figure 5. The crack has clearly been detected as a compound, 2D signal in each. The circumferential dimension of this signal in Figure 5(a) is very close to the 63 mm diameter of the induction coil, as expected from a combination of the coil diameter and the negligible width of the crack. The circumferential shape is a simple peak, again qualitatively predictable from the coil and crack configurations.

The longitudinal characteristics of the 2D signal are most easily seen in Figure 6(a), the real part of the gradiometer output from the single scan. The obvious pairs of peaks and

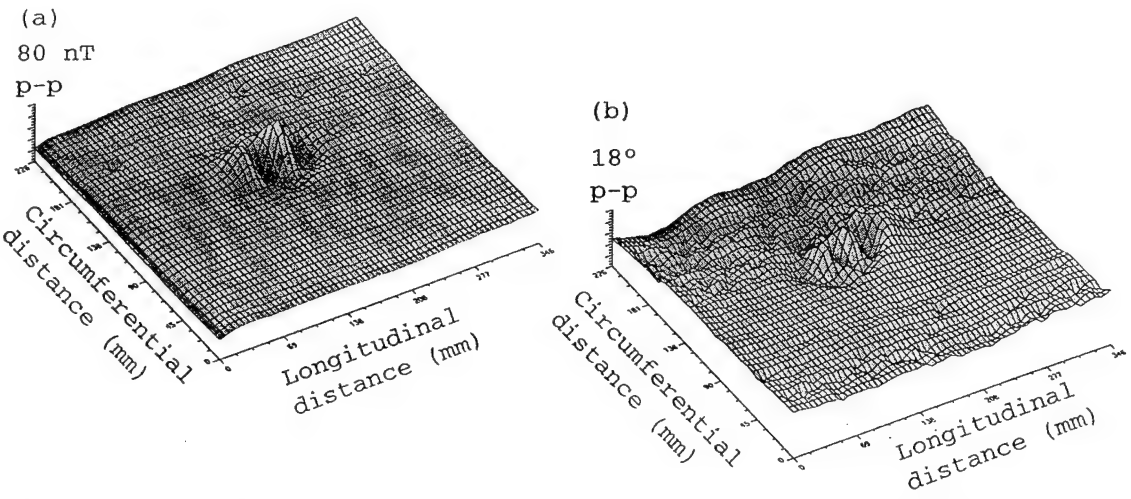

Figure 5. (a) Amplitude and (b) phase of differential circumferential magnetic field recorded around the specimen in Figure 4(b). There is an unperturbed field amplitude of approximately 80 nT in Figure 4(a).

troughs are characteristic of both our experimental and theoretical studies of the double-D coil configuration [8]. To verify the length of the crack independently, we removed the fiberglass cladding and used an ultrasonic angle probe to determine the 60 mm length of the corner echo. In this relatively simple through-crack example, we would expect the sum of this length and the 63 mm coil diameter to correspond approximately to the 121 mm long signal in the gradiometer response, as is indeed the case.

Finally, it is worth comparing the results of Figures 6(a) and (b), respectively the gradiometer and single SQUID outputs, recorded together. As expected, the peak to peak amplitude of the single SQUID output is almost exactly half that of the gradiometer. It is inverted because we recorded the subtracted channel. Though it is apparently noisy, this noise is actually interference, for example from the electrical mains field, recorded asynchronously with respect to its sources but synchronously by the SQUIDs. The distinction is important since the subtraction technique on which electronic gradiometry is based rejects only interference common to the SQUIDs. Although the signal caused by the crack can still be seen in Figure 6(b), the effect of the interference on automatic processing, including inversion [8], is likely to be very damaging.

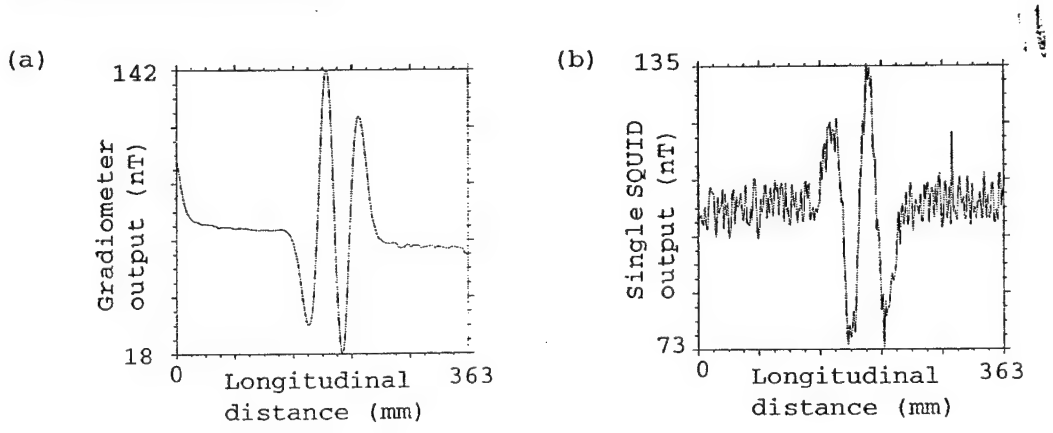

Figure 6. (a) Real part of the gradiometer output along a scan directly above the crack, and (b) single SQUID output for the same scan.

CONCLUSIONS

We are working on a wide ranging programme studying many aspects of the development of the SQUID for NDE. Although work with previous generation LTS systems is continuing at some sites, these are likely to be superseded in the short term by HTS systems based on discrete SQUIDs combined in electronic gradiometers, and in the long term by integrated devices combining superconducting pick-up coils and SQUIDs on monolithic substrates.

Already, the usability of our own HTS electronic gradiometer has allowed us to make measurements which would have taken many more months with the previous LTS system. These are of interest in themselves as solutions to previously intractable problems in NDE, such as high lift-off detection of fatigue cracks in aluminium; in providing data for verification of modelling techniques and development of inverse algorithms; and to demonstrate how very high sensitivity, wideband magnetic sensors such as the SQUID can be used successfully in environments where interference fields exceed the signal by orders of magnitude.

ACKNOWLEDGEMENTS

The authors are supported by the UK EPSRC and MoD, a BP/Royal Society of Edinburgh Research Fellowship, Oxford Instruments Ltd, Quantum Magnetics, and the US AFOSR. They also thank British Gas for supplying the pressure vessel specimen and K.J.Kirk for help with the ultrasonic testing.

REFERENCES

1. J.Clarke, in *The New Superconducting Electronics*, eds. H.Weinstock and R.Ralston (Kluwer Academic Publishers, Dordrecht, 1993) p. 123.
2. N.S.Alzayed, C-x. Fan, D.F.Lu, K.W.Wong, M.Chester and D.C.Knapp, IEEE Trans. Appl. Supercond. 4, 81 (1994).
3. N.Khare, S.Chaudhry and A.K.Gupta, Superconductors 5, 1 (1992).
4. Y.Tavrin, H.-J.Krause, W.Wolf, V.Glyantsev, J.Schubert, W.Zander and H.Bousack, Cryogenics, in press (1995).
5. U.Klein, M.E.Walker, A.Cochran, D.Hutson, R.G.Weston and C.M.Pegrum, Extended Abstracts, Int. Conf. on Supercond. Electronics, Nagoya (1995).
6. A.Cochran and G.B.Donaldson, in *Superconducting Devices and Their Applications*, eds. H.Koch and H.Lubbig (Springer-Verlag, Berlin, 1992) p. 576.
7. J.Kuznik, C.Carr, A.Cochran, L.N.C.Morgan and G.B.Donaldson, in *Proc. 2nd Eur. Conf. on Appl. Supercond.* (IoP Conf. Proc. Series, 1995) in press.
8. D.McA.McKirdy, A.Cochran, A.McNab and G.B.Donaldson, in *Proc. Int. Workshop on Electromagnetic Nondestr. Eval.* (IOS Press, Amsterdam, 1995) in press.
9. A.Cochran, J.Kuznik, C.Carr, L.N.C.Morgan and G.B.Donaldson, in *Proc. 2nd Eur. Conf. on Appl. Supercond.* (IoP Conf. Proc. Series, 1995) in press.
10. Vector Fields Ltd., Kidlington, Oxford, OX5 1JE, UK.
11. L.N.C.Morgan, C.Carr, A.Cochran, D.McA.McKirdy and G.B.Donaldson, IEEE Trans. Appl. Supercond., 5, 3127 (1995).
12. D.McA.McKirdy, A.Cochran, A.McNab and G.B.Donaldson, in *Proc. 2nd Eur. Conf. on Appl. Supercond.* (IoP Conf. Proc. Series, 1995) in press.

Presented at International Workshop on Electromagnetic NDE (ENDE '95) London September 1995.

Theoretical Consideration of Fatigue Crack Detection and Characterisation Using SQUID Sensors

David McA McKIRDY, Sandy COCHRAN and Gordon B DONALDSON
Superconducting Devices Research Group, Department of Physics and Applied Physics, University of Strathclyde, Glasgow, Scotland. G4 0NG.

Alistair McNAB
Ultrasonics Research Group, Department of Electronic and Electrical Engineering, University of Strathclyde, Glasgow, Scotland. G1 1XW.

Abstract. Conventional eddy-current NDE involves detecting the presence of cracks by monitoring the impedance of a coil. This process is limited to near-surface flaws because of the skin-depth phenomenon and the fact that coil sensors are sensitive to the first time derivative of the magnetic flux passing through them. SQUID sensors are sensitive to magnetic flux, as opposed to its derivative, and are well suited to the detection of deep subsurface flaws. The modelling of eddy current NDE has been achieved by a variety of methods, such as volume integral, finite and boundary element methods, and recent work has focused on the inversion of impedance data to obtain information about the flaw dimensions. An inversion scheme based on volume integral methods has been adapted to deal with the inversion of magnetic field data. The changes in the field components are calculated with the aid of reciprocity formulae, similar to those employed to calculate impedance changes. We examine the detection of defects in the lower surface of an aluminium plate using a "double-D" excitation coil.

1. Introduction

Eddy-current NDE has been successfully applied to the detection of surface cracks and is routinely used to locate flaws in airframes, pipelines and steel offshore oil platforms. However, there are still many problems to be solved, particularly in the aviation industry, which require the detection of deep subsurface flaws, e.g. corrosion in multi-layered structures and cracks around rivet holes which are obscured by the head of the rivet. Most systems use coils as detectors, though Hall probes are occasionally used. These coils have low sensitivity at low frequencies because the induced voltage is proportional to the rate of change of magnetic flux through the coil. Unfortunately, it is necessary to use low frequencies to detect deep subsurface flaws on account of the skin-depth effect, otherwise the electromagnetic field does not penetrate sufficiently far.

SQUIDs (Superconducting Quantum Interference Devices) are sensors ideally suited to overcome the deficiencies of coils, because they are primarily detectors of magnetic flux. Together with their high sensitivity, this makes the detection of deep subsurface flaws more likely. SQUIDs have been used successfully to measure very small magnetic fields,

particularly in biomagnetism, and it is also hoped to exploit this sensitivity to detect flaws at large stand-off distances, for example in pipelines surrounded by thick layers of cladding.

The conventional form of eddy-current NDE involves measuring the impedance of a coil and seeing how this changes when a flaw is present. Often the flaw size is obtained by comparing the impedance change with those produced by a set of simulated flaws of known size. Sometimes, separate drive and sense coils are used and it is convenient to apply the concept of transfer impedance in this case.

A different form of eddy-current NDE is the AC Field Measurement (ACFM) technique. In this method, one horizontal component and the vertical components of the magnetic field are measured by small coils in the vicinity of the flaw. The presence of a flaw is often most clearly seen as a butterfly-shaped pattern in a Lissajous plot of the two field components as the sensors are scanned along the crack. In this case, the flaw can be sized by interpolating between entries in tables of the responses of flaws of known dimensions, which have been predicted by modelling. The theory is simplified greatly by the use of the thin-skin approximation, which is really only applicable to high frequency testing or ferromagnetic test pieces, hence its application in the inspection of welds on steel offshore structures. Clearly ACFM, in this form, cannot be used to detect deep subsurface flaws.

Although SQUIDs seem suitable to overcome many of the above problems, there are new problems associated with their use. The most obvious one is that the sensors need to operate below their critical temperature, but the advent of the new high temperature superconductors (HTS) means that liquid nitrogen can now be used instead of liquid helium. In addition, the high sensitivity of the SQUID to ambient fields often forces measurements to be performed inside magnetically shielded rooms. However, careful experimental design and the use of intrinsically differential SQUID configurations or special, high frequency electronics can circumvent this expensive and restrictive solution, allowing experimental work to be carried out in open laboratories.

The configuration of SQUIDs as differential sensors is called gradiometry, involving measurement of the nth order rate of change of magnetic field with position. With the metallic, low temperature superconductors, it is usually achieved with wire-wound or integrated thin film differential sense coils. However, the new HTS materials are intractable ceramics. Although integrated HTS devices are being developed, they are not yet readily available and there is as yet no prospect of suitable wire for wire-wound coils. HTS gradiometry is therefore sometimes implemented using two SQUIDs and electronic differencing. Even then, there can be problems associated with moving the HTS SQUIDs in the Earth's magnetic field, so the scanning at Strathclyde has so far been done by moving the specimen instead..

Further details of experimental apparatus, including an electronic gradiometer designed for NDE, are given by Cochran et al. [1]; most significantly, the gradiometric system has been found to perform very much better than an earlier one based on a single HTS SQUID [2]. In this paper, however, we concentrate on theoretical topics which have become important in recent work with SQUIDs. In particular, we consider the volume integral method and how it may be applied to the parameters of SQUID systems, including typical source coil geometries, as distinct from those of more conventional impedance measurement based systems.

2. Modelling

2.1. Volume Integral Equation Modelling

The volume integral equation method was developed by geophysicists such as Weidelt [3] and Raiche [4] to study induced currents in three-dimensional structures and has been successfully adapted to eddy-current NDE by McKirdy [5] among others. Other approaches have been boundary integral equations developed by Bowler [6] and the previously mentioned thin-skin techniques of Michael and his many collaborators [7]. The volume integral equation method can be used to study isolated flaws in simple structures, such as a plate. Its main advantage is that the modelling region is confined to the flaw itself. This means that there is a smaller number of unknowns in the equation, making the storage requirements and computation times much smaller than for other techniques such as the finite element method.

It is necessary to solve for the electric field in the flaw in the following equation:

$$\mathbf{E}(\mathbf{r}) - (\sigma_f - \sigma_p) \int_{V'} \mathbf{G}(\mathbf{r},\mathbf{r}').\mathbf{E}(\mathbf{r}')dV' = \mathbf{E}^0(\mathbf{r}). \qquad (2.1)$$

Here $\mathbf{E}(\mathbf{r})$ and $\mathbf{E}^0(\mathbf{r})$ are the total and source electric fields in the flaw, σ_f and σ_p are the conductivities of the flaw (usually zero) and the plate, $\mathbf{G(r,r')}$ is the electric Green's tensor for the plate and the integration is restricted to the flaw volume *V*. Traditionally the source electric field has been calculated from analytical formulae such as those derived by Dodd and Deeds [8] for a pancake coil, but it is necessary to use numerical methods, such as the moment method, to solve Equation (2.1). The Green's functions can only be calculated for a few special geometries, which is why the modelling here is limited to the study of non-ferromagnetic aluminium plates.

2.2. Impedance Changes

The impedance change of the coil is clearly related to the change of magnetic flux through the driver coil, but it is not necessary to use this approach, as simpler formulae, derived using the reciprocity theorem, have been described by Zaman et al. [9] and give the desired ΔZ directly:

$$\Delta Z = \left(\frac{\sigma_p - \sigma_f}{I^2} \right) \int_V \mathbf{E}^0(\mathbf{r}).\mathbf{E}(\mathbf{r})dV . \qquad (2.2)$$

Here, *I* is the current in the inducing coil, usually assumed to be unity and often omitted. Clearly the impedance change can be calculated very simply once the solution to Equation (2.1) is obtained as the integration in Equation (2.2) is also over only the flaw volume.

2.3. Magnetic Field Calculation

For SQUID NDE (and indeed ACFM) it is necessary to calculate magnetic fields. This can be done directly by taking the curl of Equation (2.1) because Maxwell's equations state that

$$-i\omega\mathbf{B} = \nabla \times \mathbf{E} \tag{2.3}$$

for harmonic fields with angular frequency ω. The curl operator acts only on the unprimed co-ordinates and we can obtain another integral equation involving the magnetic Green's tensor, but this can involve considerably more computation especially when the grids for the discretisation of the flaw and the field measurements are very different:

$$\mathbf{B}(\mathbf{r}) + \frac{(\sigma_f - \sigma_p)}{i\omega} \int_{V'} \nabla \times \mathbf{G}(\mathbf{r},\mathbf{r}').\mathbf{E}(\mathbf{r}')dV' = \mathbf{B}^0(\mathbf{r}). \tag{2.4}$$

Fortunately simpler formulae, analogous to Equation (2.2), can be found, again by using the reciprocity theorem. Auld et al. [10] define the change in transfer impedance between two coils labelled by subscripts *1* and *2* as

$$\Delta Z_{12} = \left(\frac{\sigma_p - \sigma_f}{I_1 I_2} \right) \int_V \mathbf{E}_1(\mathbf{r}).\mathbf{E}_2(\mathbf{r})dV \tag{2.5}$$

The reciprocity theorem implies that the user is free to select which coil is the source and which the sensor; here we will select coil *2* as the sensor. The transfer impedance is then defined as

$$\Delta Z_{12} = \Delta V_2 / I_1 \tag{2.6}$$

if we assume a constant current I_1. If we further assume that the voltage ΔV_2 is given by the rate of change of magnetic flux through coil 2 then

$$\Delta V_2 = -i\omega\mathbf{B} \cdot \mathbf{A}_2 \tag{2.7}$$

where $\boldsymbol{A}_2$ is the directed area of the sensor. We obtain

$$\Delta B_i = \left(\frac{\sigma_p - \sigma_f}{-i\omega I_1 M_{2i}} \right) \int_V \mathbf{E}_1(\mathbf{r}).\mathbf{E}_2(\mathbf{r})dV \tag{2.8}$$

where $M_{2i} = I_2 A_2$ is the magnetic moment of coil 2 oriented in the *i*th direction, again usually taken to be unity. The complete set of magnetic field changes can be found by calculating the magnetic field due to unit magnetic dipoles in the *x*-, *y*- and *z*-directions. The field due to the vertical dipole is just the limiting case of a small pancake coil and can be found by reapplying Dodd and Deeds [8], while the horizontal dipoles can be treated in a similar way.

2.4. Double-D Coil

Double-D coils have been used by Beissner, but the problems studied have forced the use of numerical analyses only, particularly in the examination of the effects of probe tilt [11] and the addition of ferrite cores [12]. Expressions for the electromagnetic potentials can be derived in a similar way to the Dodd and Deeds formulae for a circular current loop, though these now involve infinite series. The double-D configuration induces a current pattern

similar to a horizontal magnetic dipole, so clearly two components of the magnetic vector potential are required. Therefore the analysis starts with the scalar magnetic potential instead.

As the magnetic field in the plane of any isolated loop must be perpendicular to the loop, we know that the scalar potential must be constant in this plane. The constant is usually taken to be zero outside the loop and has the values $\pm\mu_0 I/2$ on the two faces of the coil, when the current in the loop is I. If we take a double-D coil of radius a we can write the magnetic potential on one face as

$$\Phi = +\mu_0 I/2, \qquad -\pi/2 < \theta < \pi/2, \qquad r < a$$

$$\Phi = -\mu_0 I/2, \qquad \pi/2 < \theta < 3\pi/2, \qquad r < a$$

$$\Phi = 0, \qquad r > a. \tag{2.9}$$

This can be written as a Fourier-Bessel expression:

$$\Phi(r,\theta) = \pm(\mu_0 I/2)\sum_{n=0}^{\infty}\int_0^{\infty} f_{2n+1}(\lambda)J_{2n+1}(\lambda r)\lambda d\lambda \cos(2n+1)\theta \tag{2.10}$$

and standard Fourier-Bessel analysis shows that

$$f_{2n+1}(\lambda) = \frac{(-1)^n 4}{\pi(2n+1)}\int_0^a rJ_{2n+1}(\lambda r)dr \tag{2.11}$$

It is now straightforward to derive the vector magnetic potential which gives the same magnetic field and the methods of Dodd and Deeds can be used to deal with a multi-turn coil of finite length and with the inclusion of a workpiece. Test studies, though not exhaustive, have been done on some NDE problems showing that it is sufficient to use only five terms in the series and often only three are adequate.

3. Inversion

Generally speaking the inversion of electromagnetic data is a far more complex problem than forward modelling. However, there is an advantage to some forward modelling methods which permits inversion without much more computational effort, provided the discretised system of equations is solved directly rather than iteratively. This approach has been used by Eaton [13] and Marcuello-Pascual et al. [14] to invert geophysical data and can also be found in Oldenburg's review paper [15].

If the discretised form of Equation (2.1) is written as

$$\mathbf{A}\,\mathbf{e} = \mathbf{e}^0 \tag{3.1}$$

where $\mathbf{A}$ denotes the discrete form of the integral equation operator, $\mathbf{e}$ and $\mathbf{e}^0$ denote the discrete total and source electric fields., and we define a set of flaw parameters

$\{m_k, k = 1,.....,M\}$ and differentiate Equation (3.1) with respect to these parameters we obtain

$$\mathbf{A}\frac{\partial \mathbf{e}}{\partial m_k} = -\frac{\partial \mathbf{A}}{\partial m_k}\mathbf{e} \tag{3.2}$$

This has the same form as Equation (3.1) and provided it has been solved by a direct method, such as LU decomposition, we can solve the M equations in Equation (3.2) with comparatively little extra effort. This is simplified by the fact that the Green's tensors and unflawed electric fields are independent of the flaw model and calculation of the new right-hand sides is straightforward. The derivatives of the response function can be found by differentiating the appropriate formulae with respect to the model parameters, that is, Equation (2.2) for the inversion of impedance data or Equation (2.8) for magnetic field data.

If we now have N such data, denoted by $\{d_k^*, k = 1,...., N\}$, we can construct the $N \times M$ sensitivity matrix $\boldsymbol{G}$, where

$$G_{ij} = \frac{\partial d_i}{\partial m_j}, \tag{3.3}$$

that is, it contains the derivatives of the modelled responses, $\boldsymbol{d}$, with respect to the model. We wish to find the change in the model parameters, $\delta \boldsymbol{m}$, which minimises the misfit to the data $\delta \mathbf{d} = ||\mathbf{d}\text{-}\mathbf{d}^*||$. To obtain an overdetermined set of equations, we clearly require $N > M$. The tutorial review by Lines and Treitel [16] shows that the least squares solution is given by

$$\delta\mathbf{m} = (\mathbf{G}^T\mathbf{G})^{-1}\mathbf{G}^T\delta\mathbf{d} \tag{3.4}$$

which is also called the Gauss-Newton (G-N) solution. However, Lines and Treitel warn of various pitfalls in using the G-N method and go on to describe constrained solutions to the problem, particularly the Marquardt-Levenberg method. Nevertheless, the G-N method has been successfully used to obtain 5-parameter inversions of eddy-current impedance data, and it should therefore also work for low-number parameter inversions of magnetic field data. Here we study 3-parameter inversions of circular arc flaws which have been produced by cutting aluminium plates with a fine-bladed rotary saw. The three parameters are therefore the maximum depth and the location of the two ends of the flaw. Work on the Marquardt-Levenberg method is still in progress. It is hoped that this method of inversion is conceptually simpler than the approach of Norton and Bowler [17] which is based on the use of the adjoint problem.

4. Results

4.1. Practical Considerations

The development of the inversion code was done with synthetic data rather than actual experimental data, though the parameters we give below correspond very closely with experimental ones. Using synthetic data has involved calculating the response of a flaw with a fine numerical grid and performing the inversions with a slightly coarser one. Errors

in the data can be simulated by adding numerical noise, usually Gaussian, to the data, but that has not been done here.

A model of a 6.5 mm deep circular arc flaw in a 12.7 mm thick aluminium plate was constructed on a 16 x 8 rectangular grid. The diameter of the rotary saw used for experimental work was 44.45 mm (1.75 in.) so we would expect the length of such a flaw to be 31.41 mm. The width has been taken to be the experimental value of 0.15 mm and the conductivity of the aluminium alloy to be 1.817×10^7 Sm^{-1}, corresponding to a skin depth of 7.18 mm at the chosen frequency of 270 Hz. Although a rectangular grid has been used, the conductivity has been allowed to vary throughout the model to take account of the proportion of each cell located inside the flaw. This effectively makes σ_f a function of position, $\sigma_f(\mathbf{r}')$, so that the factor $(\sigma_f(\mathbf{r}') - \sigma_p)$ should now be taken inside the integral sign. The inversions have been done on the coarser 12 x 6 numerical grid, but this grid is defined over a larger area than the original flaw: 40 x 11 mm as opposed to the original 31.41 x 6.5 mm.

Originally the eddy-current modelling code was written to deal with fully three-dimensional problems, but it is known that for narrow cracks only the electric field component across the crack is of any real importance, as this has a singularity in the limit of an infinitely thin crack. The other field components can also be ignored when the inducing coil is directly over the crack, when the unperturbed induced currents would be normally incident on the location of the flaw. By considering only one component of the electric field, we reduce the time for the LU-decomposition by a factor of 27 and, as this is often the longest stage of the program, it makes it faster to find the iterative solution to the inverse problem, though we are presently limited to studying narrow flaws.

4.2. Inversions

For the purposes of calculation, the double-D coil has a lift-off of 1.5 mm, while the two SQUID sensors have lift-offs of 12.5 mm and are displaced laterally by ±12.5 mm from the centre of the double-D along the straight section of conductor.

For the 6.5 mm deep flaw we have 41 data points in the range [-20, 20] mm and both the real and imaginary parts of the magnetic field B_x are used in the inversion scheme with equal weighting, though the larger imaginary part is dominant. The initial flaw model chosen is a semi-circle of radius 10 mm, which is shown in Figure 1, together with the results of subsequent iterations. This initial model is actually too deep and too short and overestimates the response. It shrinks down for two iterations before lengthening and finally shrinking

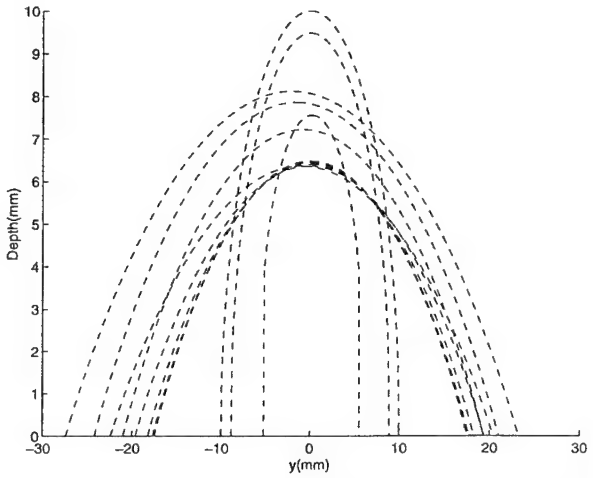

Figure 1. Results of successive iterations converging to the 6.5 mm deep circular arc flaw.

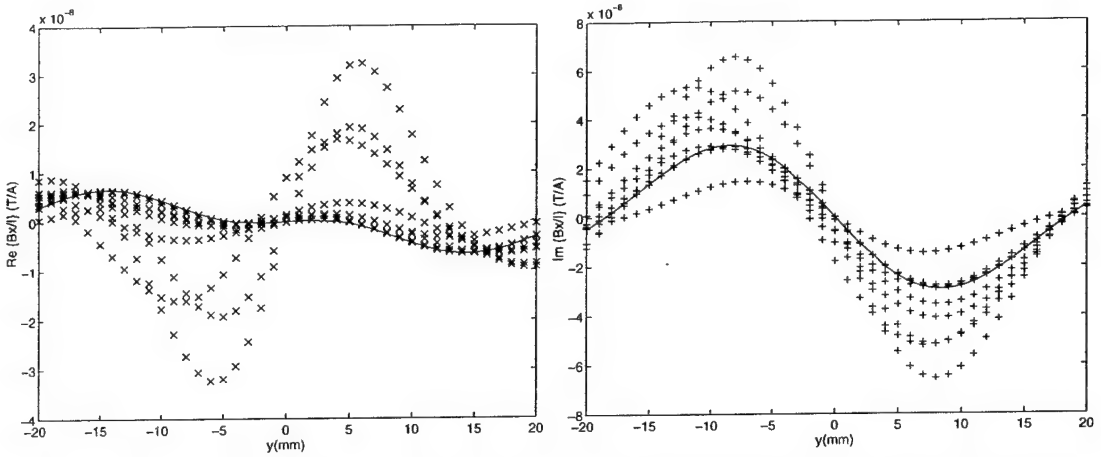

Figure 2. Real (x) and imaginary (+) parts of magnetic fields converging to the original data (solid lines) obtained with the 6.5mm deep circular arc flaw.

down to the correct shape after about 9 - 10 iterations. It should be noted that some of the intermediate models extend beyond the modelled region [-20, 20] mm, but the scheme is sufficiently robust for this not to cause problems.

The G-N method does not always converge and can diverge from a poor starting model. The fits to the data in Figure 2 show the real and imaginary parts of the magnetic field and the solid lines denote the input data. The final fits to the data lie close to the lines and the apparent larger spread in the real part is only an effect of the different scaling used in the graphs. The final depth and length of 6.49 mm and 32.04 mm from the inversion compare well with the true values of 6.5 mm and 31.41 mm. The graphs assume a driving current of 1 A which produces fields of the order of tens of nanoteslas. We have successfully detected the equivalent, scaled case of nanotesla fields produced by currents of the order of 100 mA.

The 6.5 mm flaw is not particularly deep, in that it goes almost half way through the plate and is less than a skin depth down from the top surface at a frequency of 270 Hz. Among our circular arc flaws is one only 1.8 mm deep [1] which was made with the same saw and has an expected length of 17.6 mm. The initial modelling was done over the range of the flaw on a 20 x 3 grid, while the inversions were done over a 24 x 3.6 mm area on a 12 x 2 grid.

The initial model was a circular arc of depth 3.6 mm and length 24 mm. Again the effect of overestimating the depth more than compensates for the shorter length and the initial predicted fields are too large. The intermediate models are shown in Figure 3 and the fields

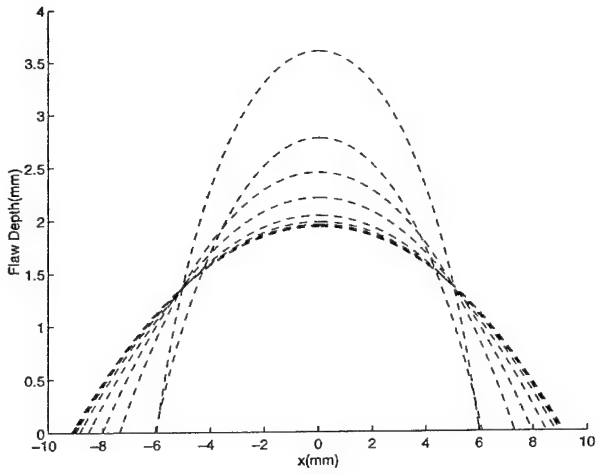

Figure 3. Results of successive iterations converging to the 1.8 mm deep circular arc flaw.

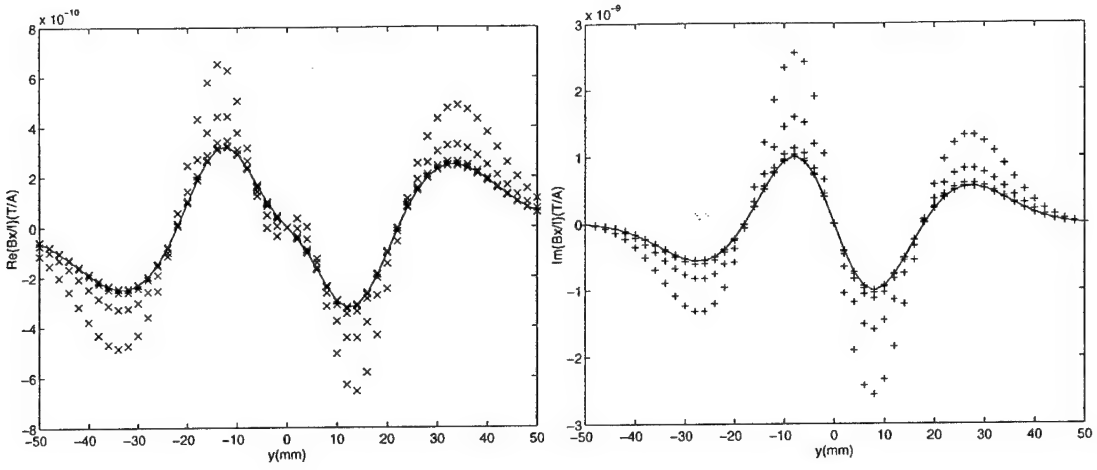

Figure 4. Real (x) and imaginary (+) parts of the magnetic field converging to the original data (solid lines) obtained with the 1.8mm deep circular arc flaw.

in Figure 4. Convergence can be said to have occurred after 5 or 6 iterations. This time 51 data points in the range [-50, 50] mm have been used and the characteristic twin peaks and twin troughs in the field produced by the double-D coil are clearly seen. An earlier attempt using the same scan as the 6.5 mm flaw actually converged to an incorrect length, but here the depth was predicted to be 1.93 mm and the length to be 18.26 mm, which should be compared with true values of 1.8 mm and 17.6 mm. It should be noted that the fields are about an order of magnitude smaller than those found with the deeper flaw.

5. Conclusions

It has been possible to extend earlier work on the simulation of conventional eddy-current NDE to model the magnetic fields detected by a simple SQUID gradiometer and to invert these fields to obtain information about the length and depth of a defect. Although there is qualitative agreement between the modelled and measured fields, the inversion of experimental data must wait until there is better agreement. The largest cause of uncertainty with the experimental data comes from measuring the lift-off of the inducing coil, but this is a common problem in any kind of electromagnetic NDE. In our case it can be easily solved by careful experimental procedure intended to produce data for inversion rather than to demonstrate the performance of the equipment.

Acknowledgements

The authors are grateful for the support of UK EPSRC and MoD, and BP/The Royal Society of Edinburgh. The first author developed the original versions of the volume integral modelling and inverse code with the support of Defence Research Establishment Pacific, Canada.

References

[1] A. Cochran, C. Carr, D. McA. McKirdy, M. E. Walker, A. McNab, U.Klein, J. Kuznik, and G. B. Donaldson, Recent Progress in SQUIDs as Sensors for Electromagnetic NDE, *These Proceedings.*

[2] A. Cochran, J. C. Macfarlane, L. N. C. Morgan, J. Kuznik, R Weston, L Hao, R. M. Bowman and G. B. Donaldson, Using a 77K SQUID to Measure Magnetic Fields for NDE, *IEEE Trans. on Appl. Supercond.* **4** (1994) 128-135.

[3] P. Weidelt, Electromagnetic Induction in Three-Dimensional Structures, *J. Geophysics* **41** (1975) 85-109.

[4] A. P. Raiche, An Integral Equation Approach to Three-Dimensional Modelling, *Geophysical J. of the Royal Astronomical Society* **36** (1974) 363-376.

[5] D. McA. McKirdy, Recent Improvements to the Application of the Volume Integral Method of Eddy Current Modeling, *J. Nondestr. Eval.* **8** (1989) 45-52.

[6] J. R. Bowler, Eddy-Current Interaction with an Ideal Crack. 1. The Forward Problem, *J. Appl. Phys.* **75** (1994) 8128-8137.

[7] D. H. Michael, A. M. Lewis, M. McIver and R. Collins, Thin-Skin Electromagnetic Fields in the Neighbourhood of Surface-Breaking Cracks in Metals, *Proc. Roy. Soc. A* **434** (1991) 587-603.

[8] C. V. Dodd and W. E. Deeds, Analytical Solutions to Eddy-Current Probe-Coil Problems, *J. Appl. Phys.* **39** (1968) 2829-2383.

[9] A. J. M. Zaman, C. G. Gardner and S. A. Long, Change in Impedance of a Single-Turn Coil Due to a Flaw in Conducting Half Space, *J. Nondestr. Eval.* **3** (1989) 37-43.

[10] B. A. Auld, J. C. Moulder, S. Jeffries, P. J. Shull, S. Ayter and J, Kenney, Eddy-Current Reflection Probes: Theory and Experiment, *Res. in Nondestr. Eval.* **1** (1989) 1-11.

[11] R. E. Beissner and J. A. G. Temple, Calculation of Eddy Current Fields for Coils of Arbitrary Shape, *Rev. Prog. Quantitative Nondestr. Eval.* **9** (1990) 257-264.

[12] R. E. Beissner and J. S. Graves, Computer Modelling of Eddy Current Probability of Crack Detection, *Rev. Prog. Quantitative Nondestr. Eval.* **9** (1990) 885-891.

[13] P. A. Eaton, 3D Electromagnetic Inversion Using Integral Equations, *Geophysical Prospecting* **37** (1989) 407-426.

[14] A. Marcuello-Pascual, P. Kaikonnen and J. Pous, 2-D Inversion of MT Data with a Variable Model Geometry, *Geophysical J. Int.* **110** (1992) 297-304.

[15] D. Oldenburg, Inversion of Electromagnetic Data: An Overview of New Techniques, *Surveys in Geophysics* **11** (1990) 231-270.

[16] L. R. Lines and S. Treitel, Tutorial Review of Least-Squares Inversion and its Application to Geophysical Problems, *Geophysical Prospecting* **32** (1084) 159-186.

[17] S. J. Norton and J. R. Bowler, Theory of Eddy-Current Inversion, *J. Appl. Physics* **73** (1993) 501-512.

Presented at European Conference on Applied Superconductivity (EUCAS '95) Edinburgh, July 1995

First order electronic gradiometry with simple HTS SQUIDs and optimised electronics

J Kuznik*, C Carr , A Cochran , L N C Morgan+ and G B Donaldson

University of Strathclyde, Department of Physics and Applied Physics, John Anderson Building, 107 Rottenrow, Glasgow, G4 0NG, UK.

* Presently visiting from Institute of Physics, Czech Academy of Sciences, Prague, Czech Republic.

+ Now with BT Laboratories, Martlesham Heath, Ipswich, IP5 7RZ, UK.

Abstract. We have constructed a complete system for first order electronic gradiometry, including instrumentation and cryostat, based on two commercial high temperature superconductor Mr SQUID devices. The combined white noise level of the two SQUIDs is 10^{-11} T/√Hz. The system was designed for non-destructive evaluation in unshielded environments and therefore has a bandwidth of at least 30 kHz, needed to provide enough slew rate to stay in the flux locked loop under laboratory conditions. The SQUIDs are oriented vertically to measure a component of horizontal field depending on probe rotation. Their separation is 25 mm and they are positioned approximately 7 mm from the base of the cryostat, which is 4 mm thick in total. Here, we outline the electronic and cryogenic hardware and present results demonstrating fundamental performance. These are based on noise measurements in low noise and unshielded environments; on mapping a V-shaped current-carrying wire to illustrate spatial resolution; and on eddy current detection of a slit in an aluminium specimen.

1. Introduction

The problems to be overcome to use high temperature superconductor (HTS) SQUIDs (superconducting quantum interference devices) for nondestructive evaluation (NDE) are quite different from those for many other applications. For example, consider the simple biomagnetic magnetocardiographic measurement [1], in which SQUID noise levels are critical, particularly at low frequencies, necessitating relatively large pick-up areas and films and Josephson junctions of the highest quality for HTS implementations.

In contrast, HTS SQUIDs for NDE can be simple commercial devices such as the Conductus Mr SQUID [2]. Although low frequency measurements are of interest, this probably indicates a minimum of as much as 10 Hz or more, since lower frequencies may make inspection too slow to be practical. The maximum frequency is also higher; typically a few tens of kHz: above this the performance of other sensors makes it difficult to justify using SQUIDs. A further difference is that it is unlikely that practical NDE can involve magnetic shielding

In summary, a SQUID NDE system should have the following attributes: as much insensitivity as possible to external interference; an adequate white noise level (relatively high 1/f noise is possible); and a bandwidth from 10 Hz to a few tens of kHz. Other positive attributes include high spatial resolution and convenient, easy to handle cryogenics.

In the past, we have tried to satisfy these requirements [3] with systems based on single HTS SQUIDs (and with low temperature superconductor (LTS) devices [4]: the requirements are the same. No matter how familiar liquid helium seems to those working with LTS SQUIDs, the dominant LTS problem has always been cryogenic inconvenience.) However, although the intrinsic white noise level and field sensitivities of the HTS systems were adequate, upper bandwidth was poor and susceptibility to external interference without resorting to magnetic shielding made the signal to noise ratio (SNR) too low for many measurements.

2. Electronic gradiometer

In our new system, shown in Figure 1, the two Mr SQUIDs are mounted vertically 25 mm apart. They are standard commercial items, the only difference being truncation of the PCB immediately below the SQUID encapsulation to allow them to be positioned as close as possible to room temperature specimens outside the cryostat (i.e. with minimum lift-off). The probe itself is spring-loaded to press the PCBs on the bottom of the cryostat. This both minimises lift-off (about 11 mm including cryostat tail thickness) and provides the positive location for the SQUIDs which is essential for accurate computer modelling. There is no adjustment of relative SQUID position: the SQUIDs are bolted to a Tufnol mounting piece, oriented back to back.

Each SQUID is connected to a separate channel in the electronics via its own multicomponent matching circuit. The bandwidth of each channel extends from DC to 30 kHz, and the white noise level is $10^{-4}\Phi_0/\sqrt{\text{Hz}}$. Typical SQUID NDE field amplitudes in the range of nT or hundreds of pT provide signals from a few mV down to hundreds of μV. The electronics themselves are fabricated in a modular fashion in a multiboard headbox mounted directly on the SQUID probe. Only the ±15 V DC power supply is separate.

Individual outputs from each SQUID are available and the electronics also include a simple circuit to provide the difference (quasi-first order gradient) signal directly. The output range is ±10 V. To maintain the flux-locked loop in the presence of large fields, for example when inspecting steel specimens, multiple resets may occur, triggered by either SQUID separately or by an out of range difference. The short, 1 ms reset period is therefore valuable.

The SQUID probe and electronics are mounted in our own cryostat with the usual refine-

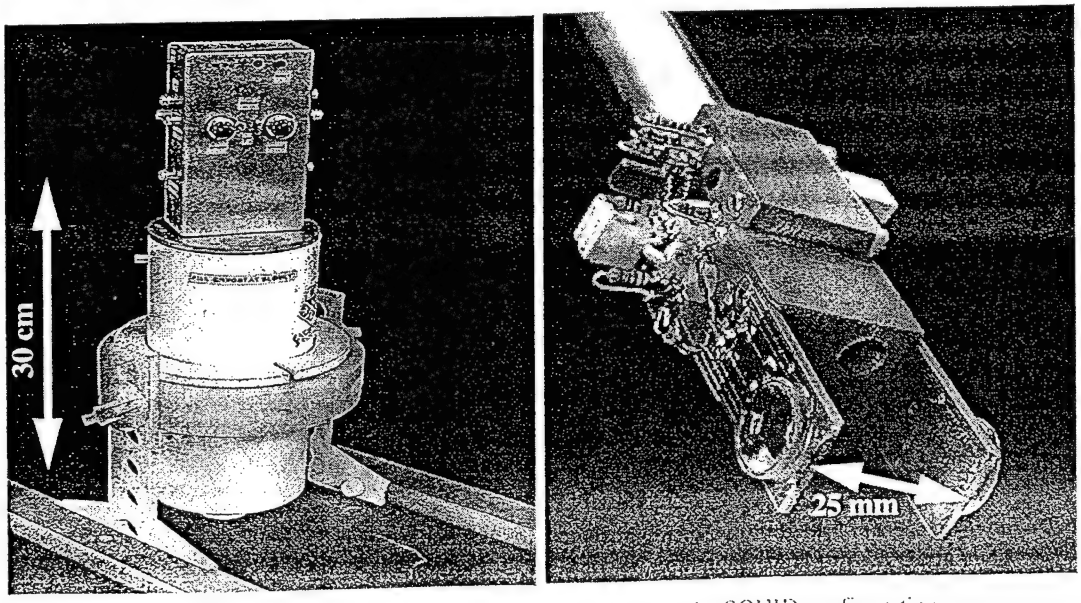

Figure 1. The complete electronic gradiometer, and the SQUID configuration.

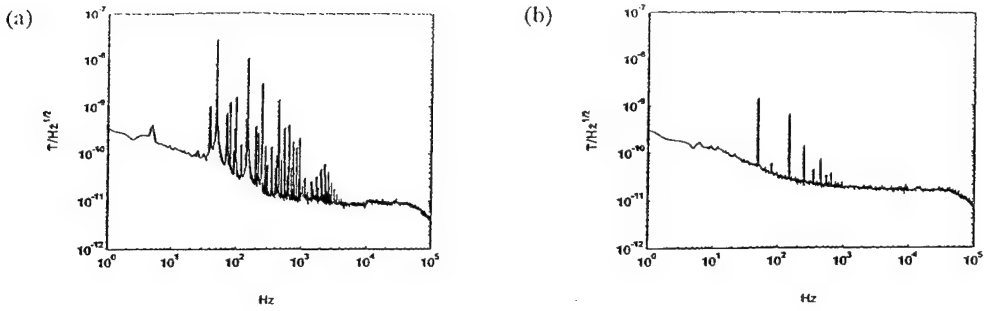

Figure 2. Noise measurements made in the open laboratory (a) single SQUID (b) electronic gradiometer.

ments of an insulating vacuum space, superinsulation and an activated charcoal getter. The cryostat's unusual characteristics are small size (diameter 150 mm, overall length 300 mm) chosen to provide a 24 hour hold time, all-Tufnol (cotton-epoxy composite) construction to obviate electromagnetic screening, and relatively small, 4 mm tail thickness.

3. Performance

We tested the system first in the Wellcome Biomagnetism Unit at the Southern General Hospital, Glasgow. This has an eddy current shielded aluminium room [5] to which an RF-shielding door has recently been added for low noise measurements. Our results showed that the white noise floor was less than 10^{-11} T/√Hz for the two SQUIDs and slightly higher for the gradiometer. The 1/f corner frequency was 100Hz. According to a comparison with noise measurements made in mumetal shielding, most of the 1/f noise component is environmental but the white noise level is given by the SQUIDs themselves.

We repeated the measurements with the equipment in position unshielded in the NDE scanner in the Superconducting Devices Research Group laboratory at Strathclyde University, with the results shown in Figure 2. Clearly, the single SQUID is susceptible to a great deal of interference, while the gradiometer, despite its simplicity, gets rid of all but the largest peaks.

Figure 3 is an x-y scan above a >-shaped wire carrying a 14 mA, 270 Hz current. In the present apparatus, the SQUIDs are aligned vertically and measure horizontal field. We would have preferred horizontal alignment (to measure vertical fields) but reorientation would have meant either making the tail of the cryostat inconveniently large or truncating the other end of the SQUID-mounting PCBs, including cutting through tracks. Figure 3 therefore illustrates how the present 11 mm minimum lift-off gives relatively poor spatial resolution. However, it also demonstrates the stability and adequate SNR of both the single SQUID and the gradiometer in the open laboratory, even during computer-controlled, stepper-motor energised scanning.

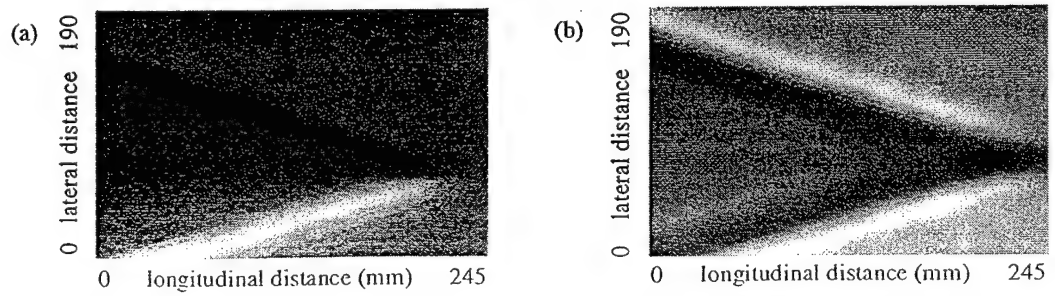

Figure 3. Maps of >-shaped current-carrying wire from (a) single SQUID (520 nT p-p) (b) electronic gradiometer (353 nT p-p). Dark areas are negative, light positive.

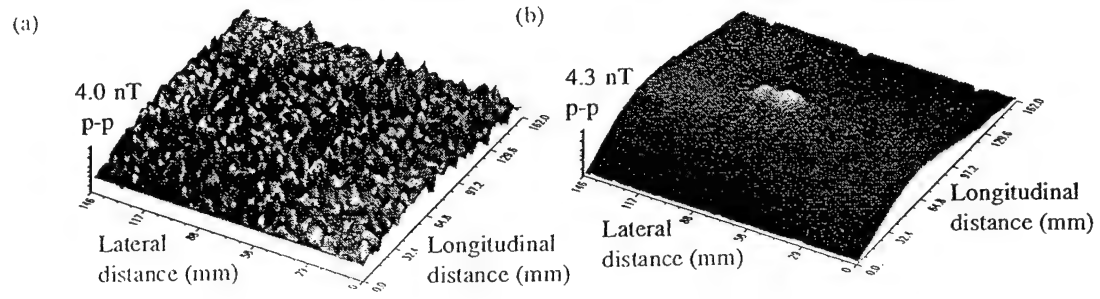

Figure 4. Eddy current maps of an aluminium plate with a single small surface slit. (a) single SQUID and (b) electronic gradiometer.

Although the current-carrying wire illustrates the response of the system to a particular source, it gives no indication of real performance for NDE. This is dealt with in more detail elsewhere [6]. Here, we give the single example in Figure 4. This shows maps of an aluminium plate with a small slit in the surface. This slit has an arc section with a 45 mm diameter. Its maximum depth is 1.8 mm, surface length approximately 20 mm and width 150 μm. It was mapped by applying a 77 mA 2.7 kHz current to a 5 turn, 4.5 mm diameter spiral coil fabricated on epoxy glass PCB. The inner to outer connection was made by aluminium wire bonding. This coil was mounted beneath the cryostat centrally between the SQUIDs. The aluminium plate was positioned as close as possible to the coil.

Figure 4 clearly shows that spatial resolution is improved if a small, well defined source is positioned close to the specimen, no matter what the SQUID lift-off. Also apparent is that the fundamental SNR of this experiment is much lower than the one illustrated in Figure 3 and the difference in noise (i.e. interference) level between the single SQUID and gradiometer is much greater - in fact, the experiment would have failed if only a single SQUID had been used.

4. Conclusions

We have designed and built a complete two SQUID electronic gradiometer based on Conductus Mr SQUIDs and optimised for NDE. With it, we are able to exploit the fundamental performance of the SQUIDs properly for the first time in an open laboratory environment. We have demonstrated this here and elsewhere [6] with a selection of typical experimental results.

The authors acknowledge support from the US AFOSR, UK EPSRC, Oxford Instruments, The Royal Society of Edinburgh and the UK DRA.

References

[1] Wikswo J P Jnr 1995 *IEEE Trans. Appl. Superconductivity* 5 2

[2] Conductus Inc.1992 *Mr SQUID: A high T_c superconductor SQUID system for undergraduate laboratories*

[3] Cochran A, Macfarlane J C, Morgan L N C, Kuznik J, Weston R, Hao L, Bowman R M and Donaldson G B 1994 *IEEE Trans. Appl. Superconductivity* 4 3 123 - 234

[4] Cochran A, Morgan L N C, Bowman R M, Kirk K J and Donaldson G B1993 *IEEE Trans. Appl. Superconductivity* 3 1 1926-1929

[5] Bain R J P, Donaldson G B, Pegrum C M, Maas P, and Weir A I 1991 *Extended abstracts of the 8th International Conference on Biomagnetism*, Munster, Germany

[6] Cochran A, Kuznik J, Carr C, Morgan L N C and Donaldson G B *Presented at EUCAS '95.*

Presented at European Conference on Applied Superconductivity (EUCAS '95) Edinburgh, July 1995

Experimental results in non-destructive evaluation with HTS SQUIDs

A Cochran, J Kuznik*, C Carr, L N C Morgan+ and G B Donaldson

University of Strathclyde, Department of Physics and Applied Physics, John Anderson Building, 107 Rottenrow, Glasgow, G4 0NG, UK.

* Presently visiting from Institute of Physics, Czech Academy of Sciences, Prague, Czech Republic.

+ Now with BT Laboratories, Martlesham Heath, Ipswich, Suffolk, IP5 7RZ.

Abstract. Until now, most experiments demonstrating the use of superconducting quantum interference devices (SQUIDs) for non-destructive evaluation have been based on liquid helium temperature equipment. However, experience of high temperature superconductor (HTS) SQUIDs is growing and we have recently begun to make almost routine measurements with them. Here we outline the developments in experimental apparatus which have allowed this and present some of our results, obtained in the open laboratory using a first order electronic gradiometer based on two simple bare HTS SQUIDs.

1. Introduction

We have been carrying out experiments in non-destructive evaluation (NDE) using superconducting quantum interference devices (SQUIDs) at Strathclyde University for more than ten years. Initially, we used low temperature superconductor (LTS) SQUIDs, gradiometers and cryostats similar to those in use at the time for biomagnetic measurements. However, we soon realised that the needs of NDE were quite different, and a long development process began.

Once it was known, soon after their discovery, that high temperature superconductors (HTSs) could be used for SQUIDs, efforts began to exploit them for NDE. Only simple experiments were possible with the first crude devices [1] but it was immediately clear that the convenience of liquid nitrogen cooling (LN_2) would be a vital factor in the adoption of SQUIDs by the wider NDE community.

The Conductus Mr SQUID [2] can now, arguably, be seen as a breakthrough in SQUID NDE. For the first time, an HTS SQUID was available which needed little special handling and which could be guaranteed to work through a series of experiments. However, few people considered that such a small sensor (with an effective pick-up area 70 μm square [3]) could have practical applications. Here, we demonstrate that this may not be true, at least in NDE.

2. Recent developments

For our first investigations of NDE with HTS SQUIDs, we used systems based on single SQUIDs. These showed that the sensors merited further investigation, though the results

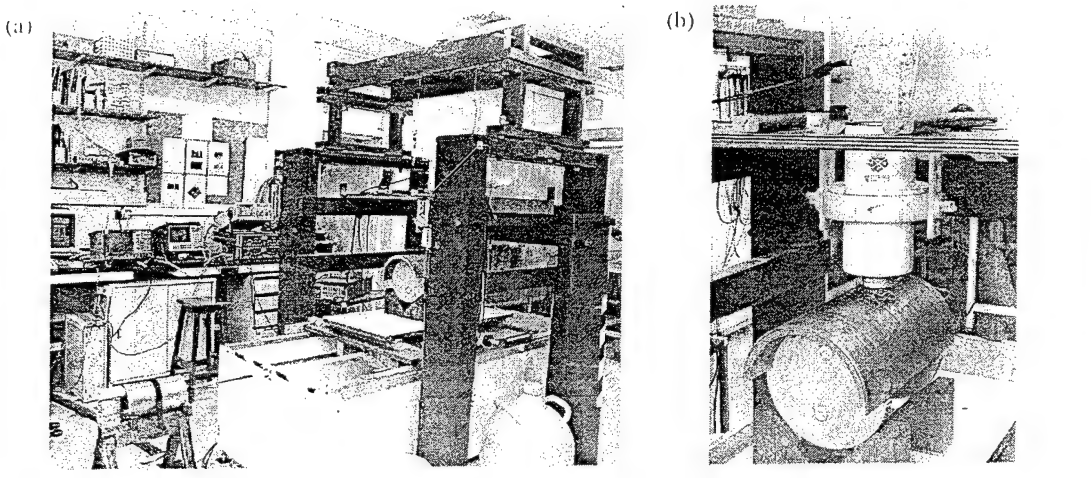

Figure 1. The NDE system in the open laboratory at Strathclyde University. (a) overall view and (b) detail showing HTS SQUID system, in this case above a section of pressure vessel

themselves, in NDE terms, were indicative only of possible future developments.

More recently, we have developed a system based on two Mr SQUIDs for simple electronic gradiometry. The other parameters of this system (described in more detail elsewhere [4]) were also optimised for NDE. They include a bandwidth of more than 30 kHz and a non-magnetic, non-conductive cryostat with a small (4 mm) LN_2 to room temperature separation.

After basic characterisation in low noise and open laboratory environments, the new gradiometer was incorporated into our existing SQUID NDE scanning, data acquisition and processing system. This has four major parts, some recently enhanced, as shown in Figure 1.

The *cryostat support gantry* is a timber frame (intended for large LTS cryostats) from which the small HTS system is suspended on two nylon arms. Precise lift-off adjustment is achieved by moving the specimen on an adjustable marble plinth.

Primary movement of the *x-y scanning bed* is longitudinal, effected by a lead screw from a shielded stepper motor and controlled via feedback from a non-magnetic shaft-encoder driven by the bed. Lateral motion is by a ratcheted rack and pinion mechanism to avoid the need for another stepper motor which, moving bodily, would act as a magnetic anomaly in its own right. Recent improvements include a choice of eight different scan patterns, one of them step and repeat which has proved crucial in the inspection of a mild steel specimen.

The stepper motor and the instrumentation for ac excitation signal generation (a two channel waveform synthesiser) and SQUID output demodulation (two EG&G 5210 dual channel lock-in amplifiers) are controlled by C++ software running on a *PC*. This also performs data acquisition, directly from the lock-ins via GPIB, or through an analogue input card.

After acquiring a complete magnetic map, it is transferred to our HP 9000/700 series *workstations* for examination and archival. Since a single scan produces at least four x-y sets of data at mm resolutions - for example quadrature ac components from one SQUID and the gradiometer - rapid processing and display is essential.

3. Experimental results

The results we present here were obtained using the three different excitation methods shown in Figure 2: direct injection of ac current, and eddy current induction using either a single turn

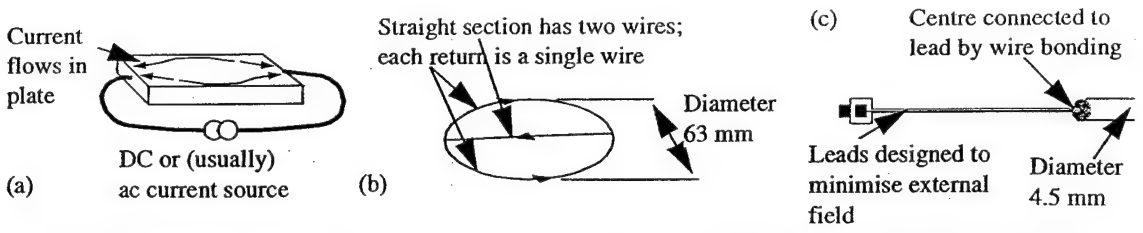

Figure 2. Excitation methods. (a) direct current injection, (b) double-D induction coil and (c) spiral coil

63 mm diameter coil with a double-D layout or a 4.5 mm diameter, 5 turn spiral coil made as a PCB with an aluminium wire bond from the centre out.

3.1. Direct injection of current

The specimen we used for this was an aluminium plate approximately 300 mm square and 13 mm thick, with a central slot 6.5 mm deep, 6 mm wide and 40 mm long. Although this is not a realistic NDE specimen, it serves to illustrate the performance of our system. Injecting a 140 mA ac signal at 530 Hz into it perpendicular to the slot gave the results shown in Figure 3.

The single SQUID result shows no indication of the slot because large signals from the current spreading out around the sides of the plate dominate and because the small signals from the slot are buried in environmental interference, itself too small to be seen on the same scale as the large signals. However, the gradiometer result clearly shows the expected peak at one end of the slot and trough at the other. There are two benefits of using a gradiometer here: the large *but distant* signals from spreading current are reduced, and interference is also reduced.

3.2. Eddy current induction with a double-D layout

For this experiment, we used the specimen described in Section 3.1, but turned over so that the slot was 6.5 mm beneath the scanned surface. In this case, although the slot is large, the 6.5 mm subsurface distance is also large in NDE terms. Note that superficially similar specimens made from separate layers [5] are electromagnetically quite different since in them current flows only around the sides of a slot whereas in our case current also flows over the slot, making the distortion more diffuse and difficult to detect.

The double-D coil of Figure 2(b) was used because field decay into the plate because of coil geometry is much slower than with a smaller coil. The ac signal in the coil was 140 mA at 270 Hz. The result from the gradiometer only is shown in Figure 4. In this case, we would expect the response to be given by two dimensional convolution of the gradiometer's spatial response, the shape of the coil (modified by lift-off), and the shape of the slot. This is indeed what appears.

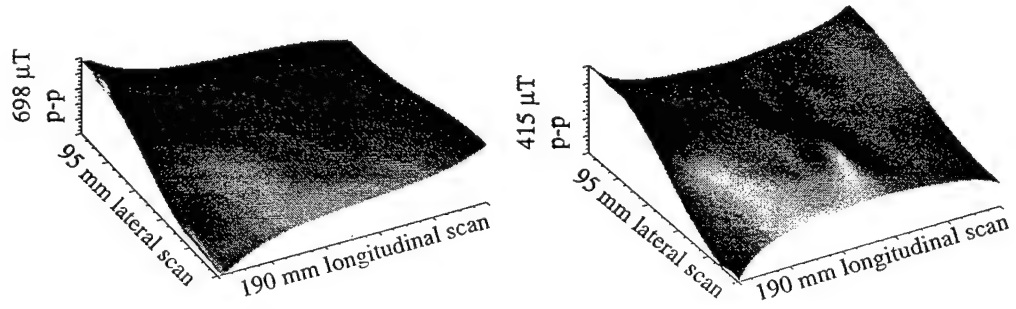

Figure 3. Directly injected current mapping. (a) single SQUID and (b) gradiometer

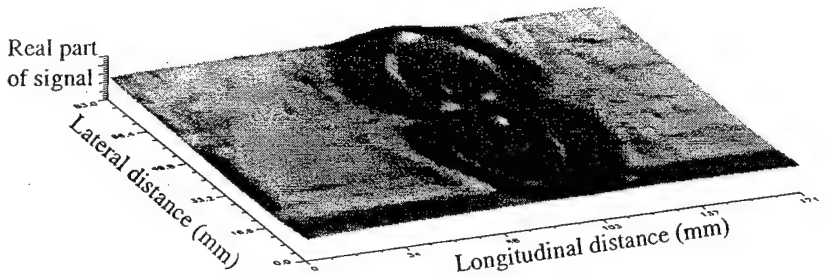

Figure 4. Eddy current mapping of a subsurface feature. The complicated response is mainly the result of the geometry of the double-D induction coil

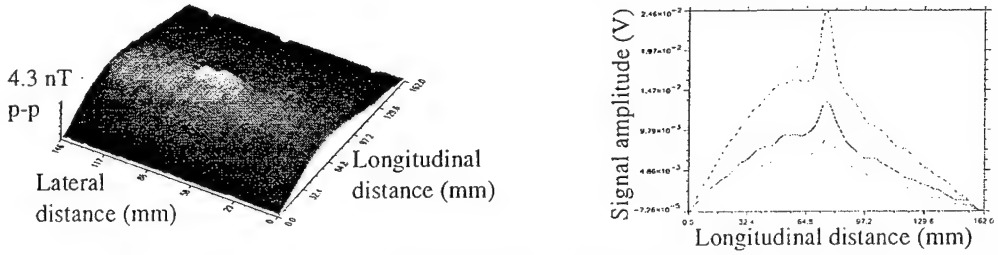

Figure 5. Eddy current mapping of a surface slit with a spiral coil. (a) Complete gradiometer result at 4.5 mm lift-off and (b) sections at lift-offs of 1.5 (upper), 3 (middle) and 4.5 mm (lower).

3.3. Eddy current induction with a small spiral coil

For our third experiment, we attached the spiral coil in Figure 2 to the cryostat and used a 47 mA 2.7 kHz ac signal. The specimen was another aluminium plate, 12.5 mm thick with a much smaller slit in its upper surface with a surface length around 20 mm, a width of 150 μm, with an arc profile 1.8 mm at its deepest and 45 mm in diameter. The results shown in Figure 5, and compared with Figure 4, clearly indicate how high spatial resolution can be achieved using a small source, even with relatively distant SQUIDs. Detection of such a small feature at lift-offs corresponding to thick layers of surface protection is noteworthy in itself for NDE.

4. Conclusions

We have demonstrated how the simplest possible HTS SQUID first order electronic gradiometer can be used as part of a well-specified SQUID NDE system working entirely without shielding to achieve results approaching the quality of those obtained with LTS systems.

The authors are supported by UK EPSRC, UK MoD/DRA, The Royal Society of Edinburgh and Oxford Instruments Ltd.

References

[1] Bowman R M, Macfarlane J C, Cochran A, Kirk K J, Pegrum C M and Donaldson G B 1993 *Supercond. Sci. Technol.* **6** 2 91 - 95

[2] Conductus Inc. 1992 *Mr SQUID: A high T_c superconductor SQUID system for undergraduate laboratories*

[3] Cochran A, Macfarlane J C, Morgan L N C, Kuznik J, Weston R, Hao L, Bowman R M and Donaldson G B 1994 *IEEE Trans. Appl. Superconductivity* **4** 3 123 - 234

[4] Kuznik J, Carr C, Cochran A, Morgan L N C and Donaldson G B *Presented at EUCAS'95*

[5] Alzayed N S, Fan C-x, Lu D F, Wong K W, Chester M and Knapp D C, 1994 *IEEE Trans. Appl. Superconductivity* **4** 2 81 - 86

Presented at European Conference on Applied Superconductivity (EUCAS '95) Edinburgh, July 1995

Using SQUIDs to solve some current problems in eddy current testing

D McA McKirdy, A Cochran, A McNab* and G B Donaldson

University of Strathclyde, Department of Physics and Applied Physics, John Anderson Building, 107 Rottenrow, Glasgow, G4 0NG, UK.
*University of Strathclyde, Department of Electronic and Electrical Engineering, Royal College, 204 George St., Glasgow, G1 1XW, UK.

Abstract. The development of SQUID-based systems for non-destructive evaluation has now reached the point at which results are not just useful as demonstrations of the technology but also show how some of the current problems in eddy current testing may be solved. The examples we consider here are the development of modelling techniques which can be tested by comparing simulated results with high quality SQUID-based experimental data; the detection of deep subsurface flaws in aluminium; and the detection of small surface flaws at quite high lift-offs, equivalent to inspection through surface coatings several millimetres thick.

1. Introduction

Much of the work on the use of the superconducting quantum interference device (SQUID) for non-destructive evaluation (NDE) has been aimed, of necessity, more at improving the superconducting technology [1] than tackling existing problems in NDE research. However, recent advances in low and high temperature superconductor (LTS and HTS) systems [2,3] show that SQUID-based eddy current testing (ECT) will soon be routinely possible, at least in the NDE research lab. This will in turn allow some current problems in ECT [4] to be tackled, including, for example, verification of modelling, and detection of deep subsurface flaws in aluminium or flaws in pipework beneath thick protective or insulating layers.

Here, we deal with each of the three problems mentioned above, first concentrating on modelling then comparing modelled and experimental results for the two practical problems.

2. Modelling techniques

SQUIDs are a good subject for numerical modelling because they behave as close to ideal macroscopic sensors. Before selecting a model, though, typical ECT experimental procedures must be taken into account. We have used two: in most cases, we attach the induction coil to the outside of the tail of the cryostat then move the specimen under this in an x-y fashion, recording the SQUID signals as we scan; in some cases, however, we have made measurements at multiple frequencies at a very small number of points above the specimen [5].

The two most relevant modelling techniques are the finite element method (FEM) [6] and the volume integral method (VIM) [7]. Their properties are summarised in Table 1.

Table 1: Properties of the FEM and the VIM

	FEM	VIM
Solves for	Potentials at all points inside and outside specimen	Electric field only in flaw
Problem definition	As graded mesh of 3D (not necessarily regular) volume elements	As regular 3D mesh of cuboid volume elements
Magnetic properties of specimen	Material can be non-magnetic ($\mu_r \approx 1$) or ferromagnetic ($\mu_r >> 1$), with appropriate code	Material must be non-magnetic (e.g. aluminium)
Geometrical properties of specimen	Arbitrary, according to mesh	Planar only
Possible flaws	Arbitrary, according to mesh	Surface (or subsurface) breaking, with major faces perpendicular to surface
Computational demands	Very high: typical run time 4 hrs for single SQUID/induction coil position	Low: typical run time 1 hr for 50 x 50 SQUID/induction coil positions
Form of output	Principally electric and magnetic fields and current densities calculated from potentials	Principally electric and magnetic fields, and induction coil impedance changes
Available as	Commercial packages with pre- and post-processing including graphical user interface	Specially written source code sometimes requiring editing to solve different problems

Although the FEM is, in theory, more flexible than the VIM, in practice this is reflected in much greater runtimes. Two dimensional (2D) problems can be solved rapidly but SQUID ECT needs 3D solutions which take several hours for a single induction coil position. At present, therefore, we restrict our use of FEM to the calculation of current densities in a specimen, particularly to observe the effects of different coil geometries and excitation frequencies.

The VIM is less familiar than the FEM. For ECT, it may be expressed by [7]:

$$\boldsymbol{E}(\boldsymbol{r}) - (\sigma_f - \sigma_h) \int_{V'} (\boldsymbol{G}(\boldsymbol{r}, \boldsymbol{r}') \cdot \boldsymbol{E}(\boldsymbol{r}'))\, dV' = \boldsymbol{E}^0(\boldsymbol{r}) \qquad (1)$$

where

$\boldsymbol{E}(\boldsymbol{r})$ ≡ total electric field,

σ_f and σ_h ≡ flaw and specimen conductivities respectively,

$\boldsymbol{G}(\boldsymbol{r}, \boldsymbol{r}')$ ≡ Green's tensor appropriate to unflawed specimen,

V' ≡ volume occupied by flaw,

and $\boldsymbol{E}^0(\boldsymbol{r})$ ≡ electric field induced in unflawed specimen by induction coil.

$\boldsymbol{r} \equiv (x,y,z)$ and $\boldsymbol{r}' \equiv (x',y',z')$ are, as usual, the observer and source coordinate vectors. The electric field, $\boldsymbol{E}(\boldsymbol{r})$, must in turn be transformed into external magnetic field, using (for example)

$$B_y(\boldsymbol{r}) = \left(-\frac{\sigma_h - \sigma_f}{i\omega m_y^0} \right) \int_V (\boldsymbol{E}(\boldsymbol{r}) \cdot \boldsymbol{E}^0(\boldsymbol{r}))\, dV \qquad (2)$$

where

$\omega \equiv 2\pi f$, f = excitation frequency

m_y^0 ≡ magnetic moment of y-oriented sense coil, usually 1 (since reciprocity is used)

and $\boldsymbol{E}^0(\boldsymbol{r})$ is the electric field induced in the unflawed specimen, in this case by the sense coil.

To model the measurement of this field by a SQUID, it can be integrated over the pick-up area or, as here, the SQUID can be assumed to be an ideal point sensor. In our work, the actual VIM implementation is in Fortran 77, running on a Sun SparcStation. As noted in Table 1, even a 50 x 50 point scan is quicker than a single point FEM calculation.

3. Results

3.1. Subsurface detection

The most common subsurface NDE method is ultrasound. However, it has the practical disadvantage of needing high quality surface contact. Although ECT has no similar need, conventional instruments are generally limited to shallow inspections (1 - 2 mm) by the skin effect. Because of the high sensitivity of the SQUID at low frequencies, this limitation can be overcome, leading to considerable interest in deep subsurface NDE, including ECT, with SQUIDs.

To demonstrate this, we performed the experiment outlined schematically in Figure 1, with the results shown in Figure 2. Clearly the experimental measurement was successful, and the VIM model has correctly predicted the shape of the complicated response which is the result of the combination of the non-negligible cross-section of the slot, the use of two SQUIDs rather far apart, and the geometry of the double-D induction coil. However, there is a discrepancy in amplitude which requires further investigation.

3.2. High lift-off inspection

Our second illustration concerns high lift-off inspection. In conventional ECT there is a very significant drop in sensitivity as lift-off increases because a usually small coil (with a strongly

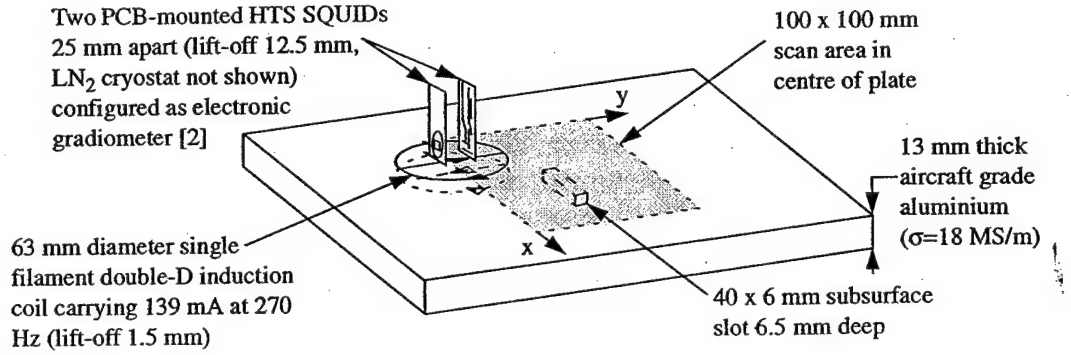

Figure 1. Experiment to detect subsurface feature

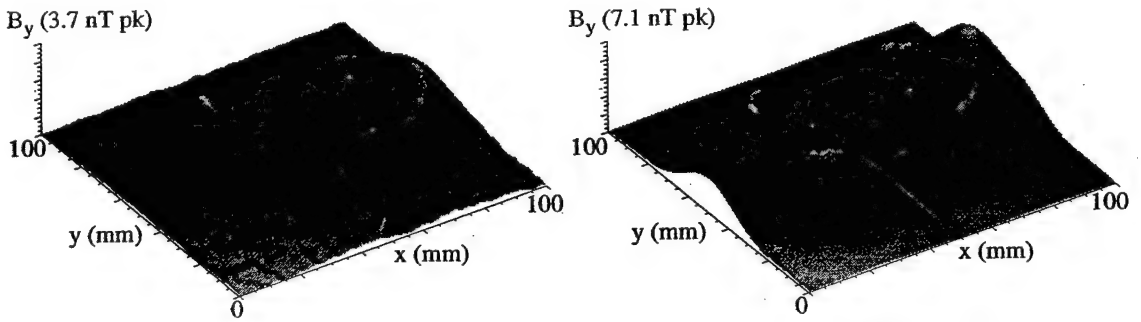

Figure 2. (a) Experimental response of subsurface slot and (b) result of VIM simulation

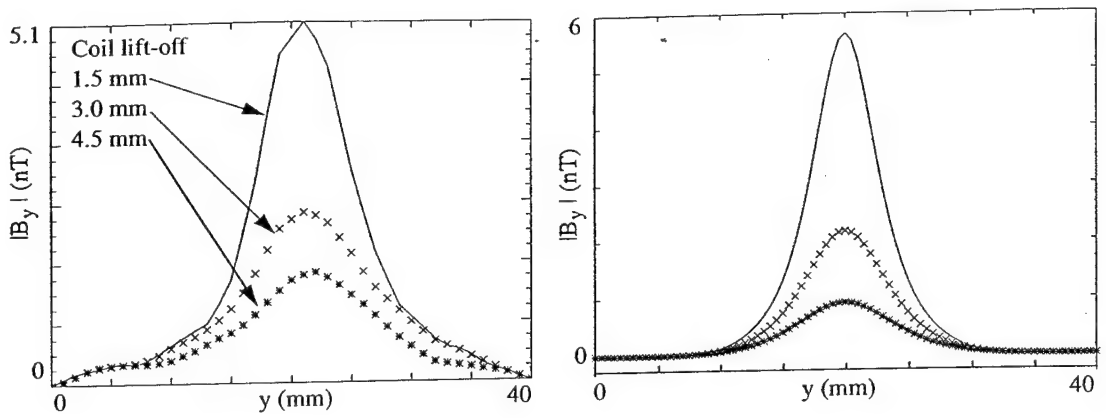

Figure 3. (a) Experimental response of surface slot at different lift-offs and (b) result of VIM simulation

distance-dependent amplitude response) is used both for induction and signal detection. In our work, even with an induction coil such as the 4.5 mm diameter 4-turn planar spiral we now consider, the sensitivity of the SQUIDs is so high that the problem is very much reduced.

To obtain the results shown in Figure 2, we scanned another aluminium plate, this time with an arc section slit in its upper surface 150 μm wide, of 1.8 mm maximum depth on a 22.5 mm radius with a surface length of 17.8 mm. We applied 77 mA at 270 Hz to the small spiral coil and made three scans, at coil lift-offs of 1.5, 3 and 4.5 mm. Again, there is reasonable correspondence between theory and experiment. In this case, the shape of the response is much simpler because of the smaller slit dimensions and simpler coil, and the response peak becomes smaller and wider as one would expect as lift-off increases.

4. Conclusions

In a previous paper we demonstrated SQUID NDE simulation using the finite element method [5], essentially for single point measurements. Here, we have considered the alternative volume integral method [7]. We have shown how it can be used to obtain simulated results in the form of x-y maps which correspond well with experimental results. This is valuable in itself, since it allows the model to be tested in a way which is difficult with the limited experimental data available from more conventional eddy current testing. With the VIM, we have considered two particular current problems in ECT: deep subsurface flaws in aluminium, and high lift-off inspection, and shown by simulation and experiment how SQUIDs may be used to solve them.

The authors are supported by UK EPSRC and MoD, and The Royal Society of Edinburgh.

References

[1] Cochran A, Donaldson G B, Morgan L N C, Bowman R M and Kirk K J 1993 *Brit. J. NDT* 35 4 173 - 182
[2] Kuznik J, Carr C, Cochran A, Morgan L N C and Donaldson G B 1995 *Presented at EUCAS'95*
[3] Klein U, Walker M E, Hutson D, Cochran A, Weston R G and Pegrum C M 1995 *Presented at EUCAS'95*
[4] See for example Thompson D O and Chimenti D E (Eds.) 1994 *Review of Progress in Quantitative NDE* **13A** Plenum Press, New York
[5] Morgan L N C, Carr C, Cochran A, McKirdy D McA and Donaldson G B 1995 *IEEE Trans. Appl. Supercond.* 5 2
[6] Vector Fields Ltd., Kidlington, Oxford, OX5 1JE, UK 1995 *OPERA* and *ELEKTRA FEM software*
[7] McKirdy D McA 1989 *J. Nondestr. Eval.* **8** 1 45 - 52
[8] Cochran A, Kuznik J, Carr C, Morgan L N C and Donaldson G B 1995 *Presented at EUCAS'95*

Presented at European Conference on Applied Superconductivity (EUCAS '95) Edinburgh, July 1995

Experimental characterisation of planar SQUID gradiometers in niobium technology

U Klein, M E Walker, A Cochran, D Hutson, R G Weston, and C M Pegrum

University of Strathclyde, Department of Physics and Applied Physics, John Anderson Building, 107 Rottenrow, Glasgow, G4 0NG, UK.

Abstract. High temperature superconductors (HTSs) are the most attractive technology for practical superconducting magnetic field sensors in the long term, but present difficulties mean that work on integrated HTS SQUID-gradiometer devices is still based on solving fabrication problems. However, low temperature superconductor technology is already well enough established to allow different sensor designs to be tested immediately. Here we consider integrated sensors optimised for electromagnetic non-destructive evaluation (NDE) in unshielded environments. We are studying both symmetric and asymmetric first-order gradiometers; the symmetric ones have two identical rectangular loops; the others have an additional loop making them singly asymmetric. Devices have been fabricated using a *Nb/Al-Al$_2$O$_3$/Nb* trilayer process established for similar devices for biomagnetism. Here we outline the practical and theoretical reasons for the NDE sensor designs we have chosen and present initial experimental results.

1. Introduction

Superconducting quantum interference devices (SQUIDs) have unparalleled magnetic field sensitivity down to very low frequencies. This makes them attractive for some electromagnetic non-destructive evaluation (EM NDE) applications for which existing sensors have inadequate frequency response, sensitivity or spatial resolution [1]. A typical example of an application is inspection of aircraft, parts of which comprise layered aluminium structures riveted together [2]. The acoustic opacity of the layer interfaces usually prevents the use of ultrasound while the total thickness restricts eddy current techniques to low frequencies at which conventional equipment has poor sensitivity.

Recent results using low and high temperature superconductor (LTS and HTS) equipment [2, 3] suggest that the theoretical sensitivity and low frequency advantages of SQUIDs can be translated into functionally satisfactory systems i.e. they can detect flaws under ideal conditions. However, there are still two problems. The first is to produce SQUID-based sensors which have adequate sensitivity to second layer flaws but are still sufficiently insensitive to interference to work in unshielded, sometimes magnetically hostile environments. The second problem is to engineer a system which is acceptable to the user in terms of cost and is convenient and reliable. This will probably demand an HTS solution, but LTS technology is well enough established to allow experimental investigations of SQUID-based sensors for unshielded operation.

To measure a single magnetic field component, e.g. B_x, there are three possibe types of planar gradiometer: symmetric, singly asymmetric and doubly asymmetric [4]. In each case,

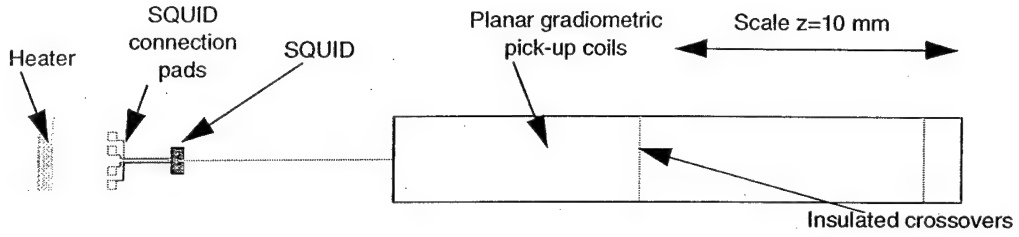

Figure 1. Layout of a first-order singly asymmetric planar gradiometer integrated with a double-washer SQUID.

we consider only long, narrow rectangular outlines. An example of a singly asymmetric design is shown in Figure 1. In a symmetric gradiometer, the number of loops is one more than its order (i.e. the lowest order of field gradient N in $\delta^N B_x/\delta z^N$ which the gradiometer does not reject). In singly asymmetric designs, an extra loop is added; this does not change the order but alters the spatial response beyond the ends of the gradiometer, most distinctly at one end for highly asymmetric designs. In doubly asymmetric designs, two extra loops are added, still maintaining the order but altering the response close to both ends independently.

2. Practical design constraints

Theoretical issues of gradiometer design are dealt with elsewhere [4, 5]. Here, we concentrate on implementing and testing first order symmetric and asymmetric designs.

The first part to be considered is the SQUID, shown in Figure 2. We have chosen to work with the common DC washer type. Although magnetic shielding is physically possible, with the SQUID fabricated on the same substrate as the gradiometer it is undesirable because the shield would act as a very significant magnetic anomaly. Instead, the SQUID itself is gradiometric. We use a first order configuration in which the SQUID body is a double washer. The gradiometer is coupled to it by two 19-turn spiral coils counterwound around the two loops [6]. The SQUID must also be as small as possible so that its behaviour as a magnetic anomaly and its sensitivity to directly coupled environmental fields are minimised. Our present NDE design was intended for biomagnetic applications in which some degree of environmental shielding is possible so the SQUID outline is 420 x 960 μm; this will be reduced in future to take account of the much stronger signals, typically up to 10 nT, in NDE, and the much larger environmental fields, typically 200 nT for the 50 Hz electrical mains in our laboratory.

Now consider the gradiometer design. The field sensitivities typically required for NDE range from 10 nT down to about 100 pT in a 5 Hz bandwidth. This allows very small sensors to be used; we have recently worked with directly coupled HTS SQUIDs with pick-up areas only 70 x 70 μm [3] in a 25 mm baseline first order electronic gradiometer. We expect interference rejection of an integrated gradiometer to improve on this and we must also allow for the

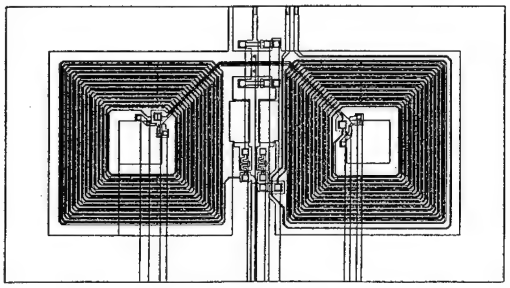

Figure 2. The double washer SQUID. The vertical lines from the interiors of the SQUID loops are construction lines for the mask design package from which the layout was taken.

inevitable sensitivity reduction caused by impedance mismatch between the pick-up coils and SQUID, and the much more significant sensitivity reduction associated with using an asymmetric pick-up coil. The outlines of the pick-up coils in our first integrated gradiometer designs are therefore 20 x 3 mm^2.

We have designed two gradiometers. The first is symmetric, with two loops 10 mm long. A SQUID positioned beyond one end is assumed to act approximately as a magnetic dipole, introducing imbalance into the otherwise balanced design. To minimise this, it is placed as far from the gradiometer as connection lead inductances and wafer real estate allow, at a distance of approximately 7.5 mm. The second gradiometer design is asymmetric, as shown in Figure 1. The three loops are approximately 8.7, 10 and 1.3 mm long. Beyond the left hand end in the diagram (the upper end during measurements), the response of the gradiometer is similar to that of the symmetric design and the SQUID is therefore placed in the same position relative to the gradiometer. However, beyond the other end, the on-axis response to a magnetic dipole, M_x, has a zero crossing at approximately 4 mm and a local amplitude maximum at 6 mm.

The presence of a thin film molybdenum resistive heater near the SQUID is important. It is there primarily to expel trapped flux from the sensors during testing without thermal cycling by withdrawal from the cryostat. Since our NDE scanner [3] allows step and repeat movement, it may also be possible to exploit the resistor to ensure that flux motion during SQUID movement in environmental fields is prevented by synchronising thermal cycling with movement of the sensor across the specimen. At this point, we must also mention our intention to use an invertible cryostat to realise the goal of a SQUID NDE system able to inspect arbitrarily oriented surfaces of a stationary specimen; an example is the underside of an aircraft.

3. Implementation and testing

Given the difficulties noted earlier with HTS fabrication, the devices we have described have been fabricated in LTS *Nb/Al-Al$_2$O$_3$/Nb* trilayer technology. This is based on processes developed in our own clean room for devices for biomagnetism. The SQUID junction dimensions are 6 x 6 μm^2 and the gradiometric pick-up coil of each device is connected to the two 180 nH spiral input coils of the SQUID.

We have fabricated a total of 18 fully integrated devices. Room temperature testing has indicated that all the devices are functional as SQUIDs. Of the five more fully tested, first indications are that one gradiometer has a short circuit and acts as a magnetometer but the other four are functioning as expected. A typical field noise spectrum is shown in Figure 3. The measurement was made in an eddy current shielded room at the Wellcome Biomagnetism Unit,

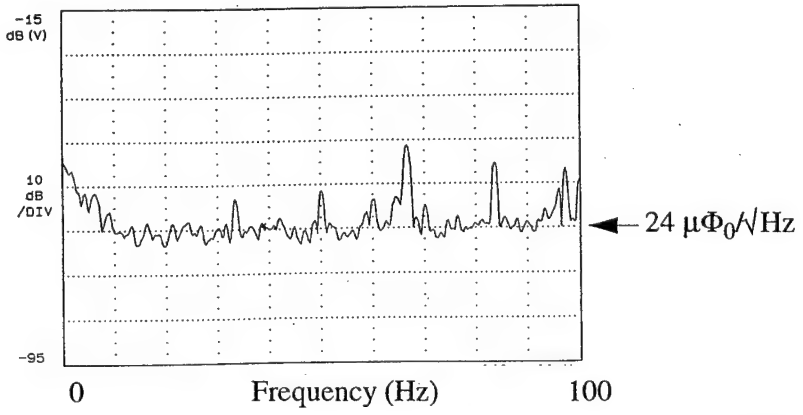

Figure 3. Noise spectrum of integrated device with asymmetric gradiometer in eddy current shielded roomt

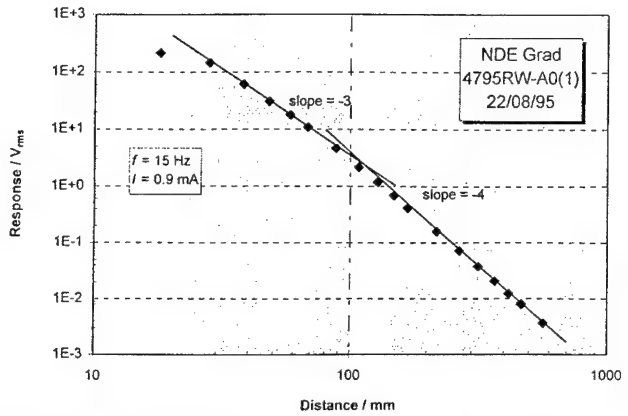

Figure 4. Response of integrated device with asymmetric gradiometer to a coil representing an on-axis magnetic dipole. The asymptotes indicated expected magnetometer and first order gradiometer responses.

Glasgow, with the SQUID connected to a Quantum Design 5000 controller. It indicates that the white noise level is approximately 25 $\mu\Phi_0/\sqrt{\text{Hz}}$ and the field sensitivity down to 420 $\text{fT}/\sqrt{\text{Hz}}$.

We have also measured the spatial response of an asymmetric device. The source was a 1000-turn coil 18.2 mm long with a diameter of 5.8 mm, representing a magnetic dipole. An ac signal of 0.9 mA at 15 Hz was applied to it and the coil was moved over a distance of almost 1 m directly beneath the gradiometer. The test took place in an rf shielded room in our laboratory, with the SQUID in a BTi fibreglass cryostat, connected to 2G 580 DC SQUID electronics. The result shows three regions. When the coil is very close to the cryostat, its dimensions are too large to approximate a magnetic dipole. Beyond this region and up to approximately 10 cm, the sensor behaves as a magnetometer: the response has a z^{-3} characteristic defined by the z^{-3} decay of the field of the coil. In the region beyond 10 cm, the response has a z^{-4} characteristic caused by a combination of the source field decay and the z^{-1} characteristic expected of a first order gradiometer. The fact that the spatial response does not level off at distances up to 1 m indicates that the intrinsic balance of the gradiometer is better than 1 part in 10^4.

4. Conclusions

Our experience of SQUID NDE has led us to believe that an integrated device is an attractive long term solution to problems including the cost of high slew-rate, wideband, multichannel electronics for electronic gradiometry, and the unsatisfactory nature of wirewound LTS devices, in terms of intrinsic imbalance and cost.

We have constructed symmetric and asymmetric first order gradiometers integrated with double washer SQUIDs in LTS technology. Our choice of fabrication process has been validated by high yields, and we have carried out initial tests on several devices, including, for the first time, a practical asymmetric gradiometer. These indicate that our design methodology is correct and that the programme is worth pursuing, with further basic and more practical tests.

References

[1] Cochran A et al 1993 *Brit. J. NDT* **35** 173 - 82
[2] Wikswo J P Jr. 1995 *IEEE Trans. Appl. Superconductivity* **5** 2
[3] Cochran A et al 1995 *Presented at EUCAS'95*
[4] Walker M E et al 1995 *Presented at EUCAS'95*
[5] Jones A E and Bain R J P 1995 *J. Comp. Phys.* **118** 191 - 9
[6] Lang G et al *Presented at EUCAS'95*

Presented at European Conference on Applied Superconductivity (EUCAS '95) Edinburgh, July 1995

Modelled Response of Planar Asymmetric Gradiometers

M E Walker, A.Cochran, U Klein, R J P Bain and G B Donaldson

University of Strathclyde, Department of Physics and Applied Physics, John Anderson Building, 107 Rottenrow, Glasgow, G4 0NG, UK.

We have numerically calculated sets of crossovers over the complete possible range of balanced first, second and third order singly asymmetric gradiometers. For the first time, we have also calculated the response of these sets of gradiometers to long current carrying wires and magnetic dipoles. Here we show that the near field response of the gradiometer can be tailored, by appropriate selection of one of the gradiometer crossover positions, to obtain desirable features. These are a null at which the SQUID can be positioned, or a region of enhanced response that can be used to improve a measurement's signal to noise ratio. We commment on the practical implications of our results.

1. Introduction

Although wire-wound gradiometers coupled to magnetically shielded SQUIDs have been studied and used for many years, they have several disadvantages, particularly for multichannel systems: poor intrinsic balance; the potential for mismatch between channels; physical constraints on minimum dimensions; and high cost per channel. To solve these problems we are studying planar gradiometers integrated with SQUIDs as shown in Figure 1. As well as overcoming practical difficulties, these may even have better fundamental performance for applications such as non-destructive evaluation (NDE), for example by allowing increased spatial resolution and measurement of alternative field components.

Symmetric planar gradiometers fabricated in LTS [1], have been considered as candidates for NDE and biomagnetism [2] for several years. However, we are more interested in asymmetric designs. Whereas symmetric gradiometers have only one response for a given order and size, asymmetric ones have a response which can be tailored by choosing the position of one or more crossovers. This allows two desirable features to be designed into their behaviour: a null at which to position the SQUID to reduce its effect as a magnetic anomaly on balance, and/or a region of enhanced response at which a specimen can be positioned to improve signal to noise ratio (SNR). To achieve both of these simultaneously requires a dou-

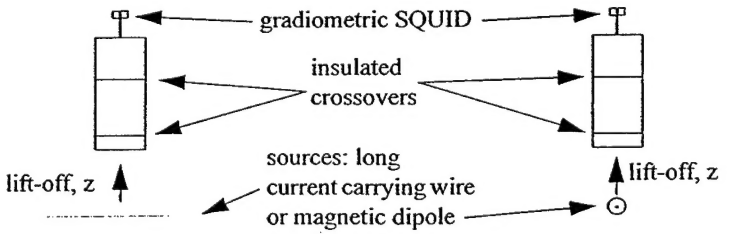

Figure 1. Gradiometer, SQUID and sources

bly asymmetric layout. Here we consider only the simpler, singly asymmetric layout which gives the choice of either a null or enhanced SNR.

2. Theory

Let

N = gradiometer order,

m = number of crossovers and

z_s = crossover position, $s = 1,2,...,m$

$-1 < z_s < 1$; i.e., the ends of the (normalised) gradiometer are at $z = \pm 1$

For symmetric gradiometers, $m = N$ and there is only one set of crossover positions that will result in a balanced gradiometer of a given size and order. However, for asymmetric gradiometers $m > N$ and there is no unique set of crossover positions: for an Nth order gradiometer with m crossovers, N of the crossover positions depend on the other $(m\text{-}N)$ positions. In practice, this means that $(m\text{-}N)$ positions are chosen and the other N positions are calculated from them. However, neither the chosen crossover positions nor the calculated ones are entirely arbitrary; each must lie within an allowed region [3]:

$$\cos((s\pi)/m) < z_s < \cos(((s\text{-}1)\pi)/m)$$

For a singly asymmetric gradiometer $(m\text{-}N) = 1$. One crossover position can therefore be chosen, allowing the response at one end of the gradiometer to be tailored. Using Fortran code on an HP 9000/715/100 workstation, we have numerically calculated sets of balanced crossovers for first, second and third order singly asymmetric gradiometers over the entire range possible. This was done by specifying, for example 100 different crossover positions in turn over the range allowed for the chosen one and calculating the others accordingly. Each chosen position (i.e. distinct gradiometer design) was given an index, as shown in Figure 2.

3. Results

3.1. Crossover positions

Figure 3 shows 100 sets of crossover positions over the entire possible range of balanced third order singly asymmetric gradiometers. This design has intrinsic $1/z^3$ behaviour on axis at large distances, so that, for example, its far field response to a magnetic dipole is $1/z^6$, neglecting balance errors. It is, of course, the near field behaviour which is of more interest here.

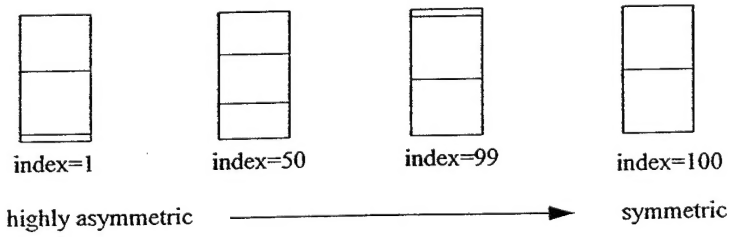

Figure 2. The scheme used to index gradiometer designs

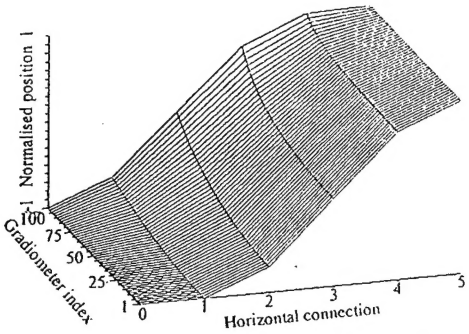

Figure 3. Sets of crossover positions for balanced third order, singly asymmetric gradiometers

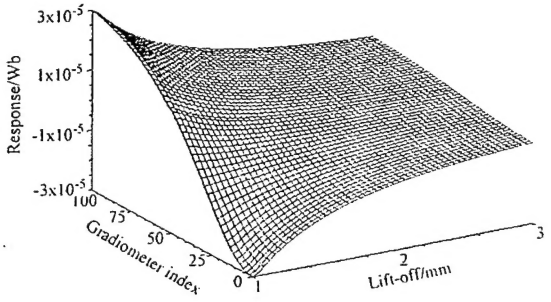

Figure 4. Response of a third order gradiometer to an on-axis magnetic dipole

3.2. Magnetic dipole responses

We have simulated the responses of asymmetric gradiometers to long current carrying wires and magnetic dipoles. While both of these models are easy to realise experimentally, they are also useful because simple demonstrations of NDE systems can be based on location and mapping of wires, and magnetic dipoles can be used as models of SQUIDs. Here we concentrate on theoretical magnetic dipole results.

Figure 4 shows the response of the complete range of third order gradiometers to a horizontally oriented magnetic dipole on the gradiometer axis (as shown in Figure 2) over lift-offs from 1 to 3 mm. Inspection reveals that there are two basic types of response as shown in Figure 5. For these graphs, we have assumed a gradiometer length of 20 mm and a width of 3 mm.

Both types decay as expected to zero as the dipole moves further from the gradiometer. However, if the dipole is considered as a model of a SQUID then Figure 5(a) shows that the

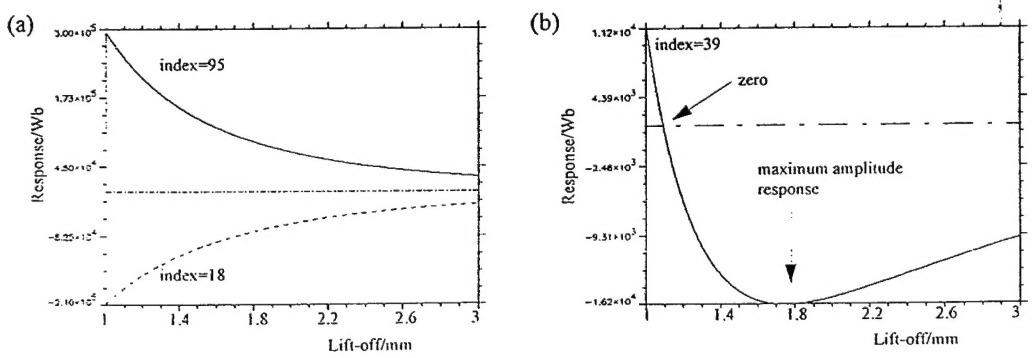

Figure 5. Different types of response to a magnetic dipole

Table 1(a) Null

index	null position
38	1.05 mm
...	...
45	1.90 mm

Table 1(b) Maximum response

index	max posn	max amp	-3dB width
34	1.16 mm	4.18×10^{-2} Wb	0.12 mm
...	...	...	...
41	2.04 mm	1.10×10^{-2} Wb	1.52 mm

SQUID should be positioned as far from the gradiometer as possible to minimise its effect on intrinsic balance. This has practical implications for the overall size of the device and the number (or maximum gradiometer size) which can be fabricated on a given size of substrate.

In contrast, Figure 5(b) indicates that the SQUID can be placed very close to the gradiometer, at the zero signal position, giving a device which is more compact overall and with potentially better balance. As an alternative, the local (here negative) peak in the amplitude response could be exploited by reversing the gradiometer in the cryostat to give maximum sensitivity to external NDE sources which behave like magnetic dipoles [4].

It must be noted that, for a 20 mm long gradiometer, the peak occurs within 2 mm of the end of the gradiometer. This would be difficult to exploit with most existing cryostat designs. Further figures emphasising the range of zero and peak positions are given in Table 1, corresponding to all gradiometers with responses similar to Figure 5(b), i.e. with a zero crossing and distinct negative peak. Note that the maximum amplitude is given for the case where the induced current in the gradiometer is 1 μA.

Similar features also exist for first and second order gradiometers. However, as the order reduces, the positions shift towards the gradiometer and occur over a smaller range of indices.

4. Conclusions and Further Work

We have obtained sets of crossovers over the entire possible range for first, second and third order singly asymmetric gradiometers and we have modelled the response of the resulting gradiometer designs to magnetic dipoles and current carrying wires. Our models have shown that the gradiometer design can be chosen to obtain a null to use as a SQUID position, or an enhanced amplitude region in which to position a specimen for signal measurement.

In future we will extend the modelling to current dipoles, then use dipole distributions and the finite element method [5] to simulate real NDE sources. We will also study doubly asymmetric gradiometers. Efforts to verify our models experimentally have already begun [6].

The authors are supported by UK EPSRC, MoD/DRA, The Royal Society of Edinburgh and Quantum Magnetics.

References

[1] Donaldson G B, Pegrum C M and Bain R J P 1985 SQUID'85 729 - 759

[2] Wikswo J P Jr. 1995 *IEEE Trans. Appl. Superconductivity* **5** 2

[3] Jones A E and Bain R J P 1995 *J. Comp. Phys.* **118** 191 - 199

[4] Cochran A, Donaldson G B, Evanson S and Bain R J P 1993 *IEE Proc. A* **140** 2 113 - 120

[5] McKirdy D McA, Cochran A, McNab A and Donaldson G B 1995 *Presented at EUCAS'95*

[6] Klein U, Walker M E, Hutson D, Weston R, Cochran A and Pegrum C M 1995 *Presented at EUCAS'95*